SYNTHESIS OF POLYTHIOPHENE AND POLYPYRROLE DERIVATIVES
AND THEIR APPLICATION IN ELECTROCHROMIC DEVICES

A THESIS SUBMITTED TO
THE GRADUATE SCHOOL OF NATURAL AND APPLIED SCIENCES
OF
MIDDLE EAST TECHNICAL UNIVERSITY

BY

METİN AK

IN PARTIAL FULFILLMENT OF THE REQUIREMENTS
FOR
THE DEGREE OF DOCTOR OF PHILOSOPHY
IN
CHEMISTRY

DECEMBER 2006

Approval of the Graduate School of Natural and Applied Sciences

Prof. Dr. Canan Özgen
Director

I certify that this thesis satisfies all the requirements as a thesis for the doctor of philosophy.

Prof. Dr. Ahmet Önal
Head of Department

This is to certify that we have read this thesis and that in our opinion it is fully adequate, in scope and quality, as a thesis and for the doctor of philosophy.

Prof. Dr. Levent Toppare
Supervisor

Examining Committee Members

Prof. Dr. Duygu Kısakürek (METU, CHEM)

Prof. Dr. Levent Toppare   (METU, CHEM)

Prof. Dr. Teoman Tinçer   (METU, CHEM)

Prof. Dr. Erdal Bayramlı   (METU, CHEM)

Prof. Dr. Mustafa Güllü   (Ankara Univ. CHEM)

I hereby declare that all information in this document has been obtained and presented in accordance with academic rules and ethical conduct. I also declare that, as required by these rules and conduct, I have fully cited and referenced all material and results that are not original to this work.

Name, Last name: Metin AK

Signature   :

ABSTRACT

SYNTHESIS OF POLYTHIOPHENE AND POLYPYRROLE DERIVATIVES
AND THEIR APPLICATION IN ELECTROCHROMIC DEVICES

Ak, Metin

PhD., Department of Chemistry

Supervisor: Prof. Dr. Levent Toppare

Different substituted thiophene and pyrrole monomers namely hexamethylene (bis-3-thiopheneacetamide) (HMTA), N-(4-(3-thienylmethylene)-oxycarbonylphenyl)maleimide (MBThi), 2,4,6-Tris-(4-pyrrol-1-yl-phenoxy)-[1,3,5]triazine (TriaPy), 2,4,6-Tris-(thiophen-3-ylmethoxy)-[1,3,5] triazine (TriaTh), and N-(2-(thiophen-3-yl)methylcarbonyloxyethyl) maleimide (NMT) were synthesized. The chemical structures of the monomers were characterized by Nuclear Magnetic Resonance (^{1}H-NMR and ^{13}C-NMR) and Fourier Transform Infrared (FTIR) Spectroscopies. Electrochemical behavior of the monomers in the presence and absence of comonomers were studied by cyclic voltammetry. Subsequently, monomers were homopolymerized and copolymerized via electrochemical methods and the resultant polymers were characterized by FTIR, Scanning Electron Microscopy (SEM) and conductivity measurements.

Second part of the study was devoted to investigate one of most interesting property of conducting polymers, the ability to switch reversibly between the two states of different optical properties, "electrochromism". In recent years there has been a growing interest in application of conducting polymers in electrochromic devices. Thus, electrochromic properties of the synthesized conducting polymers were investigated by several methods like spectroelectrochemistry, kinetic and colorimetry studies. Spectroelectrochemistry experiments were performed in order to investigate key properties of conjugated polymers such as band gap, maximum absorption wavelength, the intergap states that appear upon doping and evolution of polaron and bipolaron bands. Switching time and optical contrast of the homopolymers and copolymers were evaluated via kinetic studies. Results implied the possible use of these materials in electrochromic devices due to their good electrochromic properties.

Keywords: Thiophene and pyrrole derivatives ; Electrochemical polymerization; Conducting copolymers; Electrochromism; Spectroelectrochemistry; Electrochromic Devices

ÖZ

POLİTİYOFEN VE POLİPİROL TÜREVLERİNİN SENTEZİ VE ELEKTROKROMİK CİHAZ UYGULAMALARI

Ak, Metin

Doktora, Kimya Bölümü

Tez Yöneticisi: Prof. Dr. Levent Toppare

Aralık 2006, 114 sayfa

Bu çalışmada dört farklı tiyofen veya pirol fonksiyonlu monomerler (hekzametilen (bis-3-tiyofen asetamit) (HMTA), N-(4-(3-tiyenilmetilen)-oksikarbonilfenil)maleimid (MBThi), 2,4,6-Tris-(4-pirol-1-yl-fenoksi)-[1,3,5]triazin (TriaPy), 2,4,6-Tris-(tiyofen-3-ylmetoksi)-[1,3,5]triazin (TriaTh), N-(2-(tiyofen-3-yl)metilkarbonil oksietil)maleimid (NMT)] sentezlenmiştir. ^{1}H, ^{13}C NMR, FTIR, ve dönüşümlü voltametri teknikleri kullanılarak monomerlerin karakterizasyonu yapılmıştır. Çalışmanın ikinci aşamasında sentezlenen monomerlerin elektrokimyasal homopolimerizasyonu ve kopolimerizasyonu sonucunda elde edilen polimerlerin FTIR, SEM ve iletkenlik ölçümü gibi yöntemler kullanılarak karakterizasyonu yapılmıştır.

Son yıllarda iletken polimerlerin elektrokromik cihazlarda kullanılması çok ilgi çeken bir konu olduğu için, çalışmanın ikinci kısmı tersinir olarak uygulanan potansiyele göre iki veya daha fazla renk arasında değişim yapma özelliğine, yani iletken polimerlerin en ilginç özelliklerinden biri olan elektrokromizme

adanmıştır. Sentezlenen iletken polimerlerin özellikleri, spektroelektrokimya, kinetik ve kolorimetrik çalışmalar gibi yöntemlerle araştırılmıştır. Spektroelektrokimya deneyleri bant aralığı, maksimum absorpsiyon dalga boyu, katkılama sonucu ortaya çıkan arabant halleri ve polaron, bipolaron bantları gibi ilekten polimerlerin özelliklerini ortaya çıkarmak için yapılmıştır. Homopolimerlerin ve kopolimerlerin tepki zamanı ve optik kontrast özellikleri kinetik çalışmalarla incelenmiştir. İncelenen elekrokromik özellikler, bu malzemelerin kararlı ve kısa tepki zamanlarına sahip olduğunu ve elektromik aygıt uygulamaları için uygun olduğunu göstermiştir.

Anahtar Kelimeler: Tiyofen ve pirol türevleri, Elektrokimyasal polimeştirme, İletken polimerler, Elektrokromik özellikler, Spektroelektrokimya, Elektrokromik cihazlar

TO MY MOTHER, Fatma AK

Words can not express my gratitute.........

ACKNOWLEDGMENTS

TABLE OF CONTENTS

LIST OF FIGURES

FIGURE

xvi

LIST OF TABLES

TABLE

xviii

ABBREVIATIONS

$(SN)_x$	Poly(sulfurnitride)
ACN	Acetonitrile
BFEE	Borontrifluoride diethyletherate
CB	Conduction Band
CIE	La Commission Internationale de l'Eclairage
CP	Conducting Polymer
CV	Cyclic Voltammetry
ECD	Electrochromic Device
EDOT	3,4-Ethylenedioxythiophene
E_g	Band Gap Energy
FTIR	Fourier Transform Infrared Spectrometer
HMTA	Hexamethylene (bis-3-thiopheneacetamide)
HOMO	Highest Occupied Molecular Orbital
ITO	Indium Tin Oxide
L a b	Luminance, hue, saturation
LED	Light Emitting Diode
LUMO	Lowest Unoccupied Molecular Orbital
MBThi	N-(4-(3-thienylmethylene)-oxycarbonylphenyl) maleimide
NMR	Nuclear Magnetic Resonance
NMT	N-(2-(thiophen-3-yl)methylcarbonyloxyethyl) maleimide
OFET	Organic Field Effect Transistor
P(HMTA -co-Th)	Poly(hexamethylene (bis-3-thiopheneacetamide)-co-thiophene)
P(MBThi-co-Th)	Poly(N-(4-(3-thienylmethylene)-oxycarbonylphenyl) maleimide-co-thiophene)

P(NMT)	Poly(N-(2-(thiophen-3-yl)methylcarbonyloxyethyl) maleimide)
P(NMT-co-Th)	Poly(N-(2-(thiophen-3-yl)methylcarbonyloxyethyl) maleimide-co-thiophene)
P(TriaPy -co-Py)	Poly(2,4,6-Tris-(4-pyrrol-1-yl-phenoxy)-[1,3,5] triazine-co-pyrrole)
P(TriaPy)	Poly(2,4,6-Tris-(4-pyrrol-1-yl-phenoxy)-[1,3,5] triazine)
P(TriaTh -co-Th)	Poly(2,4,6-Tris-(thiophen-3-ylmethoxy)-[1,3,5] triazine-co-thiophene)
PAc	Polyacetylene
PAni	Polyaniline
PAT	Poly(3-alkylthiophene)
PC	Propylene carbonate
PCz	Polycarbazole
PEDOT	Poly(3,4-ethylenedioxythiophene)
PMMA	Poly(methyl methacrylate)
PPP	Poly(p-phenylene)
PPV	Poly(p-phenylene vinylene)
PPy	Polypyrrole
PTh	Polythiophene
Py	Pyrrole
SEM	Scanning Electron Microscopy
TBATFB	Tetrabutylammonium tetrafluoroborate
TEA	Triethylamine
Th	Thiophene
TriaPy	2,4,6-Tris-(4-pyrrol-1-yl-phenoxy)-[1,3,5]triazine
TriaTh	2,4,6-Tris-(thiophen-3-ylmethoxy)-[1,3,5]triazine
VB	Valance Band

CHAPTER I

INTRODUCTION

1.1 History of the Conducting Polymers

Polyaniline (PAni), known as "aniline black", is one of the oldest conductive polymers known. It was first prepared by Letheby in 1862 by anodic oxidation of aniline in sulphuric acid [1], and was used in the printing industry [2]. The first polymerization of acetylene to form polyacetylene (PAc) was reported in 1958 by Natta and coworkers [3]. Since PAc was obtained as an insoluble and infusible powder, the material received little attention at that time. The idea that conjugated polymers could be good electrical conductors has roots back to the 1960s when MacDiarmid and others discovered that poly(sulfurnitride) $(SN)_x$, a polymeric inorganic explosive [4], has a high conductivity [5]. As seen in Figures 1a and b, $(SN)_x$ chain appears to consist, besides the electrons forming the σ bonds which hold it together, of a singly-occupied π orbital on each S atom, interspersed with a π lone pair centred around each N atom. The polymer therefore, to a good approximation can be regarded as a one-dimensional chain of S atoms, with a single electron on each side. This is equivalent to a half-filled band and consequently one would predict the polymer to be metallic [6]. The interesting electrical properties of $(SN)_x$ represented a step towards conducting polymers as they are known today.
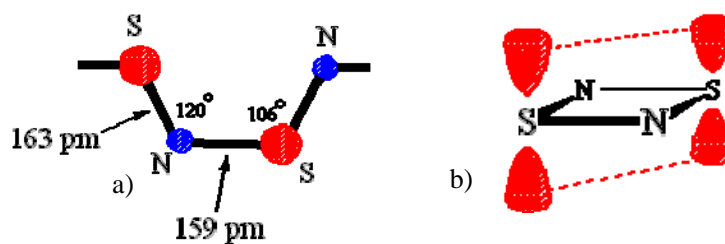
Figure 1.1 a) A section of the conducting polymer $(SN)_x$ b) Description of the bonding of S_2N_2

The modern era of conducting polymers began at the end of 1970s when the discovery that poly(acetylene) (PAc) could be synthesized to form highly conducting doped films [7]. Alan Heeger, Alan MacDiarmid, and Hideki Shirakawa were rewarded for their primary work with the 2000 Nobel Prize in Chemistry [8]. They established that polymer plastics can be made to conduct electricity if alternating single and double bonds link their carbon atoms, and electrons are either removed through oxidation or introduced through reduction. Normally the electrons in the bonds remain localized and cannot carry an electric current, but when the team "doped" the material with strong electron acceptors such as iodine, the polymer began to conduct nearly as well as a metal, with conductivity 10^{11} times higher than pure polyacetylene (PAc) [9,10].

New conducting polymer structures (Figure 1.2) have been developed over the past two decades with the hope of obtaining better properties than polyacetylene. New classes of conducting polymers include polythiophene [11] (PTh), polyfuran [12], polypyrrole [13] (PPy), poly(p-phenylene) [14] (PPP), poly(p-phenylene vinylene) [15] (PPV), polyfluorene [16], polyaniline [17] (PAn) and polycarbazole [18] (PCz). Although none have exhibited higher conductivity than PA, these polymers have been useful in designing new structures that are soluble and stable. Electron-rich heterocycle based polymers such as polythiophene and polypyrrole are very stable in the p-doped form and this has made these systems two of the most studied conducting polymers. Their stability is due to their lower polymer oxidation potentials which

follow the order of PAc>PTh>PPy. Also, these structures are more easily modified than PAc, allowing for more diversity of structures.
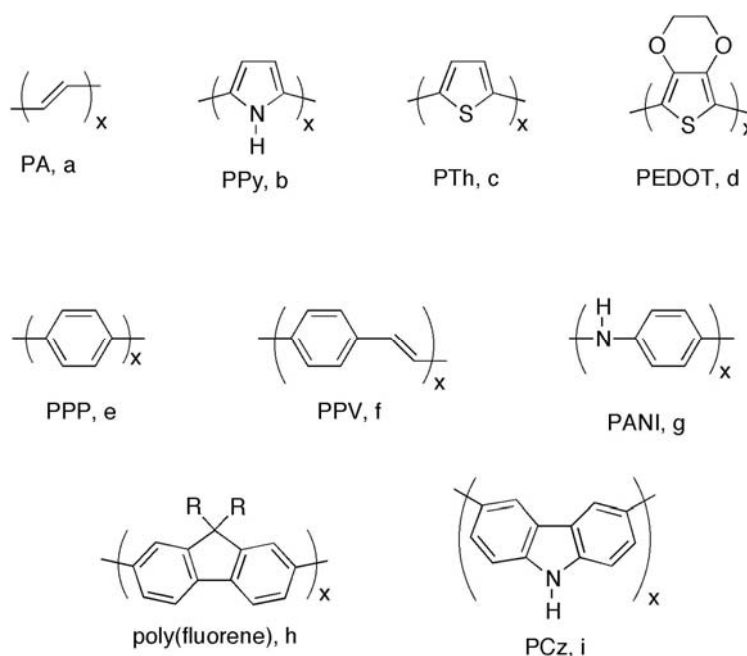
Figure 1.2 Common conjugated polymers. (a) poly(acetylene), (b) poly(pyrrole), (c)poly(thiophene), (d) poly(3,4-ethylenedioxythiophene), (e) poly(p-phenylene), (f) poly(p-phenylene vinylene), (g) poly(aniline), (h) poly(fluorene), and (i) poly(carbazole).

1.2 Extrinsically and Intrinsically Conducting Polymers

Since a conjugated polymer is a semiconductor with a finite band gap, conversion into a conductor implies introduction of charges onto the polymer chain which can be accomplished by various methods. The first method concerns the introduction of charges either by electron removal (oxidation or p-doping) or -injection (reduction or n-doping). The major part of conjugated polymers known today is built up of electron-releasing units, making them p-type semiconductors which can be doped with oxidants like I_2, $FeCl_3$ etc. The structural changes that occur in a conjugated polymer upon oxidation are

illustrated for polypyrrole (see Fig. 1.8, page10). Polythiophene oxidation [19,20] is the same as polypyrrole, the removal of one electron from the polythiophene chain produces a mobile charge in the form of a radical cation, also called a *polaron*. Further oxidation can either convert the polaron into a spinless *bipolaron*. In either case, introduction of each positive charge also means introduction of a negatively charged counterion.

The second method consists of *acid doping* of conjugated polymers having a site that can be protonated, which process introduces charges in the main chain. The best known example is polyaniline (Figure 1.3). The neutral leucoemeraldine form **2a** can be oxidized to the emeraldine base **2b** without introduction of counterions. However, the emeraldine base **2b** only becomes conductive after treatment with a sufficiently strong acid (HX) which protonates the imine nitrogens and, at the same time, introduces a counterion (X^-). The conducting emeraldine **2c** can also be represented by the mesomeric structure **2d**, in which all phenyl rings are aromatic and radical cations are present on every second nitrogen atom. This degenerate mesomerism is thought to account for a high charge-carrier mobility, and thus high conductivity, but conformational factors like the crystallinity of polyaniline films also play a crucial role. In the above two examples, introduction of charge carriers is inevitably accompanied by the introduction of counter-ions. It is defined here that extrinsically conducting polymers are π-conjugated polymers that become conductive after doping, i.e. after the introduction of charged species that are delocalized along the conjugated main chain (charge carriers), accompanied by the introduction of counter-charged species that are not delocalized along the conjugated main chain. The definition covers all π-conjugated polymers that are made conductive either by means of doping with an oxidizing or reducing agent, or by means of acid doping or selfdoping.

In contrast, intrinsically conducting polymers are conducting π-conjugated polymers which do not need additional doping and are characterized by electrically neutral conjugated systems in which some π-electron bands are only partially filled. The character of their conductivity may range from

"hopping" to metallic, depending on the degree of overlap of the π-orbitals of neighboring molecules.
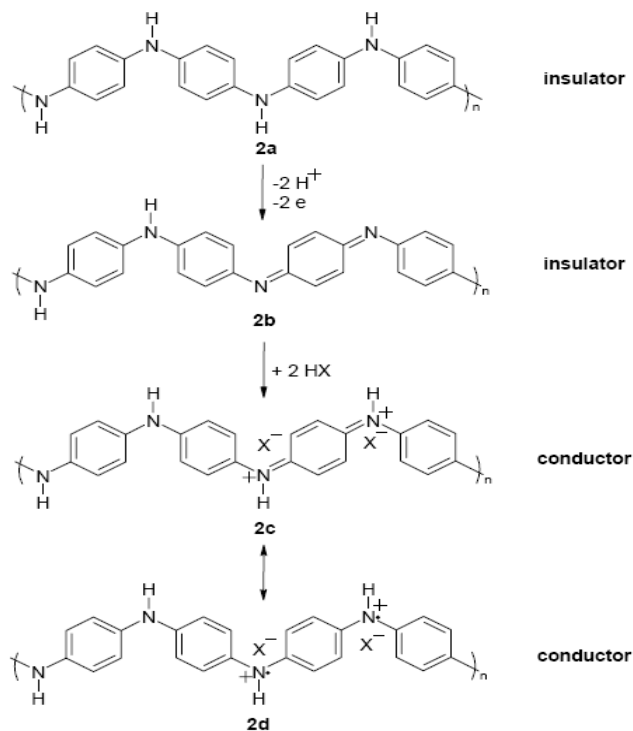
Figure 1.3. Primary forms of poly(aniline) (PANI).

1.3 Band Theory and Doping-Induced Transitions in Conjugated Polymers

The excitation and/or removal/insertion of electrons in conjugated polymers as a result of electrochemical or photochemical doping processes necessitate discussion of band theory. In its most simple form for conjugated polymers, the high extent of conjugation gives rise to two discrete energy bands, the lowest energy containing the highest occupied molecular orbital (HOMO), also known as the valence band (VB); and that containing the lowest unoccupied molecular orbital (LUMO), known as the conduction band (CB). The energy distance between these two bands is defined as the band gap (E_g), and in neutral conjugated polymers refers to the onset energy of the π-π*

transition. The Eg of conjugated polymers can be approximated from the onset of the π-π* transition in the UV-Vis spectrum. In their neutral form, conjugated polymers are semiconducting, but upon oxidation (p-doping) or reduction (n-doping), interband transitions form between the VP and CB, lowering the effective band gap, resulting in the formation of charge carriers along the polymer backbone.

The band structure of a conjugated polymer originates from the interaction of the orbitals of the repeating units throughout the chain.This is exemplified in Figure 1.4 where the calculated (frontier) energy levels of oligothiophenes with n = 1 - 4 and of polythiophene are shown as a function of oligomer length [21]. Addition of every new thiophene unit causes hybridization of the energy levels yielding more and more levels until a point is reached at which there are bands rather than discrete levels.
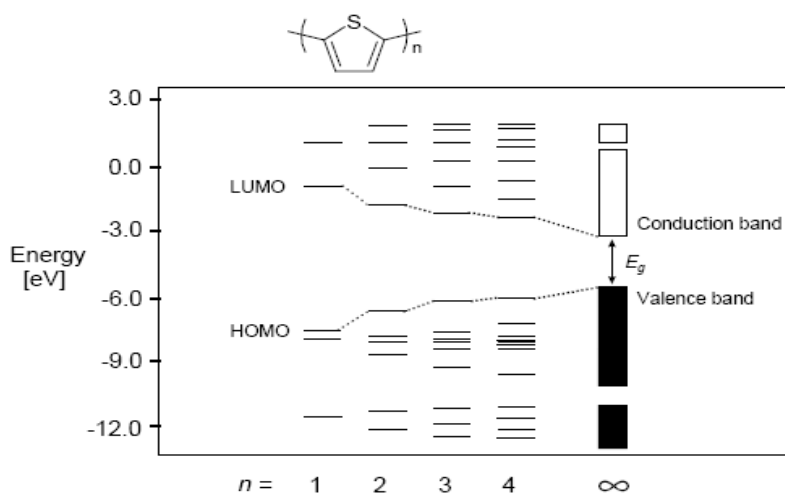
Figure 1.4. Calculated (frontier) energy levels of oligothiophenes with n = 1-4 and of polythiophene, where Eg =band gap; adapted from reference [21]

Polymerization of 3-substituted thiophenes can lead to three different type of coupling of thiophene ring along the polymer main chain, head to tail (HT), head to head (HH) and tail to tail (TT). This leads to a mixture of four chemical distinct triad regioisomers (Figure 1.5).

6
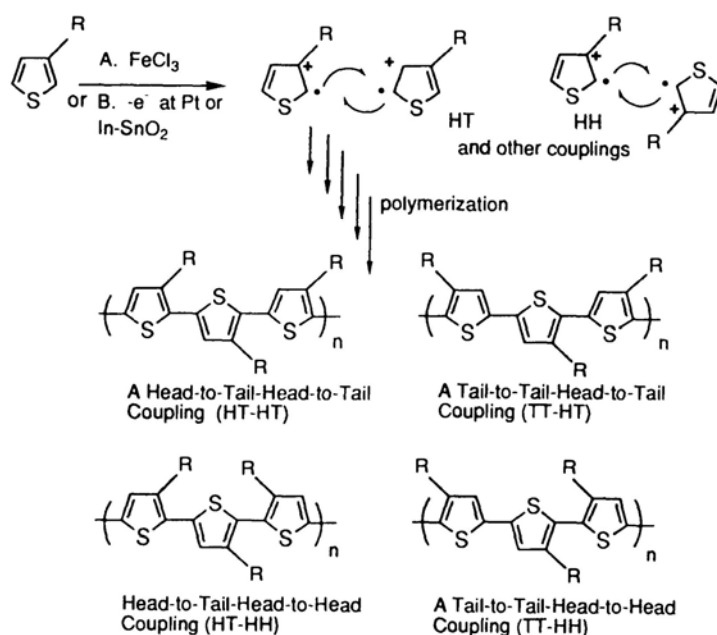
Figure 1.5 Classical synthetic methods lead to a number of regiochemical isomers.

The presence of HH coupling in irregular polythiophenes causes an increased twist of the thiophene units (due to steric repulsion) with loss of conjugation. These results in increased band gap (blue shift in absorption) decreased conductivity [22]. On the other hand, regioregular, head-to-tail poly(3-substituted) thiophene can easily access a low energy planar conformation, leading to highly conjugated polymer (Figure 1.6)

Initial studies of band theory as applied to conjugated polymers focused on poly(acetylene). PAc is unique in that both resonance forms of the neutral polymer are degenerate, leading to the formation of solitons on oxidation. The localized electronic state associated with the soliton is a nonbonding state at an energy lying at the middle of the π-π^* gap, between the bonding and antibonding levels of the perfect chain. The soliton is a defect both topological and mobile because of the translational symmetry of the chain [24]. Soliton model was first proposed for degenerated conducting polymers (PAc in particular) and it was noted for its extremely one dimensional character, each soliton being confined to one polymer chain (Figure 1.7). Thus, there was no

conduction via interchain hopping. Furthermore, solitons are very susceptible to disorder, and any defect such as impurities, twists, chain ends or crosslinks will localize them [25,26].
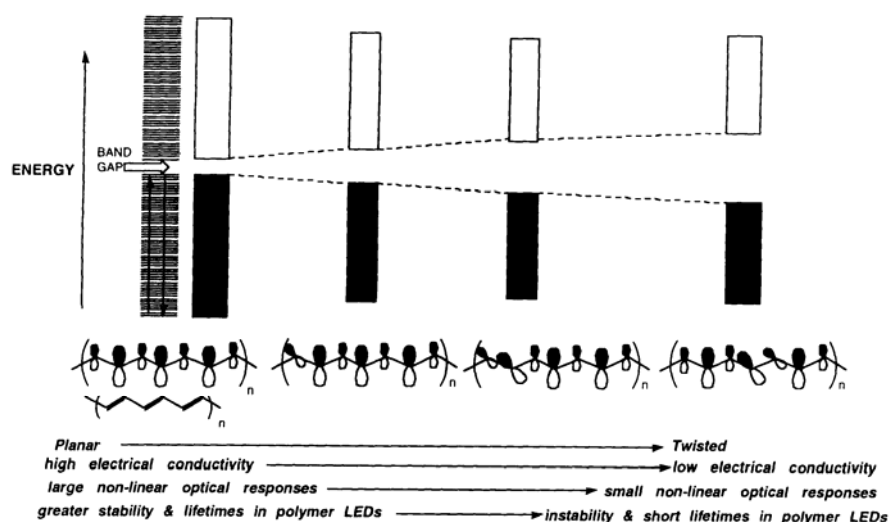
Figure 1.6 Bands gaps and electrical and optical properties vary with planarity. (Adopted from reference [23])
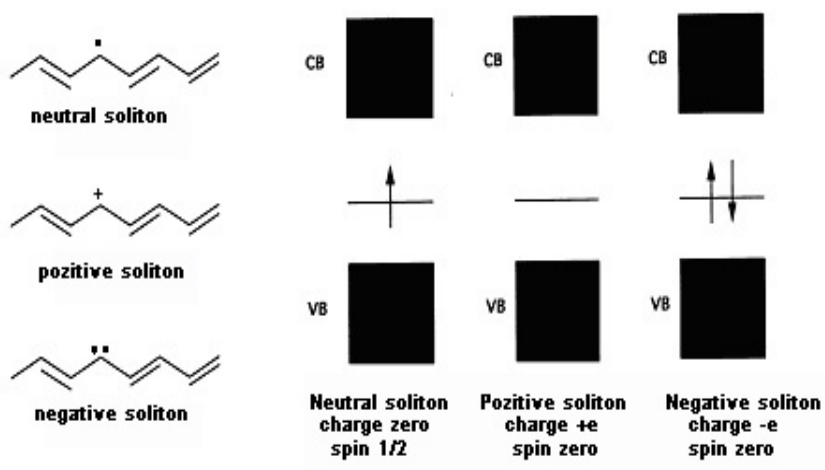
Figure 1.7 Schematic representations of solitons

8

A different scenario exists for aromatic polymers because of their nondegenerate ground states. As an example, the oxidative doping of PPy is shown in Figure 1.8(a). Application of an oxidizing potential destabilizes the VB, raising the energy of the orbital to a region between the VB and CB. Removal of an electron from the estabilized orbital results in a radical cation or polaron. Further oxidation results in the formation of dications or bipolarons, dispersed over a number of rings. These radical cations and dications are the charge carriers responsible for conductivity in conjugated polymers. Because of the nondegenerate energy transitions of conjugated polymers (excluding PA), structural changes result and are based on the most widely accepted mechanism as shown for PPy in Figure 1.8(b) [27]. Electron paramagnetic resonance (EPR) spectroscopy results support this mechanism, showing that neutral and heavily doped polymers possess no unpaired electrons, while lightly doped polymers do display an EPR signal [28,29]. The theory presented above is based on the seminal work of Fesser, Bishop, and Campbell, whose FBC theory is one of the most widely cited by scientists attempting to interpret optical transitions in their conjugated polymers [30].

Another increasingly accepted model for oxidative doping in conjugated polymers is the formation of p-dimers instead of bipolarons. In the p-dimer theory, polarons from separate polymer chains interact, forming a diamagnetic species with no EPR signal [31-33]. Apperloo et al. performed studies on thiophene-based oligomers building a persuasive case for p-dimer formation [34,35]. However, it is not yet clear which mode of oxidative doping is responsible for the observed properties in conjugated polymers, leaving the door open for continued study. Through both of these theories, organic chemists have been able to interpret and modify the band structure of conjugated polymers to tune their optical and electrical properties. Much of the work performed on these materials was inspired by the color changes observed in inorganic and organic small molecules. The ability to control the electronics and structure of polymers set them apart from the traditional materials and opened up a huge area of research that has seen tremendous success over the past several decades.

9
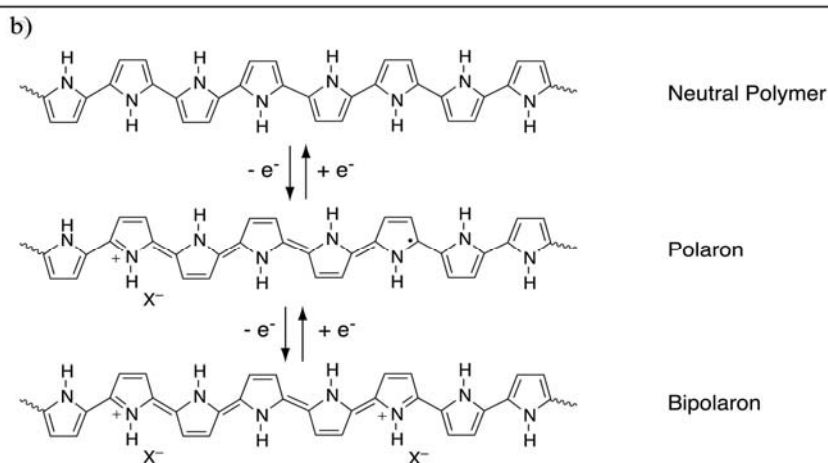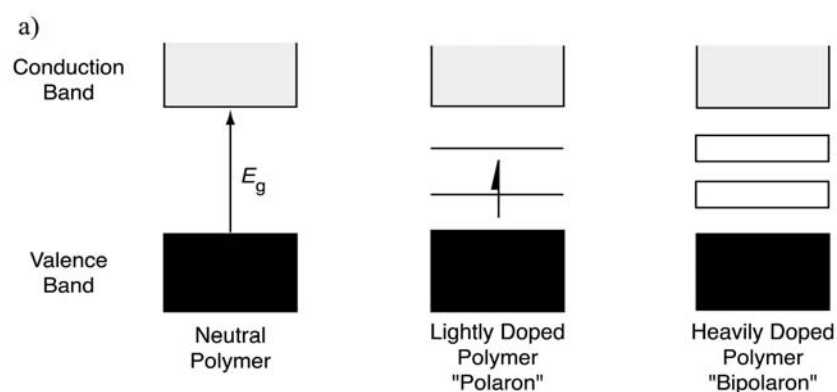
Figure 1.8 Band theory and doping-induced structural transitions of polypyrrole.(a) Band theory of conjugated polymers. (b) Structural changes associated with polaron and bipolaron formation as a result of oxidative doping in polypyrrole.

1.4 Electrochemical Synthesis of Conducting Polymers

Conducting polymers can be prepared by using chemical and electrochemical methods. Electrochemical formation of conducting polymers such as PT, PPy and PEDOT proceeds via oxidation of the neutral monomer at the anode surface [36-38]. This oxidation step requires 2 electrons per molecule, the excess of charge passed during synthesis being necessary for oxidation of the resulting polymer film.

Figure 1.9a represents the mechanism proposed for the polymerization of heterocycles, where X can be S, O or N-R. The first step consists oxidation of

the monomer that yields the radical cation. Monomer diffusion towards the anode is the rate-determining step, being much slower than the electron-transfer reaction. Consequently, a high concentration of radical cations is constantly maintained near the anode. The further fate of these highly reactive species depends on the experimental conditions including electrolyte composition, temperature, applied potential, nature and morphology of deposition support, etc. In favorable cases, the next step is a dimerization reaction (coupling of two radical cations) that produces a dihydro dication dimer. Further, this species loses two electrons and rearomatizes to form the neutral dimer. Due to extended conjugation over two rings, the dimer has a lower oxidation potential than the monomer itself, and therefore it gets oxidized easily to form the radical cation. Stepwise chain growth proceeds via association of radical ions or, less likely, through coupling of a radical cation with a neutral monomer. As chain length increases, resulting oligomers become insoluble in the electrolytic medium and precipitate onto the anode.

First generation heterocycles such as thiophene and pyrrole have two possible reaction pathways, as shown in Figure 1.9b. Polymerization proceeding exclusively through α−α couplings affords polymers with a linear backbone and enhanced electrical properties. The occurrence of a α−β linkage in a given chain modifies its electronic distribution and could promote the formation of branching in energetically favorable sites. Furthermore, the presence of these linkage defects generates twists in adjacent chains, and thus, modifies their electronic distribution promoting the propagation of more defects in the resulting material. The relative reactivity of the α and β positions is about 95/5 for thiophene and decreases as the polymerization proceeds, leading to an increase of the number of undesired couplings and consequently to a decrease in the polymer effective mean conjugation length [39]. This is consistent with the considerable increase in the content of disorder as well as the decrease in conductivity as the polymerization proceeds. Therefore, limitation of the polymer growth to very thin films allows for the synthesis of a highly compact material with fewer defects and enhanced electrical properties [40-42].
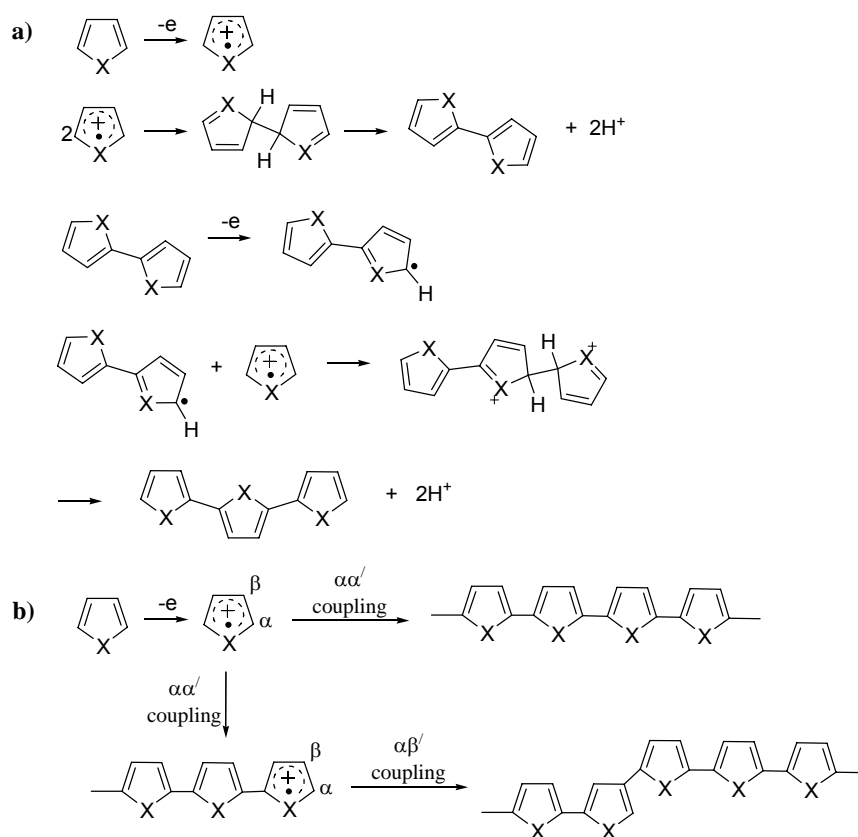
Figure 1.9 Electropolymerization mechanism. a) Polymerization of heterocycles (X = S, O, NH), b) Competitive reaction pathways in unsubstituted poly(heterocycles)

Most conductive polythiophene films prepared by electrochemical polymerization of thiophene in an organic solvent, in which the electroxidation of thiophene is achived at potentials above 1.6 V vs SCE. It is reported that at potentials higher than 1.4 V polythiophene degrades due to side reactions [43]. This phenomenon is call as polythiophene paradox [44] which signifies the presence of competition between electrodeposition and degradation, especially at high potentials or very low monomer concentrations [45]. It was concluded that, in order to obtain high quality electrochemically synthesized polythiophene, the oxidation potential of thiophene must be lowered.

Undesired α−β and β−β couplings can be eliminated through monomer substitution at β positions. Substitution of thiophene by electron donating

groups leads to a decrease in monomer oxidation potential, allowing for electrosynthesis under milder conditions and thus, decreasing the possibility of obtaining overoxidized material. For example, in 3,4-ethylenedioxythiophene (EDOT), both β positions are substituted and the polymerization proceeds exclusively through the desired α-α couplings. Judicious selection of the substituent affords materials that are soluble, easily polymerizable and possess an enhanced degree of order.

1.4.1 Electrochemical techniques used in the synthesis of the conducting polymers

1.4.1.1 Constant Current Electrolysis (Galvanostatic)

In constant current electrolysis (CCE), the current is kept constant throughout the electrolysis while the potential is allowed to alter in a cell containing working and counter electrodes. It is simple in application but it has some disadvantages. The variation of the potential may cause all possible redox process and the nature of the generated species may be unknown because of the side reactions. In order to overcome these difficulties, electrolyte or substrate can be added at the same rate as that of monomer consumption.

1.4.1.2 Constant Potential Electrolysis (Potentiostatic)

This method is carried out in a three electrode cell, which ensures effective potential control and maximize the reproducibility of the polymerization process. The potential of the working electrode with respect to a reference electrode is adjusted to a desired value and kept constant by a potentiostat. This potential may be called the polymerization potential (E_{pot}) and it is determined by means of cyclic voltammetry. Since the potential is constant during the electrolysis, unwanted electroactive species are eliminated and the initiation proceeds only through monomer.

1.4.1.3 Cyclic Voltammetry

Cyclic voltammetry is one of the most useful methods, which provides a great deal of useful information about the electrochemical behavior of electroactive species. In this method, the potential of the working electrode is scanned in the anodic and cathodic directions and the current flow as a function of this potential is measured. A voltammogram provides us to understand the electroactivity and redox potential of a material, mechanism of the electrochemical reactions, reversibility of electron transfer, whether the reaction products are further reduced or oxidized and the growth rate of the conducting polymers.

1.4.2 Effect of Synthesis Conditions on Electrochemical Polymerization

The nature of the process occurring and final properties of the electrogenerated polymers are affected by many parameters such as the nature and shape of the electrodes, solvent, electrolyte, temperature, synthesis potential, cell geometry and monomer concentration.

Since the polymerization proceeds via oxidation and reduction reactions, it is necessary that the electrode should not be oxidized concurrently with the aromatic monomer [46]. For this reason, inert electrodes, such as Pt, Au and ITO are mostly used when preparing conductive films. Saturated calomel electrode (SCE), Ag/Ag^+ and $Ag/AgCl$ electrodes can be used as the reference electrodes [47].

Solvent should be capable of dissolving monomer and counterion at appropriate concentrations. In addition, it should present a high dielectric constant to ensure the ionic conductivity of the electrolytic medium and a good electrochemical resistance against decomposition at potentials required to oxidize the monomer. The solvents with poor nucleophilic character should be used since more nucleophilic solvents are likely to attack the free radical intermediates. Therefore, aprotic solvents such as acetonitrile may be used during electropolymerization.

The requirements in selecting the supporting electrolyte are basically; the solubility of the salt, its degree of dissociation and the reactivity of both the anion and the cation [48]. In addition to these, the counterion should be stable both chemically and electrochemically; otherwise, breakdown products can interfere in the polymerization process [49].

Temperature is the other parameter that should be taken into consideration during electropolymerization. It has a substantial influence on the kinetics of polymerization as well as on the conductivity, redox properties and mechanical characteristics of the films [50]. At high temperatures, lower conducting films are produced as a result of the side reactions such as solvent discharge and nucleophilic attacks on polymeric radicals [51] .

1.5 Application of conducting polymers

There are two main groups of applications for conducting polymers. The first group utilizes their conductivity as its main property whereas the second group utilizes their electroactivity. The extended π-systems of conjugated polymer are highly susceptible to chemical or electrochemical oxidation or reduction. These alter the electrical and optical properties of the polymer, and by controlling this oxidation and reduction, it is possible to precisely control these properties. Since these reactions are often reversible, it is possible to systematically control the electrical and optical properties with a great deal of precision. It is even possible to switch from a conducting state to an insulating state. The two groups of applications are shown in Figure 1.10.
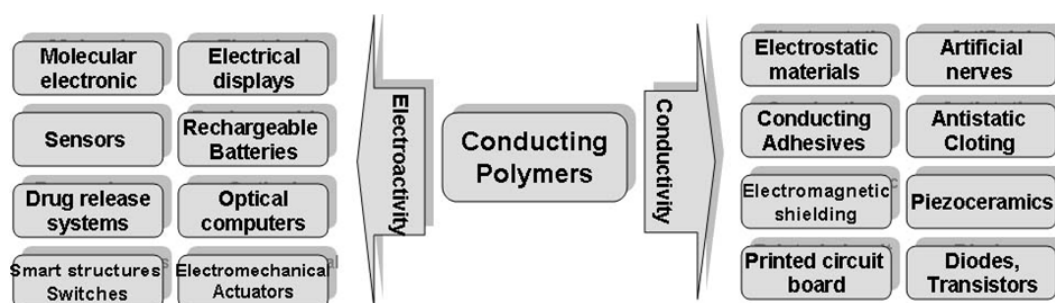
Figure 1.10 Application of Conducting Polymers

1.5.1 Applications that utilizes conductivity

These applications make use of the polymer's conductivity only. The polymers are used due to either their light weight, biological compatibility for ease of manufacturing or cost.

By coating an insulator with a very thin layer of conducting polymer, it is possible to prevent the buildup of static electricity. This is particularly important where such a discharge is undesirable. Such a discharge can be dangerous in an environment with flammable gasses and liquids and also in the explosives industry. In the computer industry the sudden discharge of static electricity can damage microcircuits. This has become particularly acute in recent years with the development of modern integrated circuits. To increase speed and reduce power consumption, junctions and connecting lines are finer and closer. The resulting integrated circuits are more sensitive and can be easily damaged by static discharge at a very low voltage. By modifying the thermoplastic used by adding a conducting plastic into the resin results in a product that can be used for the protection against electrostatic discharge [52].

By placing monomer between two conducting surfaces and allowing it to polymerize it is possible to stick them together. This is a conductive adhesive and is used to stick conducting objects together and allow an electric current to pass through them.

Many electrical devices, particularly computers, generate electromagnetic radiation, often radio and microwave frequencies. This can cause malfunctions in nearby electrical devices. The plastic case used in many of these devices are transparent to such radiation. By coating the inside of the plastic case with a conductive surface, this radiation can be absorbed. This can best be achieved by using conducting plastics. They are cheap, easy to apply and can be used with a wide range of resins. The final finish generally has good adhesion, gives a good coating, thermally expands approximately the same as the polymer it is coating, needs just one step and gives a good thickness [53].

Many electrical appliances use printed circuit boards. These are copper coated epoxy-resins. The copper is selectively etched to produce conducting lines used to connect various devices. These devices are placed in holes cut

into the resin. In order to get a good connection the holes need to be lined with a conductor. Copper has been used, however the coating method, electroless copper plating, has several problems. It is an expensive multistage process, the copper plating is not very selective and the adhesion is generally poor. This process is being replaced by the polymerization of a conducting plastic. If the board is etched with potassium permanganate solution, a thin layer of manganese dioxide is produced only on the surface of the resin. This will then initiate polymerization of a suitable monomer to produce a layer of conducting polymer. This is much cheaper, easy and quick to do, is very selective and has good adhesion [54].

Due to the biocompatability of some conducting polymers they may be used to transport small electrical signals through the body, i.e. act as artificial nerves. Perhaps modifications to the brain might eventually be contemplated [55].

Weight is a premium importance for aircraft and spacecraft. The use of polymers with a density of about 1 g cm^{-3} rather than 10 g cm^{-3} for metals is attractive. Moreover, the power ratio of the internal combustion engine is about 676.6 watts per kilogram. This compares to 33.8 watts per kilogramme for a battery-electric motor combination. A drop in magnitude of weight could give similar ratios to the internal combustion engine [55]. Modern planes are often made with light weight composites. This makes them vulnerable to damage from lightning bolts. By coating aircraft with a conducting polymer the electricity can be directed away from the vulnerable internals of the aircraft.

1.5.2 Applications that utilizes electroactivity

Molecular electronics are electronic structures assembled atom by atom. One proposal for this method involves conducting polymers. A possible example is a modified polyacetylene with an electron accepting group at one end and a withdrawing group at the other. A short section of the chain is saturated in order to decouple the functional groups. This section is known as a "spacer" or a "modulable barrier". This can be used to create a logic device (Figure 1.11). There are two inputs, one light pulse which excites one end and

another which excites the modulable barrier. There is one output, a light pulse to see if the other end has become excited. To use this there must be a great deal of redundancy to compensate for switching "errors" [56].

Figure 1.11 Insertion of a "spacer" to decouple the functionalized chain ends

Depending on the conducting polymer chosen, the doped and undoped states can be either colorless or intensely colored. However, the color of the doped state is greatly redshifted from that of the undoped state. Because conducting polymers are intensely colored, only a very thin layer is required for devices with a high contrast and large viewing angle. Unlike liquid crystal displays, the image formed by redox of a conducting polymer can have a high stability even in the absence of an applied field. The switching time achieved with such systems has been as low as 100 μs but a time of about 2 ms is more common. The cycle lifetime is generally about 10^6 cycles. Experiments are being done to try to increase cycle lifetime to above 10^7 cycles [57].

The chemical properties of conducting polymers make them very useful for use in sensors. This utilizes the ability of such materials to change their electrical properties during reaction with various redox agents (dopants) or via their instability to moisture and heat. An example of this is the development of gas sensors. It has been shown that polypyrrole behaves as a quasi 'p' type material. Its resistance increases in the presence of a reducing gas such as ammonia, and decreases in the presence of an oxidizing gas such as nitrogen dioxide. The gases cause a change in the near surface charge carrier (here electron holes) density [58]. Another type of sensor developed is a biosensor. This utilizes the ability of triiodide to oxidize polyacetylene as a means to measure glucose concentration. Glucose is oxidized with oxygen with the help

of glucose oxidase. This produces hydrogen peroxide which oxidizes iodide ions to form triiodide ions. Hence, conductivity is proportional to the peroxide concentration which is proportional to the glucose concentration [59].

Probably the most publicized and promising current applications are light weight rechargeable batteries. Some prototype cells are comparable to, or better than nickel-cadmium cells now on the market. The polymer battery, such as a polypyrrole-lithium cell operates by the oxidation and reduction of the polymer backbone. During charging the polymer oxidizes anions in the electrolyte enter the porous polymer to balance the charge created Simultaneously, lithium ions in electrolyte are electrodeposited at the lithium surface. During discharging electrons are removed from the lithium, causing lithium ions to reenter the electrolyte and to pass through the load and into the oxidized polymer. The positive sites on the polymer are reduced, releasing the charge-balancing anions back to the electrolyte. This process can be repeated about as often as a typical secondary battery cell [60].

Conducting polymers can be used to convert electrical energy into mechanical energy. This utilizes large changes in size undergone during the doping and dedoping of many conducting polymers. This can be as large as 10%. Electrochemical actuators can function by using changes in a dimension of a conducting polymer, changes in the relative dimensions of a conducting polymer and a counter electrode and changes in total volume of a conducting polymer electrode, electrolyte and counter electrode. The method of doping and dedoping is very similar as that used in rechargeable batteries discussed above. The applications of this include microtweezers, microvalves, micropositioners for microscopic optical elements, and actuators for micromechanical sorting (such as the sorting of biological cells) [61].

One of the most futuristic applications for conducting polymers are "intelligent" structures. An *intelligent material* is capable of recognizing appropriate environmental stimuli, processing the information arising from the stimuli and responding to it in an appropriate manner and time frame. A further desirable feature is that the material should ideally be self-powered, having energy conversion and storage functions. Conducting electroactive polymers

have emerged as one of the champions in intelligent materials research. CEPs have all the desirable properties:

• They are readily engineered at the molecular level to recognize specific stimuli.
• Because they are conductive, they facilitate transport of electrical information.
• They are capable of localized processing as well as actuation of response mechanisms.

Recent research has suggested that conducting polymers are set to emerge in devices used to store energy in the form of super capacitors. The intense interest in these applications is driven by developments in electric-powered vehicles and alternative energy in general. Supercapacitors are those devices able to store a charge of 50 F/g (or 30 F/cm^3) of the device, or higher. This high storage capacity and ability to deliver high power density can be utilized in electronic equipment and electric vehicles [62]. The fast discharge rate obtainable from capacitors means that high power can be delivered for short periods. Conducting polymers are being researched for "redox supercapacitors." In these devices, the redox chemistry of the polymer is used in the same way as described above for batteries. However, the design of the device is such that the conducting polymer is applied as a thin coating on a high-surface-area substrate. This design allows for very rapid charging and discharging of the polymer so that capacitor-like performance is obtained. All solid-state redox supercapacitors using PTh and PPy with a solid polymer electrolyte have been reported [63] as having storage capacities of 18 F/g.

Polymer photovoltaics using conducting polymers are also being developed. In a typical arrangement, the photosensitive polymer (such as polyphenylene vinylene (PPV) and its derivatives) is sandwiched between two electrodes (Figure 1.12). One is a transparent material, typically indium tin oxide (ITO)-coated glass, and the other electrode is a low-work-function metal such as aluminum or calcium. It is necessary the put hole transport layer (HTL) and electron transport layer (ETL) in this sandwich confugration. Light is

absorbed by the polymer, creating excitons (electron-hole pairs) that dissociate at an appropriate interface to give charge separation and, hence, current flow. Efficiencies of polymer-based photovoltaics are very low compared with silicon semiconductor materials. However, polymer photovoltaics have the potential to be manufactured very cheaply and can be applied to very large areas, such as roof tops and exterior walls of buildings. The large surface areas can compensate for the lower efficiencies to provide an adequate supply of electricity. Of course, efficiencies are being improved by chemical modification of the polymer and better design of the photovoltaic device. One approach to polymer modification is to attach "light harvesting" groups to the polymer chains so as to increase the amount of light absorbed. Once again, the fabrication of the device is critical in determining device performance. It has been shown that formation of interpenetrating networks of donor- and acceptor-type polymers results in marked improvements in photovoltaic efficiency, as reviewed recently [64].
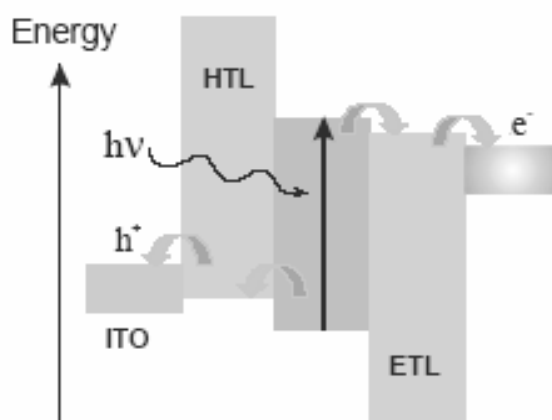
Figure 1.12 Device design for polymer a photovoltaic device

The process used for the photovoltaic device can be reversed to produce a light emitting diode (LED). When an electric field is applied to the two electrodes shown in Figure 1.13, electrons are injected into the conduction

band of the polymer layer from the cathode (usually a low-work-function metal such as aluminum or calcium). At the ITO anode, electrons are removed from the valence band of the polymer to produce vacancies, or holes. The free electrons and holes move in opposite directions under the influence of the electric field and, when they combine, a photon of light is emitted. The color of the light emitted depends on the band gap between the valence and conduction bands in the polymer. Appropriate derivation of PPV polymers has produced PLEDs that emit the three colors red, blue and green.
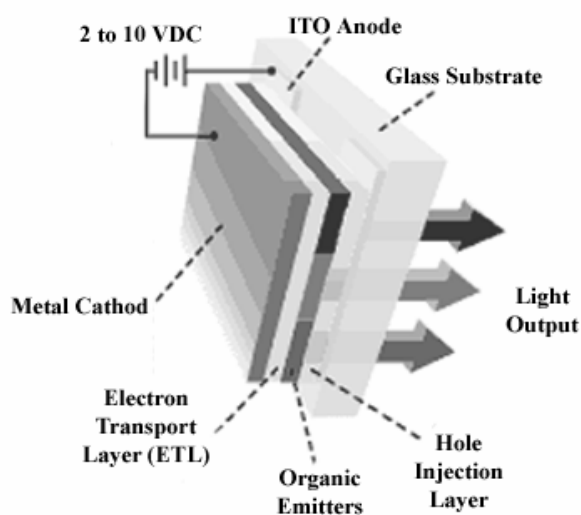
Figure 1.13 Device design for a polymer light emitting diode

1.6 Electrochromism

Electrochromism is the reversible and visible change in transmittance and/or reflectance that is associated with an electrochemically induced oxidation–reduction reaction. It results from the generation of different visible region electronic absorption bands upon switching between redox states. The color change is commonly between a transparent ("bleached") state and a colored state, or between two colored states. The electrochromic materials

may exhibit several colors and termed as polyelectrochromic and the process is called to be multicolor electrochromism. [65].

Basically three classes of electrochromic materials are known; metal oxide films, molecular dyes and conducting polymers. A typical and most widely studied example of metal oxides is the tungsten trioxide (WO_3) system. Tungsten oxide has a nearly cubic structure which may be simply described as an "empty-perovskite" type formed by WO_6 octahedral that share corners. The empty space inside the cubes is considerable and this provides the availability of a large number of interstitial sites where the guest ions can be inserted. Tungsten trioxide, with all tungsten sites as oxidation state W_{VI}, is a transparent thin film. On electrochemical reduction, W_V sites are generated to give the electrochromic (blue coloration to the film) effect. Although, there is still controversy about the detailed coloration mechanism, it is generally accepted that the injection and extraction of electrons and metal cations (Li^+, H^+, etc.) play an important role [66]. WO_3 is a cathodically ion insertion material. The blue coloration in the thin film of WO_3 can be erased by the electrochemical oxidation. The generalized equation can be written as below equation

$$WO_3 \quad + \quad xM+ \quad + xe^- \rightarrow \quad M_xWO_3$$
$$\text{(transparent)} \qquad\qquad \text{(blue)}$$
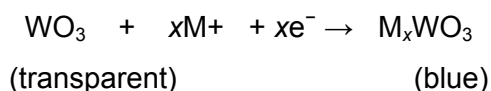
Diquaternization of 4,4'-bipyridyl produces 1,1'-disubstituted-4,4'-bipyridilium salts, commonly known as "viologens" [67] Of the three common viologen redox states (Fig. 1.14), the dication is the most stable and is colorless. Reductive electron transfer to viologen dications forms radical cations. Generally the viologen radical cations are intensely colored, with high molar absorption coefficients, owing to optical charge transfer between the (formally) +1 and zero valent nitrogens. A suitable choice of nitrogen substituents in viologens to attain the appropriate molecular orbital energy levels can, in principle, allow color choice of the radical cation.
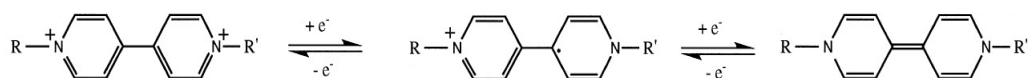
Figure 1.14 The three common viologen redox states, dication, radical cation, neutral species from left to right respectively.

1.6.1 Electrochromism in Conducting Polymers

Electrochromism can be exploited in a series of optical devices with potential use in various applications, such as in information display and storage, in the automotive industry (as rear-view mirrors and visors), and in architecture (as smart windows) to control luminosity and save energy thought the control of sunlight transmission [68]. Among organic molecules, conducting polymers have attached significant interest in the field of electrochromism, since they offer additional advantages, such as, low processing cost, enhanced mechanical properties, no dependence with angle of vision, good UV stability high coloration efficiency, fast switching ability and fine-tuning of the band gap through the modification of polymer's chemical structure. By adjusting the electronic character of the π system along the neutral polymer backbone, the π-π^* transition can be adjusted across the electromagnetic spectrum from the UV, through the visible and into the near-infrared [69].

The redox switching of conjugated polymers is accompanied by changes in electronic transitions. Figure 1.15 shows the expected transitions in a conjugated polymer [70]. In the neutral state the polymer exhibits single broad transition from the valence band to the conduction band. The energy difference between these two levels is the band gap (Eg), and it is measured as the onset of the π to π^* absorption in the neutral state of the polymer. Upon oxidation, removal of an electron from the valance band, there is the formation of polaron. This results in state with an unpaired electron whose energy state is higher than the valance band. Accordingly, there occurs the lowering of the corresponding antibonding level in the conduction band; leading to formation of new two intragap states. This should lead to possible four new transitions.

24

Figures 1.15, a, b, c, d and e, f show possible electronic transitions in polaronic and bipolaronic states.
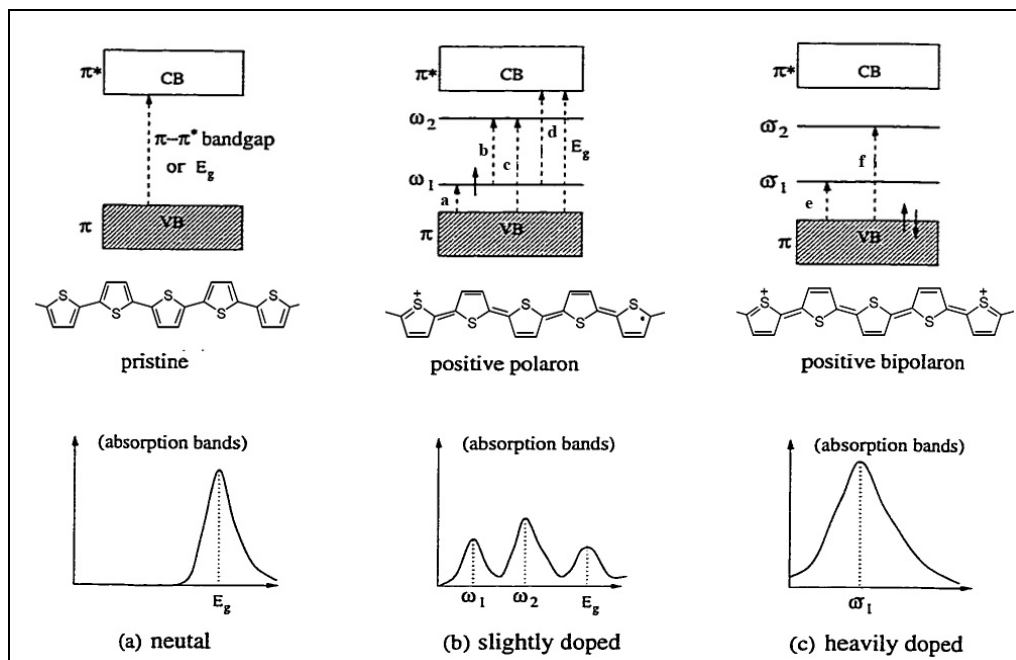
Figure 1.15 Polaron and bipolaron band diagrams in non-degenerate ground state polymers: (a) neutral, (b) slightly doped and (c) heavily doped polymer

Among the conducting polymers polypyrrole is the one of the first to be investigated both in terms of electropolymerization mechanism and optical properties. Doped (oxidized) polypyrrole film is blue-violet (λ_{max} = 670 nm). Electrochemical reduction yields the yellow-green (λ_{max} = 420 nm) "undoped" form. Removal of all dopant anions from polypyrrole yields a pale-yellow film. However, complete dedoping is only achieved if the PPy films are extremely thin. This means that thick films of polypyrrole (this is necessary to achieve high optical contrast) can not be used in device construction. This material is also highly susceptible to degradation of the film on repetitive color switching.

Color changes involve the movement of counter ions into and out of the matrix. The charged species enters the polymer matrix and migrates slowly

through the film. The speed of the color change dependents on the speed at which the dopant ions can migrate in and out of the polymer matrix. As the response time is dependent on the movement of charge compensating counter ions, open polymer morphology often results in a reduced response time [71]. The ideal electrochromic polymer should have a high contrast between its extreme states, having short switching time. Stability and maintenance of color after the current has been switched off are also among the expected features to be fulfilled.

1.6.2 Factors Affecting the Color of a Conducting Polymer

In its neutral state, the color of the polymer dependent on the energy gap between the valence and conduction bands. The energy gap between bipolaron band and conduction band determines the color in oxidized state. These are all dependent on the conjugation of the polymer, the electrochemical nature of side groups and their effects on the polymer backbone. Energy related to the bond alternation ($E^{\Delta r}$), the mean deviation from planarity (E^{θ}), the aromatic resonance energy (E^{Res}), the inductive and mesomeric electronic effects of substituents (E^{Sub}) and interchain interactions (E^{Int}) (Figure 1.16) [72].

$$E_g = E^{\Delta r} + E^{\theta} + E^{Res} + E^{Sub} + E^{int}$$
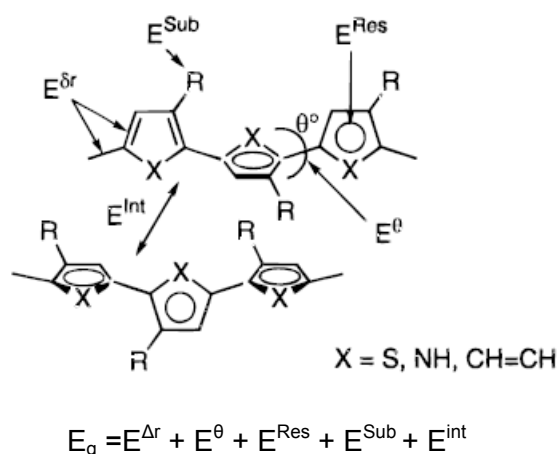
Figure 1.16 Schematic representation of parameters that play a determining role on E_g [72]

Bond alternation is defined as the maximum difference between the length of a C-C bond inclined relative to the chain axis and a C-C bond parallel to the chain axis [73]. Poly(aromatics) such as polythiophene have non degenerate ground state, namely aromatic and quinoid which are energetically not equivalent. Up to a certain extent, the band gap is known to decrease as the contribution of the aromatic geometry decreases or the quinoid geometry increased. The classical example of aromaticity control in conjugated polyheterocycles is polyisothianaphthene, a polythiophene with a benzene ring fused at the 3- and 4-positions along the polymer backbone [74].

The existence of single bonds between the aromatic cycles causes interannular rotations in conjugated polymers. The overlap of the orbitals varies with this twist angle, which causes the departure from co-planarity. The decline in the extent of overlap results in an increase of E_g by a quantity of E^Q. Introduction of flexible side chains cause steric interactions with sulphur groups of neighboring monomeric units and with each other which increases the rotational distortions in polythiophenes [75]. As mentioned in Section 1.3, regioregular poly(3-alkylthiophene)s has shown much lower band gaps and better electrochemical properties due to the ordering of the polymer films. Especially, head-to-head regiochemical defects are found to cause large twist around the bonds, leading to lowering of π electron configuration.

Aromaticity in poly(aromatics) results in a competition between π-electron confinement within the rings and delocalization along the chain. It was shown that the band gap of conjugated polymer generally decreases with decrease in the resonance energy per electron [74].

The introduction of electron-donating substituents onto a conjugated chain is a commonly used approach to decrease the polymer's oxidation potential by raising the energy of the valence band electrons ("HOMO" of the conjugated chain) and thereby band gap decreases by E^{Sub}. Electron releasing or withdrawing substituents are known to increase the HOMO and lower the LUMO respectively. Among the electrochromic materials conducting polymers, polythiophene derivatives, gained special interest owing to their facile switching

properties, processability, ease of color tuneability and their comparatively low cost [76]. Polythiophene thin films are blue (λ_{max}=~800 nm) in their doped (oxidized) state and red (λ_{max}=490 nm) in their `"undoped" form. Tuning of color states is possible by suitable choice of thiophene monomer, and this represents a major advantage of using conducting polymers for electrochromic applications.

In principle, di-substitution at the β positions should provide the synthetic basis to perfectly stereoregular polymers since di-substitution eliminates the possibility of β coupling and reduces the likelihood of cross-linking. However, this approach is severely limited by the steric interactions between substituents, which lead to a decrease in polymer conjugation length. In fact, poly(3,4-dialkylthiophenes) have higher oxidation potentials, higher optical band gaps, and lower conductivities than poly(3- alkylthiophenes).This problem was solved by fusing the ring onto the heterocycle, effectively pinning the substituents back from the main chain, like in the case of poly(3,4-ethylenedioxythiophene). Cyclization between the 3 and 4 positions relieves steric hindrance in thiophenes.

In the literature there are series of studies that acknowledge the combination of heterocycles, phenylenes and/ or vinylenes in extended conjugation monomers. Several polymers containing both EDOT and arylene moieties are synthesized. Indeed a series of electron rich, low oxidation potential bis(EDOT) arylenes, including benzene [77] and carbazole [78], has been reported. Also use of vinylene group in similar approach resulted polymers with even lower band gap [78]. These are basically donor-acceptor or so called push-pull substituted polymers. By this approach both electron donating and withdrawing groups are combined in a 1:1 ratio alternating across the polymer backbone. The resultant polymer has the valence band of the donor and the conduction band of the acceptor.

1.6.3 Electrochromic Devices

In the recent years, a lot of attention is been paid in understanding the physical and chemical properties of various electrochromic materials and

28

particularly on CPs, not only from basic research point of view but also from the commercial view [65]. It has brought various electrochromic materials and devices actually in the market also, such as, in automobile sector rear view mirrors and several others like sunroofs and visors are under prototype production. Widespread applications of ECDs, particularly, for architectural applications depend on reducing costs, increasing device lifetime and overcoming the problem of ECD degradation. Commercial production of all plastic electrochromic devices, smart windows, for monitoring time–temperature application has been already achieved.

An electrochromic device (ECD) is essentially a battery in which the electrochromic electrode is separated by a suitable solid or liquid electrolyte from a charge balancing counter electrode, and the color changes occur by charging and discharging the electrochemical cell with the application of few volts [65]. The arrangements of these layers depend on the operation mode. [68]

1.6.3.1 Types of Electrochromic Devices (ECD)

The smart window is only one of the interesting application areas for electrochromism and not necessarily the one where electrochromism will first be introduced on a large scale. In fact, there are four different fields within which electrochromic devices offer distinct advantages over alternative technologies. The smart windows are likely to have important applications in innovative and energy-efficient architecture where they would adjust the inflow of luminous radiation and solar energy through glazing in buildings.

Dual type ECDs are constructed in a sandwich cell device configuration with electrochromically complimentary high and low band gap polymers on top of the transparent ITO coated glass electrodes. These electrodes are separated by a thin layer of gel electrolyte to allow switching. These devices provide highly transparent and colored states which could be useful in controlling the lighting in offices etc. By replacing one of the transparent electrodes of the smart window with a metallic reflector, one reaches the variable reflectance device. Its possible applications include anti dazzling rear view mirrors for cars. If one integrates a white pigment in electrochromic

device, it can serve for information display purposes like, signs and labels. Another possible device area concerns surfaces with variable thermal emittance such surfaces are of interest for temperature stabilization or camouflage applications.

As shown in Figure 1.17 the dual type polymer ECDs are constructed in a sandwich cell device configuration with electrochromically complementary high and low band gap polymers on top of the transparent ITO coated glass electrodes. These electrodes are separated by a thin layer of gel electrolyte to allow switching. In order to prepare an ECD that can undergo a distinct switch from a highly transmissive state to a deeply absorptive state, material choice is extremely important.

Change in the color of the device is achieved by the change in the electronic properties of the polymers due to applied potential across the device. Since this is a two-electrode electrochemical cell, during functioning of the device, one of the polymers should be oxidized while the other is reduced. A change in applied voltage results in the neutralization of the doped polymer with simultaneous oxidation of the complementary polymer, generating color change in the device.
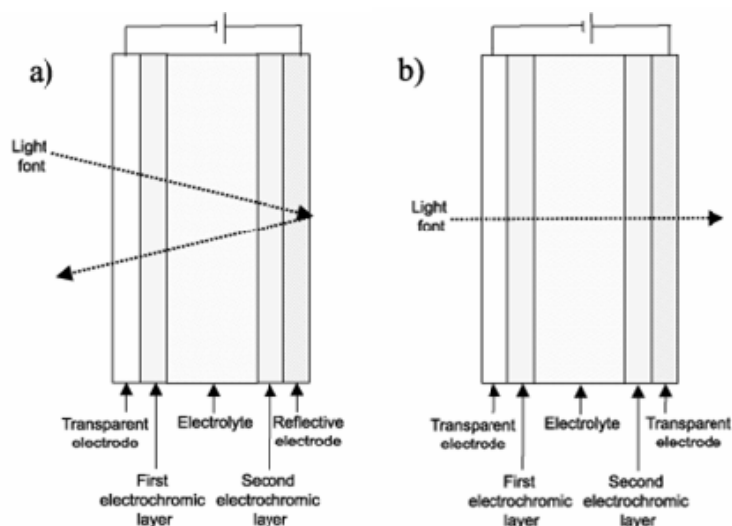
Figure 1.17 Schematic representation of an electrochromic device operating at a) reflective mode and b) transmissive mode.

Figure 1.18 represents the schematic representation of visible spectra for both anodically and cathodically coloring polymer demonstrating the concept of dual polymer ECDs. As seen, the ideal device represents no significant absorption within the visible region in one of its states (Figure 1.18 a) yet the other extreme state reveals high coloration (Figure 1.18 b). At bleached state high band gap polymer is in neutral and low band gap polymer is in oxidized state where both of which do not reveal any absorption within the visible region. Upon applied potential high band gap polymer is oxidized and low band gap polymer is reduced to its neutral state and device turned to colored state.
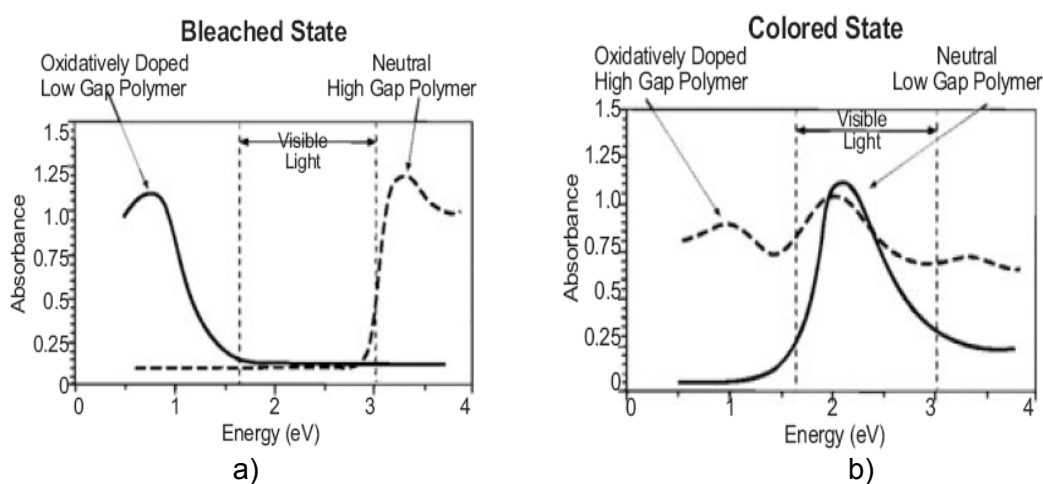
Figure 1.18 Schematic representation of the visible spectra for both and anodically and cathodically coloring polymer demonstrating the concept of dual polymer ECDs for absorptive/ transmissive windows [79]

An ideal cathodically coloring material is the one that has highly colored neutral state and highly transparent oxidized state. For this, a material should have a band gap around 1.8-2.2 eV revealing $\pi-\pi^*$ transition with in the range of 550-650 nm, where the human eye is highly sensitive. On the contrary, an anodically coloring polymer is chosen to have a high band gap (E_g) > 3.0 eV (π to π^* transition onset < 410 nm) with all of the absorption lying in the ultraviolet region of the spectrum.

Basic requirements for high performance electrochromic devices are: a) short response time; b) good stability; c) optical memory, defined as the color stability under open circuit potential conditions; d) optical contrast, also called write-erase efficiency, and e) color uniformity [68].

1.7 The Composition of Color

The sensation of color depends primarily on the composition of light which is a mixture of white light and colored light (which in itself can be a mixture of wavelengths as in the case of purple). There are 3 receptors in the eye that respond to different wavelengths. This leads to attempts to chart colors by a mixture of three primary lights.

Figure 1.19 shows James Clerk Maxwell's color triangle with the three apexes representing three primary colored lights: blue-violet, orange-red, and green. A great number, but not all colors can be produced by mixing lights of the three primary colors. A specific color, for example an unsaturated greenish blue, can be represented by a point on the triangular grid.

In order to represent all colors, 3 imaginary or "ideal" primaries are used. The Commission Internationale de l'Eclairage (CIE) defined in 1931 (modified in 1967) the chromaticity curve with standard observer and 3 ideal standard sources. The chromaticity diagram is constructed (Fig. 1.20) by drawing a color triangle with 3 ideal (but non-existent) primary colors at each corner. The x-axis is the amount of ideal green that would be mixed with blue. The y-axis is the amount of ideal red that would be mixed with blue. A given color is represented by values along the two axes.

Superimposed on the triangle is the CIE chromaticity curve which places the band of pure spectral colors as a solid curved-line from violet up to green down to red. The dashed line connecting 380 nm and 700 nm are the nonspectral colors of purple obtained by mixing violet and red light beams. All the colors that we can see are contained within the area bounded by the solid and dashed lines. The central point W of the diagram is the white produced by an equal mixture of the three primaries.
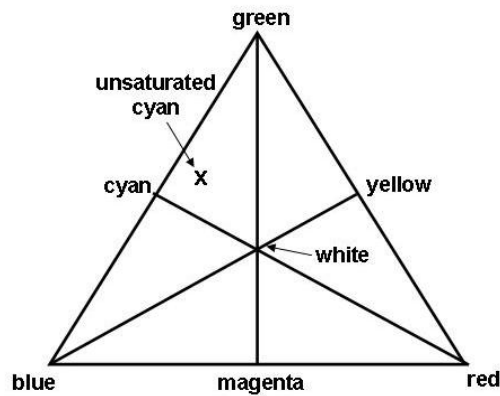
Figure 1.19 The color triangle attributed to James Clerk Maxwell. (adapted from Ref. 80)

We can represent a mixture of two spectral lights as a point on the line joining the light point on the spectral curve. The dotted line in Fig. 1.20 joins the blue light at 480 nm with the yellow light at 580 nm. Following the dotted line we would proceed from spectral (or saturated) blue to pale blue to white to pale yellow to saturated yellow. Thus, a mixture of the correct amounts of 480 nm blue light and 580 nm yellow light gives any of the colors located in between. Similarly the purple colors can be formed by a mixture of red light with violet light as specified by the dashed line. Pair of colors which can produce white (the line joining the two colors passes through the white point, W) are called a complementary pair. Thus, blue light and yellow light form a complementary pair as do orange (600 nm) and blue-green 488 nm, also called "cyan". We can now use the point W as the origin and describe color as a mixture, in a certain proportion, of white light of a given wavelength. This wavelength is referred to as the dominant wavelength and the color associated with this dominant wavelength is called the **hue**. We thus describe the sensation of color in terms of hue. The amount of hue that makes up the composition of light is known as **saturation** (also designated as "chroma"). The dominant wavelength points on the spectral curve (solid line in Fig. 1.20) are fully saturated. As the dominant wavelength or hue is diluted with white light, the saturation decreases. For example, to describe a beam of pink-appearing light as unsaturated orange hue of 620 nm.

33
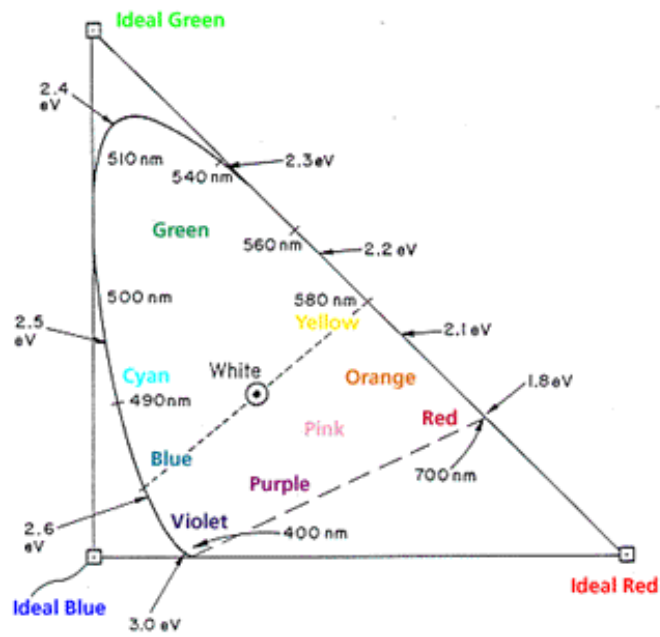
Figure 1.20 The CIE chromaticity diagram showing wavelengths in nanometers (nm) and energies in electron volts (eV). (Adapted from Ref. 81)
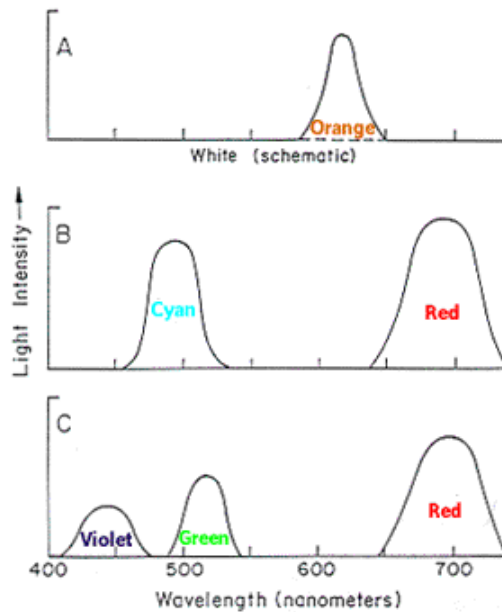
Figure 1.21 Different ways of obtaining metameric beams of pink light. Each implies mixture with white light to obtain pink light, A) by orange light, B) by mixing red with cyan, or C) by mixing red, green, and violet. (Adapted from Ref. 81)

There are many ways to produce the light at point for pink color in Figure 1.20 (or any other point): one hue plus white, two spectral colors or three. These light mixtures are illustrated in Fig. 1.21 where A) shows orange and white, B) blue-green (cyan) and red, and C) violet, green, and red. These three mixtures would appear the same to the standard observer. To the eye, these metameric colors would all appear the same.

1.8 Color and Light

1.8.1 Light: Photons and Waves

Isaac Newton discovered in 1672 that light could be split into many colors by a prism, and used this experimental concept to analyze light. The colors produced by light passing through a prism are arranged in a precise array or spectrum from red through orange, yellow, green, blue, indigo and into violet. The order of colors is constant, and each color has a unique signature identifying its location in the spectrum. The signature of color is the wavelength of light.

Somewhat less than 100 years after Newton's discoveries, James Clerk Maxwell showed that is a form of electromagnetic radiation. This radiation contains radio waves, visible light and X-rays. Figure 1.22 shows electromagnetic radiation as a spectrum of radiation extending beyond the visible radiation to include at one end radio waves and at the other end gamma rays.

The visible light region occupies a very small portion of the electromagnetic spectrum. The light emitted by the sun falls within the visible region and extends beyond the red (into the infrared) and the ultraviolet (UV) with a maximum intensity in the yellow.

When we consider light as an electromagnetic wave, a color's spectral signature may be identified by noting its wavelength. We sense the waves as color, violet being the shortest wavelength and red the longest. Visible light is the range of wavelengths within the electromagnetic spectrum that the eye responds to. Although radiation of longer or shorter wavelengths are present, the human eye is not capable of responding to it.
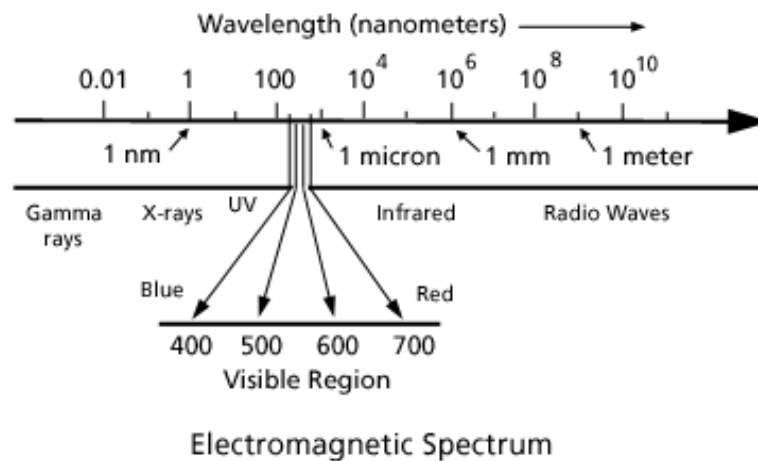
Figure 1.22 The electromagnetic spectrum, which encompasses the visible region of light, extends from gamma rays to radio waves

Three typical waves of visible light are shown in Fig. 1.23. The wavelength is the distance from one wave crest to the next, and is represented by λ. Violet light is electromagnetic radiation with wavelengths of 410 nanometers and red light has a wavelength of 680 nanometers. The nanometer is a unit of distance in the metric scale and is abbreviated as nm. One nanometer is a distance too small to be resolved in an optical microscope but one micron (μm) or one thousand nanometers can be resolved (1 micron = 1000 nm). The wavelengths of visible light are smaller than common objects such as the thickness of a sheet of paper or the diameter of a human hair. Both of these are about one hundred microns thick which translates to distances greater than one hundred wavelengths of visible light. As we move through the visible spectrum of violet, blue, green, yellow, orange and red, the wavelengths become longer. The range of wavelengths (400 - 700 nm) of visible light is centrally located in the electromagnetic spectrum (Fig. 1.22). Infrared and radio waves are at the long wavelength side while ultraviolet (UV), x-rays and gamma rays lie at the short wavelength side of the electromagnetic spectrum.

Radiation with wavelengths shorter than 400 nm and longer than 700 nm cannot be sensed by the eye. We can describe light as electromagnetic waves with color identified by its wavelength. We can also consider light as a stream

36

of minute packets of energy-photons which create a pulsating electromagnetic disturbance. A single photon of one color differs from a photon of another color only by its energy.

In the description of light, the most convenient unit of energy to use is the electron volt, abbreviated eV. The electron volt is the energy gained by an electron that moves across a positive voltage of one volt (V). For example 1.5 electron volts is the energy gained by an electron moving from a negative metal plate to a positive plate which are connected to the terminals of a common 1.5 volt "C" battery.

Visible light is composed of photons in the energy range of around 2 to 3 eV (Fig. 1.24). As the energy of the light increases, the wavelength decreases. Orange light with a wavelength of 620 nanometers is composed of photons with energy of 2 eV. It is the energy range of 1.8 to 3.1 eV which triggers the photo receptors in the eye. Lower energies (longer wavelengths) are not detected by the human eye but can be detected by special infrared sensors. Higher energies (shorter wavelengths) such as x-rays are detected by x-ray sensitive photographic film or again by special devices.
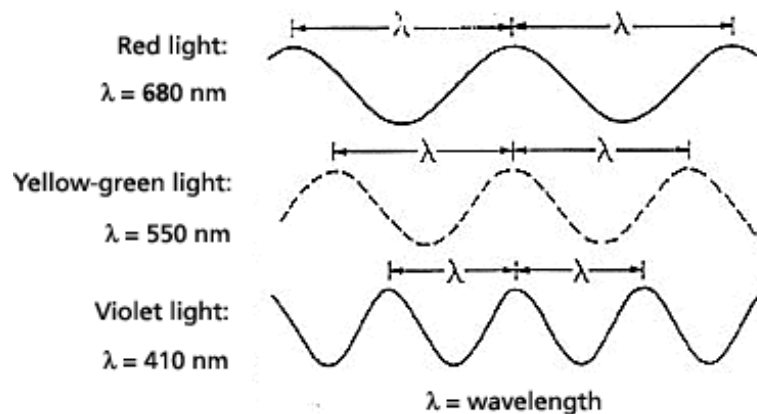
Figure 1.23 A wave representation of three different light hues: red, yellow-green and violet

Light rays are composed of photons where energy specifies a color from red to violet. The intensity or brightness of the light is defined by the flux, or

number of photons passing through a unit area in a unit time; i.e., number of photons per cm^2 per sec. If we specify a wavelength in the visible range on the electromagnetic scale, we can attribute a color to it. That is, laser light with a single wavelength of 650 nanometers looks red. We show the major spectral colors in Fig. 1.25a as a linear sequence from red (at 700mm) to violet at 400 nm.
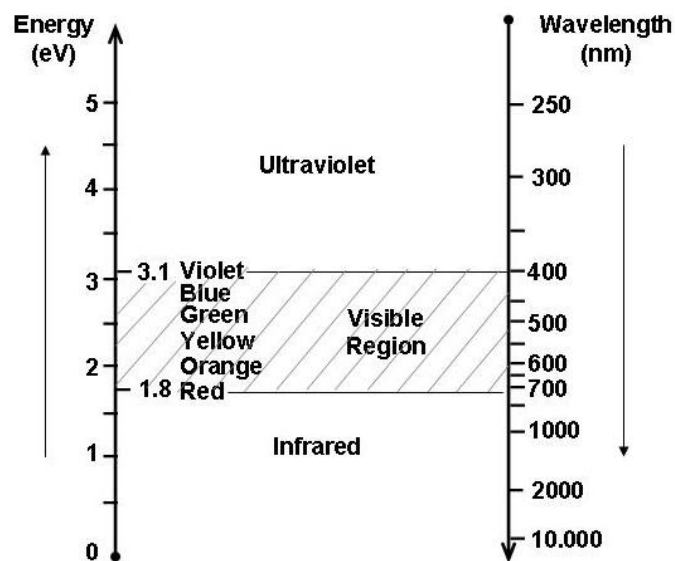
Figure 1.24 Diagram showing the visible region of the electromagnetic spectrum in terms of wavelength and corresponding energies

A circular sequence of these same spectral colors, the color wheel first attributed to Isaac Newton, is shown in Fig. 1.24b. The progression of colors from red through violet is identical to that on the linear scale. The circular wavelength scale outside the color wheel shows the wavelength connection between the linear and circular sequences. The purple region in the color wheel is a notable difference between the two sequences. Colors in this purple portion of the color wheel are composed of mixtures of wavelength and cannot be represented by a single wavelength. Brown requires a more complex mixture of wavelengths from at least three regions of the sequence.

38
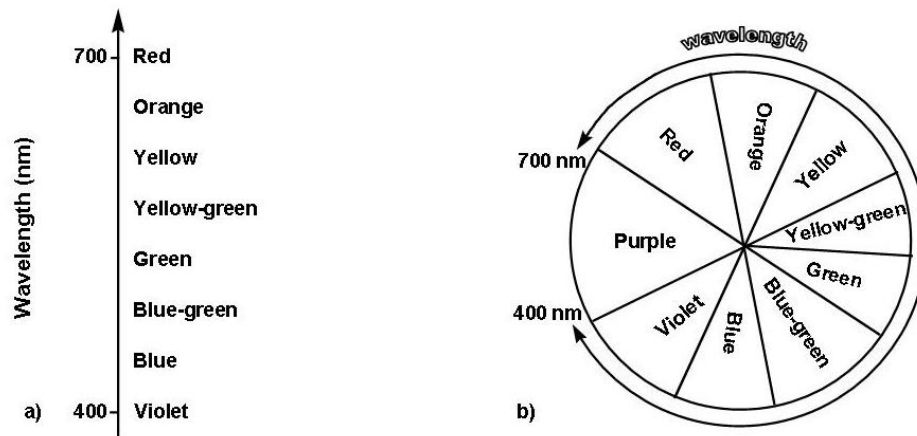
Figure 1.25 The region of visible light in wavelengths shown as a linear arrangement (a) and as a circle (b)

1.8.2 The Color of Objects

Color is produced by the absorption of selected wavelengths of light by an object. Objects can be thought of as absorbing all colors except the colors of their appearance which are reflected as illustrated in Fig. 1.26. A blue object illuminated by white light absorbs most of the wavelengths except those corresponding to blue light. These blue wavelengths are reflected by the object.
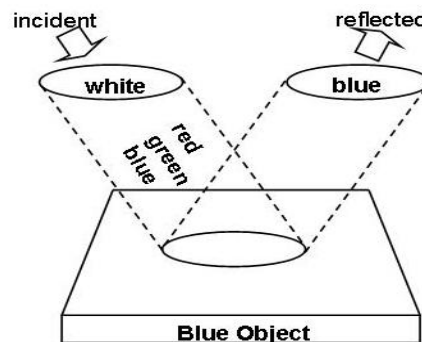
Figure 1.26 Schematic representation of white light composed of all wavelengths of visible light incident on a pure blue object

39

1.8.3 The Eye and Color Sensation

Our perception of color arises from the composition of light - the energy spectrum of photons - which enters the eye. The retina on the inner surface of the back of the eye (Fig. 1.27) contains photosensitive cells. These cells contain pigments which absorb visible light. Of the two classes of photosensitive cells, rods and cones, it is the cones that allow us to distinguish between different colors. The rods are effective in dim light and sense differences in light intensity - the flux of incident photons - not photon energy. So in dim light we perceive colored objects as shades of grey, not shades of color.
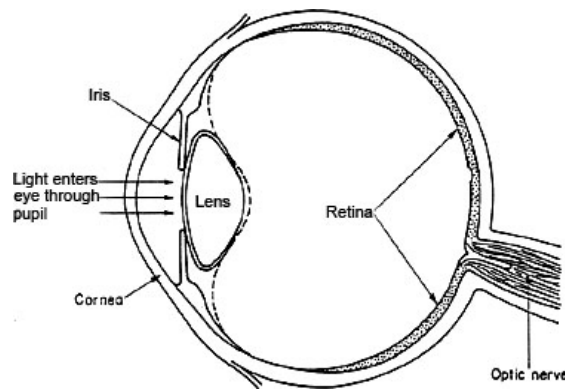
Figure 1.27 A cross-sectional representation of the eye showing light entering through the pupil

Color is perceived in the retina by three sets of cones which are photoreceptors with sensitivity to photons whose energy broadly overlaps the blue, green and red portions of the spectrum. Color vision is possible because the sets of cones differ from each other in their sensitivity to photon energy. The sensitivity of the cones to light of the same intensity (the same photon flux) but different wavelengths (energy) is shown in Fig. 1.28. The maximum sensitivity is to yellow light, but cone R has a maximum in the red-orange, G in the green-yellow, and B in the blue. The sensitivities of the three comes

40

overlap. For every color signal or flux of photons reaching the eye, some ratio of response within the three types of cones is triggered. It is this ratio that permits the perception of a particular color.
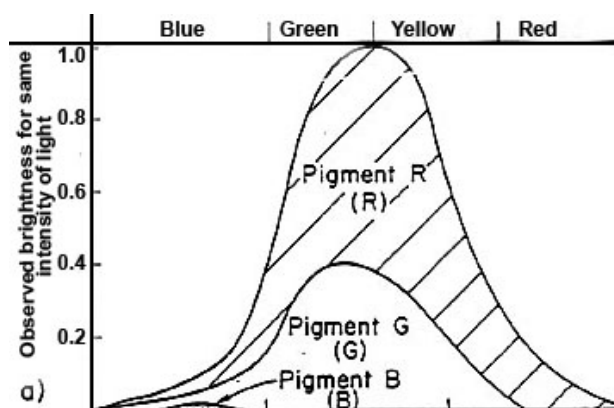
Figure 1.28 The response of the tree cones to incident light

For electrochromic windows an ideal cathodically coloring material has a low band gap around 1.8-2.0 eV in order for the π-π* transition to occur in the visible region where the human eye is highly sensitive. An anodically coloring polymer is chosen to have a high band gap (E_g) > 2.0 eV with all of the absorption lying in the ultraviolet region of the spectrum. Generally cathodically coloring materials for use in ECDs are based on PEDOT and its derivatives, as they exhibit high electrochromic contrasts, low oxidation potentials and high conductivity, as well as good electrochemical and thermal stability. In this thesis, new thiophene and pyrrole based monomers used for anodically coloring materials for electrochromic windows were synthesized.

Here we report the synthesis and electrochemical and optical properties of several new thiophene and pyrrole monomers. Our goal was to obtain materials with high band gaps. Substitution is known to provide a way of controlling the band gap, as the presence of side chains induces a twist of the conjugated backbone, resulting in a decrease of the π-conjugation and therefore an increase of the band gap.

CHAPTER II

EXPERIMENTAL

2.1 Materials

Pyrrole (Aldrich), thiophene (Sigma) and acetonitrile (Merck) were purified by convential distillation procedures prior to use. 3,4-Ethylenedioxythiophene (EDOT) was purchased from Aldrich and used as received. The electrolysis solvents, acetonitrile (Merck), propylene carbonate (Aldrich) and dichloromethane (Merck) were used without further purification. The supporting electrolyte tetrabutylammonium tetrafluoroborate (Aldrich) was used as purchased. Chloroform (Merck), 3-thiophene methanol (Aldrich) 4-(1*H*-pyrrol-1-yl)phenol (Aldrich), 2,4,6-trichloro-1,3,5-triazine (Aldrich) 3-thiophene acetic acid (Aldrich), hexamethylene diamine (Aldrich), borontrifluoride ethylether (BFEE) (Sigma), maleic anhydride (Sigma), p-amino benzoic acid (Aldrich), ethanolamine (Aldrich), furan (Sigma) and thionyl chloride (Aldrich) were used without further purification.

2.2 Instrumentation

2.2.1 Potentiostat and Galvanostat

Films were electrochemically polymerized by potentiostatic methods by using Solartron 1285 and Voltalab PST50 potentiostats/galvanostats. The function of potentiostat is to maintain the potential of the working electrode (WE) at an adjusted level with respect to a fixed reference electrode (RE). The potential difference between the WE and RE is equal to input potential that can be controlled externally. The current driven by the potentiostat (between WE

and RE) can be determined by measuring the voltage drop across a small resistance R connected to the counter electrode in series.

In a three electrode potentiostatic system, the major current passes through the counter electrode (CE) and WE. The current amplifier supplies current to the cell (between the WE and CE), regardless of the solution resistance. By this way the purpose of maintaining potential control between the two electrodes has been accomplished.

2.2.2 Electrolysis Cell

Electrochemical polymerization was carried out in a H-shaped cell which can hold 50 mL solution. Working and the counter electrodes were platinum foils with an area of 1.5 cm^2. This cell is a three-compartment one which is divided into two compartments as the catholyte and anolyte with a medium porosity sintered glass disc of 2.0 cm in diameter. Reference electrode was inserted to the working side of the cell and a Ag/Ag^+ (10^{-2} M) was utilized as the reference electrode. The cell has gas inlets to pass the N_2 gas through the solution.
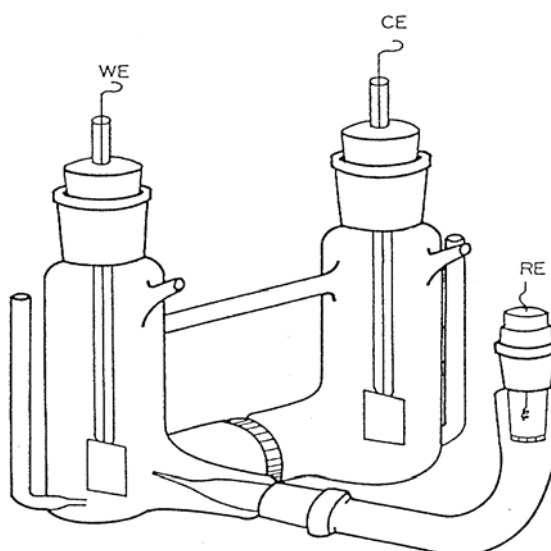
Figure 2.1 H-Shaped Electrolysis Cell

In order to investigate spectroelectrochemical properties of the conducting polymers, electropolymerizations were carryied out in UV cuvette. Basically a UV cuvette was utilized as the electrolysis cell equipped with Pt counter and Ag wire pseudo reference electrode (Figure 2.2).
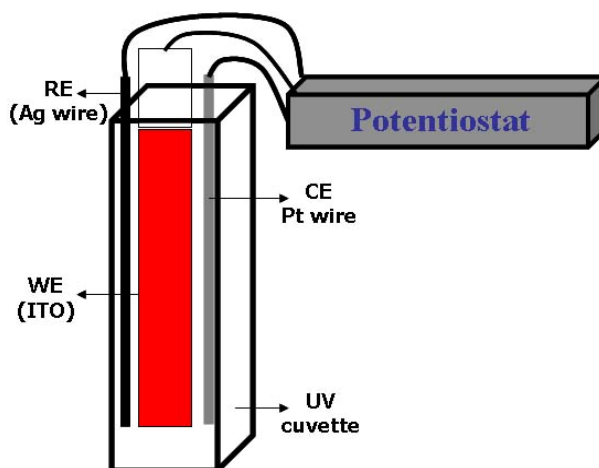
Figure 2.2 Schematic representation of electrolysis cell.

2.2.3 Cyclic Voltammetry (CV) System

Among the electrochemical methods that can be applied to the study of conducting polymer films deposited on a conducting surface, cyclic voltammetry (CV) is becoming increasingly popular as a mean to study redox states due to its simplicity and versatility. The electrode potential at which a polymer undergoes reduction or oxidation can be rapidly located by CV. Furthermore, CV reveals information regarding the stability of the product during multiple redox cycles. Since the rate of potential scan is variable, both fast and slow reactions can be followed. A very important aspect of this method is its ability to generate new redox species during the first potential scan and then probe the fate of species on the second and subsequent scans.

Therefore, CV allows the growth of a polymer film along with its further characterization during a single experiment.

The cyclic voltammety cell consists of a platinum bead working electrode of 1 cm wire in length, a platinum spiral counter electrode (3 cm coil), and a Ag/Ag$^+$ reference electrode (Fig. 2.3). The volume of the cell was about 15 mL. CV experiments were carried out by a Voltalab PST50 potentiostat/galvanostat.

2.2.3.1 Cyclic Voltammetry of Conducting Polymers

This method consists of cycling the potential of an electrode, which is immersed in an unstirred solution, and measuring the resulting current at the working electrode. Therefore, the obtained voltammogram is a display of current (vertical axis) vs. potential (horizontal axis). The reducing or oxidizing strength of the WE is precisely controlled by the applied potential. Typically, the polymerization of electron rich monomers starts at low potentials (a) where no redox reactions occurs, followed by scanning in the anodic direction (Fig.2.4). At potential (b), the electrode has sufficient oxidizing character to oxidize the monomer to its radical cation.
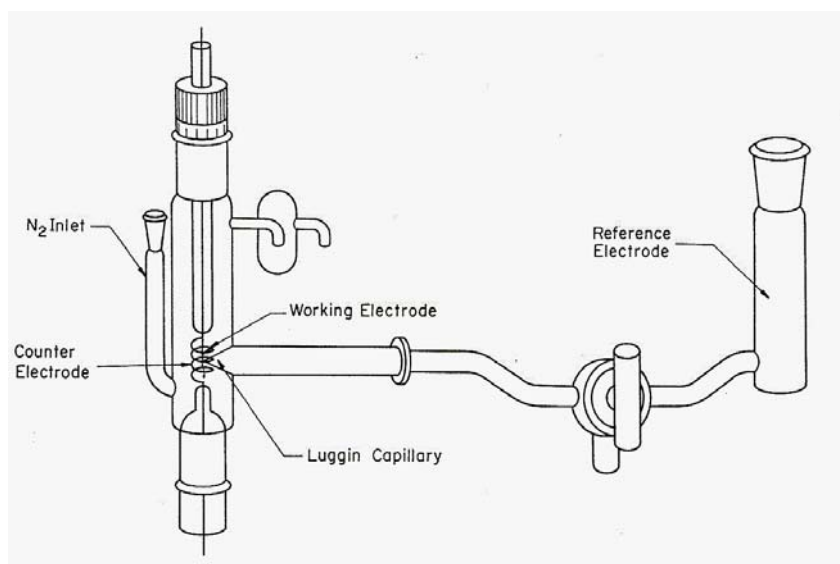
Figure 2.3 Cyclic Voltammetry Cell

The anodic current increases rapidly (b-c) until the concentration of the monomer at the electrode surface approaches zero, causing the current to peak (c), and then decay as the solution surrounding the electrode is depleted of monomer. Monomer oxidation is immediately followed by chemical coupling that affords oligomers in the vicinity of the electrode. Once these oligomers reach a certain length, they precipitate onto the electrode surface where the chains can continue to grow in length. The electroactivity of the polymer deposited onto the WE can be monitored by the appearance of a peak corresponding to the reduction of the oxidized polymer while scanning in the cathodic direction (d). A second positive scan reveals another oxidation peak at a lower potential than the monomer oxidation peak (e). This is due to the neutral polymer now becoming oxidized. Another noticeable fact is the increase in monomer oxidation peak current in the second and subsequent scans. As the peak current is directly proportional with the electrode area, this increase in the peak current could be attributed to an increase of the WE area due to a more porous morphology of the electrodeposited polymer.
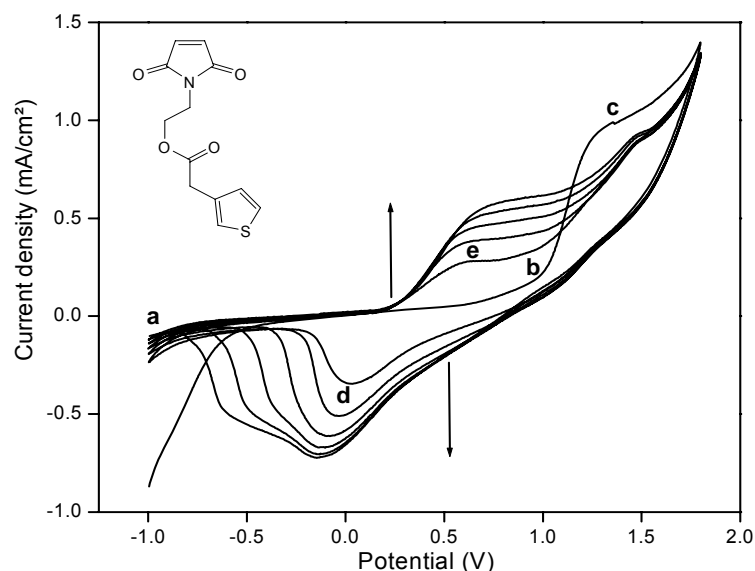
Figure 2.4 Cyclic voltammogram of an electron rich monomer

2.2.4 Fourier Transform Infrared Spectroscopy (FTIR)

FTIR is a useful method for the characterization of monomers and conducting polymers because it does not require polymers to be soluble. It is used for the detection of functional groups. In this work, the spectrometer used in order to obtain the spectra of samples was a Nicolet DX 510 FTIR. The spectra were recorded by using KBr pellets.

2.2.5 Scanning Electron Microscopy (SEM)

SEM is a surface analytical technique which is employed to study the morphology of conducting polymer film surfaces and provides valuable information on the structure of the monomer, the nature of dopant and the thickness of the film. SEM of polymer films was performed using a JEOL model JSM-6400 scanning electron misroscope at 20 kV with varying levels of magnification.

2.2.6 ^{1}H and ^{13}C Nuclear Magnetic Resonance Spectrometer

^{1}H-NMR and ^{13}C-NMR spectra of monomers were taken by Bruker Instrument-NMR Spectrometer (DPX-400) using $CDCl_3$ as the solvent and tetramethylsilane as the internal standard relative to which the chemical shifts (δ) are given.

2.2.7 UV-Vis Spectrophotometer

Agilent 8453 UV-Vis spectrophotometer was used in order to carry out spectroelectrochemical studies.

2.2.8 Four Probe Conductivity Measurements

Conductivity measurements can be performed by four probe and two probes techniques. Among available conductivity techniques, four probe

method has several advantages for measuring electrical properties of conducting polymers. First, four probe techniques eliminate errors caused by contact resistance, since the two contacts measuring the voltage drop are different from the contacts applying the current across the sample. Second, this technique allows for conductivity measurements over a broad range of applied currents, usually varying between 1 µA and 1mA for conducting polymers.

In four probe technique, four equally spaced osmium tips were placed onto a head. The head was lowered to the sample until the four probes touch the sample. A constant source was used to pass a steady current through the outermost probes and voltage drop across the inner two was measured (Figure 2.5). Conductivity was given by the equation:

$$\sigma = \ln2 \ / \ (\pi d \ x \ i/V)$$

where σ is the conductivity, i as the current applied through the outer probes, V voltage drop measured across the inner probes and d is the sample thickness.
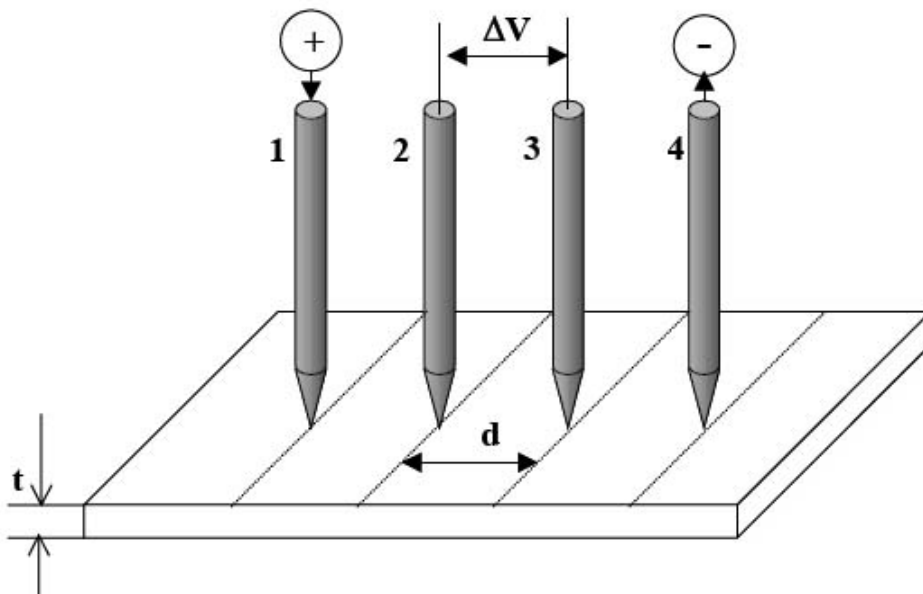
Figure 2.5 Schematic diagram of four probe technique

2.3 Procedure

2.3.1 Synthesis of Hexamethylene (Bis-3-Thiophene Acetamide)

A mixture of 3-thiophene acetic acid (0.80 g, 5.6 mmol) and thionyl chloride (0.77 g, 6.5 mmol) was placed in 25 mL round bottom flask carrying a drying tube and refluxed for 1 h. A water aspirator vacuum was applied to remove the excess thionyl chloride. The liquid product was dropwise added to hexamethylene diamine (0.32 g, 2.81 mmol) in 20 mL dry THF in an ice bath under rapid stirring. The mixture was stirred for about 30 min. The product was collected by suction filtration and washed with THF to remove unreacted hexamethylene diamine and 3-thiophene acetic acid. A light-brownish solid product was obtained in 45% yield. Figure 2.6 shows synthesis route for HMTA.
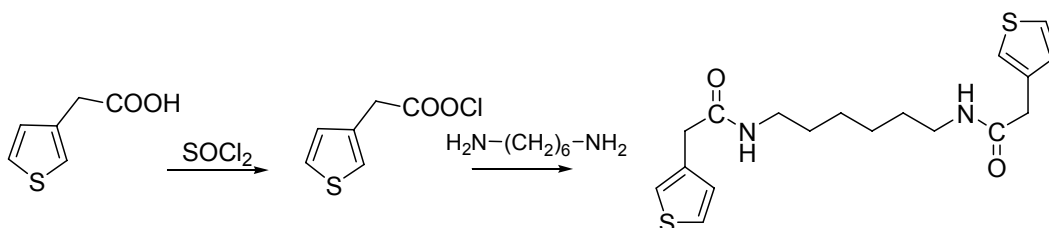
Figure 2.6 Synthesis route for HMTA

2.3.2 Electrochemical Synthesis of Copolymer of HMTA with Thiophene [P(HMTA-co-Th)]

HMTA was coated on the working electrode surface from its dichloromethane solution. The electrolyses were carried out in acetonitrile with TBAFB (0.05M) and thiophene (8×10^{-2} M) at 1.9V vs Ag^o/Ag$^+$ at room temperature. Free standing black films were formed in 1h.

2.3.3 Synthesis of N-(4-(3-thienyl methylene)-oxycarbonylphenyl) Maleimide (MBThi)

2.3.3.1. Synthesis of 4-Maleimidobenzoic Acid (MBA)

MBA was synthesized by the condensation reaction of maleic anhydride with p-amino benzoic acid followed by cyclodehydration using acetic anhydride and sodium acetate according to literature procedure (Fig. 2.7) [7]. Yield: 79%; mp: 234 ^{o}C. IR (cm^{-1}): 3460–3200 (COOH), 3105 (C=C), 2300 (COOH), 1720 (CO–N–CO), 1610 (C=C), 1400 (CH), 1217 (–C–O), 820 (phenyl), 720 (cis CH=CH).

2.3.3.2 Synthesis of 4-Maleimido Benzoic Acid Chloride (MBACl)

This intermediate was synthesized in 73% yield according to the literature procedure [7]. mp: 157–158 ^{o}C   IR (cm^{-1}): 1770 (COCl), 1715 (CO–N–CO), 1600 [(C=C), 1370 (CH)], 700 (cis CH=CH).

2.3.3.3 Synthesis of MBThi

To a mixture of 2.40 g (1.98 ml, 21 mmol) 3-thiophene methanol and 2.02 g (2.77 ml, 20 mmol) dry triethyl amine (TEA) in a two necked round bottom flask equipped with a reflux condenser and a dropping funnel, 4.71 g (20 mmol) of MBACl dissolved in 100 ml of dry chloroform were added dropwise with stirring. The reaction was kept at 30 ^{o}C for 3 days with continuous stirring. Then, the reaction mixture was washed with 1% HCl solution and distilled water (each one for four times) and dried over CaCl$_2$. The solvent was evaporated out with a rotary evaporator and the residue was extracted with hot methanol to remove unreacted traces of thiophene methanol and MBA. The crude product was purified by reprecipitation three times from THF solution to hexane and a brownish solid was obtained. After filtration, pure MBThi was dried in vacuum oven (Fig. 2.7). Yield: 55%; mp: 85-88 ^{o}C. IR (cm^{-1}): 3100 (C=C); 2900 (–CH$_2$); 1770, 1710, 1380, 1142, 699 (imide ring); 1710, 1270, 1210 (ester); 3110, 769 (C–Ha of thiophene ring); 3020, 856 (C–Hb of

thiophene ring). ^{1}H-NMR (δ, ppm from TMS in DMSO-d_6): 8.11–8.07 (d, 2H, Ar-H, ortho to ester group); 7.69 (s, 1H, Ar-H, ortho to imide group); 7.59–7.55 (m, 2H, 2- and 4-position in thiophene ring); 7.52 (s, 1H, Ar-H, ortho to imide group); 7.26–7.22 (bs, 3H, CH=CH and 5-position in thiophene ring); 5.36 (s, 2H, CH$_2$).
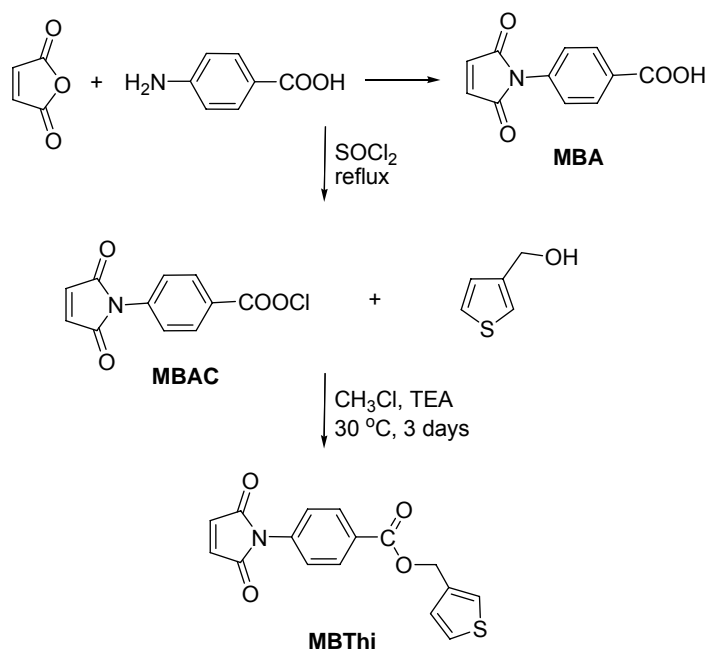
Figure 2.7 Synthesis route for MBThi

2.3.4 Electrochemical Synthesis of Copolymer of MBThi with Thiophene P(MBThi-co-Th)

Polymerizations were performed in the presence of 50 mg MBThi and 8.2×10^{-3} molL^{-1} thiophene in 0.1molL^{-1} TBAFB/AN/BFEE in a cell equipped with Pt working and counter electrodes and Ag wire pseudo reference electrode. Electrodeposition of copolymer films were performed potentiodynamically between 0.0 V and 2.0 V at a scan rate of 500 mV/s. The free-standing films which were grown on the electrode surface were peeled and vigorously washed with AN to remove unreacted monomers.

2.3.5 Synthesis of 2,4,6-tris(4-(1H-pyrrol-1-yl)phenoxy)-1,3,5-triazine (Tria-Py)

2,4,6-trichloro-1,3,5-triazine (0.92 g, 5.10^{-3} mol) was dissolved in acetone (10mL) and a solution of (2.39 g, 1.5×10^{-2} mol) 4-(1*H*-pyrrol-1-yl)phenol and NaOH (0.6 g, 1.5×10^{-2} mol) in H_2O (5 mL) was added dropwise at 0–5 ^{o}C. The reaction mixture was stirred vigorously under N_2 for 1h at 0–5 ^{o}C and than at 35-40 ^{o}C for 4h. The reaction mixture was then cooled to 0 ^{o}C. A white crystalline solid was filtered, washed with cold water, then with MeOH and finally recrystallized twice from a solution of isopropyl alcohol and acetone (3:1 v/v). Tria-Py was obtained as white crystalline solid with a 76% yield, mp 257 ^{o}C (Fig. 2.8).
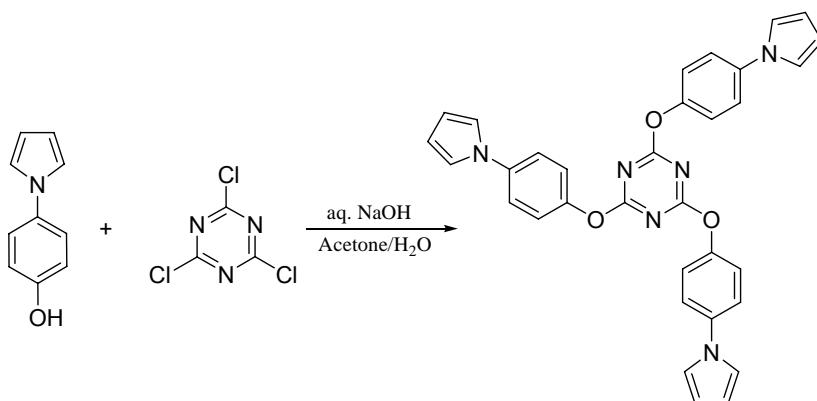
Figure 2.8 Synthesis route for TriaPy

2.3.6 Electrochemical Synthesis of P(Tria-Py)

Electrochemical polymerization of Tria-Py via constant potential electrolysis was performed in a single compartment cell, in the presence of 50 mg Tria-Py, 0.1 M TBAFB in DCM/AN (1:3) via application of 1.6 V. Limited solubility of the monomer in AN was enhanced by adding DCM in electrolysis cell. After electrolysis, the free standing film was washed with DCM several times to remove unreacted monomer. Similar procedure was applied for the synthesis of P(Tria-Py) on ITO by using a UV-cuvette as a single compartment cell. The electrochromic measurements; spectroelectrochemistry, and

switching studies of the polymer film deposited on ITO coated glass were carried out in same media in the absence of monomer.

2.3.7 Electrochemical Synthesis of Copolymer of TriaPy with Pyrrole P(TriaPy-co-Py)

Polymerizations were performed in the presence of 30 mg TriaPy and 8.2×10^{-3} molL^{-1} pyrrole in 0.1molL^{-1} TBAFB/AN in a cell equipped with Pt working and counter electrodes and Ag wire pseudo reference electrode. Electrodeposition of copolymer films were performed potentiodynamically between -0.5 V and 1.8 V at 250 mV/s scan rate. The free-standing films which were grown on the electrode surface were peeled and vigorously washed with AN to remove unreacted monomers.

2.3.8 Synthesis of 2,4,6-tris(4-(1H-pyrrol-1-yl)phenoxy)-1,3,5-triazine (Tria-Th)

2,4,6-trichloro-1,3,5-triazine (1.26 g, 7 mmol) was dissolved in DCM (10mL) and a solution of 2.40 g (1.98 ml, 21 mmol) 3-thiophene methanol and NaOH (1.2 g, 30 mmol) was added dropwise at room temperature. The reaction mixture was stirred vigorously under N$_2$ for 1h and than at 30-35 $^{\circ}$C for 4h. It was then refluxed for 12 h. A white crystalline solid was filtered, washed with cold water, then with MeOH and finally recrystallized twice from a solution of isopropyl alcohol and acetone (3:1 v/v). Tria-Th was obtained as white crystalline solid with a 76% yield, mp 91 $^{\circ}$C (Fig. 2.9).
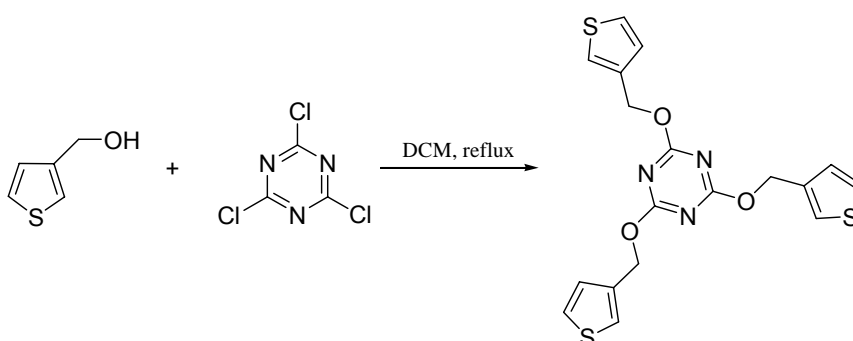
Figure 2.9 Synthesis route for TriaTh

2.3.9. Synthesis of N-(2-(thiophen-3-yl)methylcarbonyloxyethyl) maleimide (NMT)

2.3.9.1 Synthesis of 3, 6-endoxo-1, 2, 3, 6-tetrahydrophthalic anhydride (ETA)

The 3, 6-endoxo-1, 2, 3, 6-tetrahydrophthalic anhydride (ETA) (Scheme 1) was synthesized according to the method described by Narita et al [15]. Maleic anhydride (20 g, 20.4 mmol) and ethyl acetate (25.5 ml) were mixed in a 100 ml round-bottomed flask. Furan (17.35 g, 25.5 mmol) was added and the reaction mixture was stirred overnight at room temperature. The precipitate was filtered and washed with ethyl acetate producing 18.15 g (89 %) of a white solid as the final product, m.p. 107 ^{o}C (Fig 2.10).

2.3.9.2 Synthesis of 2-hydroxy-N-ethyl-3, 6-endoxo-1, 2, 3, 6-tetrahydro phthalimide (ETM)

The synthesis of 2-hydroxy-N-ethyl-3, 6-endoxo-1, 2, 3, 6-tetrahydro phthalimide (ETM) (Fig. 2.10) was carried out in accordance to the method described by Narita et al [15]. Ethanolamine (3.8 g, 6.17 mmol) in ethanol (5 ml) was added drop-wise to slurry of ETA (10 g, 6 mmol) in ethanol (15 ml) in a 50 ml round-bottomed flask. This mixture was then refluxed for 4 hours. After cooling to room temperature overnight, a white solid had formed. The crude product was filtered and washed with ethanol followed by petroleum ether yielding 7.27 g (58 %) of a white crystalline solid as the final product, m.p. 132 ^{o}C (Fig 2.10).

2.3.9.3 Synthesis of thiophen-3-yl-acetyl chloride

3-thiophene acetic acid (7 mmole) was dissolved in 10mL dichloromethane and reacted with excess thionyl chloride (14 mmole, where thionyl chloride was added dropwise while cooling in ice bath 0 ^{o}C). The

chlorination reaction was carried out overnight at room temperature, which yields thiophen-3-yl-acetyl chloride (yield 92%).

A solution of 0.8 g (0.004 mol) ETM in 10 mL dichloromethane containing 0.4 g (0.004 mol) triethylamine (TEA), was added dropwise in 0.5 h, by cooling in ice bath and nitrogen atmosphere onto 0.72 g (0,0045 mol) 3-thiophene acetyl chloride. The esterification was carried out overnight at room temperature. After cooling of the solution, solid product filtered off and washed with ethanol (Fig 2.10).
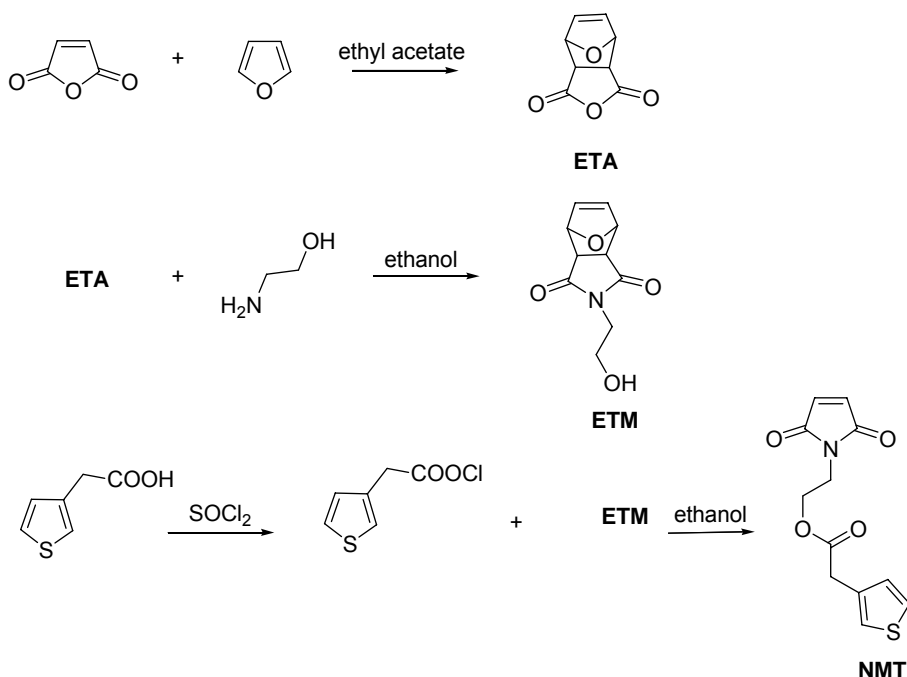
Figure 2.10 Synthesis route for NMT

2.3.10 Electrochemical Synthesis of P(NMT) and P(NMT-co-Th)

For synthesis of P(NMT), 40 mg of NMT were dissolved in 15 mL AN/BFEE (1:1, v/v) and 0.1M TBATFB were introduced into a single compartment electrolysis cell. For synthesis of P(NMT-co-Th), 15 µL thiophene were added the same cell. Electrolysis was run for 30 min at 1.7 V at room

temperature under inert atmosphere. Resulting copolymer films were washed with AN to remove BF4$^-$ after the electrolysis. Similar method was used to synthesize the copolymer on ITO coated glass plate.

2.4 Spectroelectrochemistry and Other Optical Measurements

Spectroelectrochemistry plays a key role in probing the electronic structure of conducting polymers as well as in examining the optical changes that occur upon doping. It provides information about the material's band gap and intraband states created upon doping as well as gives some insight into a polymer color through the location of the absorption maxima and the ratio of peak intensities if the material shows fine structure on the main π-π* peak.

Measurements were carried out by using a specially designed three-electrode cell to allow potential application while monitoring the absorption/transmission spectra with a UV spectrophotometer. Typical polymer samples are thin films that deposited potentiostatically on transparent ITO/glass electrodes purchased from Delta Technologies, Ltd. These electrodes have surface resistivities in the range of 10 to 20 S/cm and are cut to fit a UV cuvette (0.7 cm wide). Usually a Ag wire pseudo reference is used as the reference electrode and a Pt wire is used as the counter.

A typical spectroelectrochemical experiment is carried out with a spectrophotometer operating in single beam mode. An accurate baseline is obtained using two cuvettes containing bare ITO/glass electrodes immersed in a liquid electrolyte placed in both reference and sample compartments. After collecting the baseline, the polymer coated ITO is placed in the sample compartment. Polymer analysis is obtained by sequentially stepping the applied potential until the polymer reaches its fully oxidized and neutral forms. These extreme redox states are attained when the polymer absorption envelope stops changing with increasing/decreasing applied potential. Simplified experimental setup for the spectrofotometric measurement is shown in Figure 2.11.

Dual polymer ECDs are analyzed in a similar manner. However, devices used to collect the baseline are assemblies consisting of the bare ITOs

sandwiched together with gel electrolyte. In order to apply voltage across the device, the counter and the reference leads are connected to one another.

A kinetics experiment allows for measuring polymer and device switching times between the two extreme redox states. This measurement follows the spectroelectrochemistry experiment described above because it requires knowledge of polymer (device) potentials applied for a full switch as well as the wavelength of maximum contrast. Once these values are known, the spectrophotometer can be switched to transmission mode to monitor changes in a sample's opacity at the wavelength where the optical contrast is the highest. Concurrently, a square potential waveform is applied at desired time intervals. This allows monitoring % T as a function of time at the specified wavelength, usually located in the visible region.
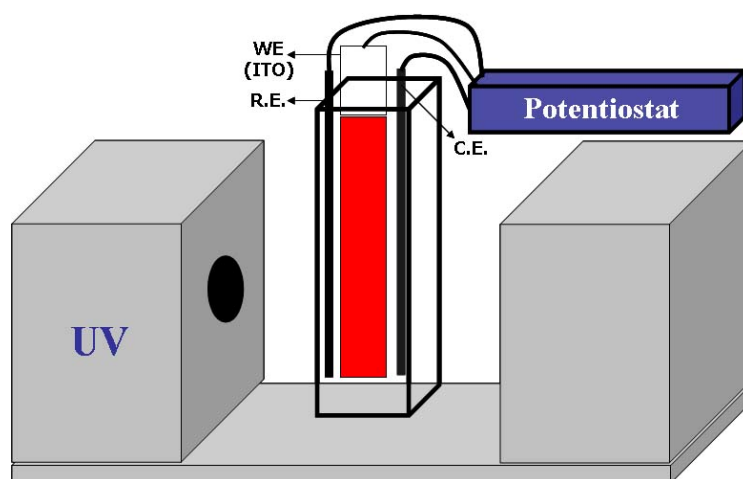
Figure 2.11 Simplified experimental setup for the spectrofotometric measurement
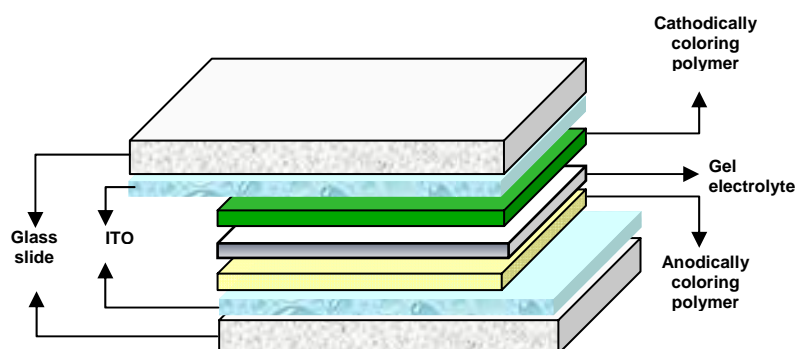
2.5 Gel Electrolyte Preparation

Gel electrolyte was prepared by using TBAFB:ACN:PMMA:PC in the ratio of 3:70:7:20 by weight. After TBAFB was dissolved in ACN, PMMA was added into the solution. In order to dissolve PMMA, vigorous stirring and heating was

required. PC, as a plasticizer, was introduced to the reaction medium when all of the PMMA was completely dissolved. The mixture was stirred and heated until the highly conducting transparent gel was produced [47].

2.6 Electrochromic Device Construction

An electrochromic device (ECD) is essentially a rechargeable battery in which the electrochromic electrode is separated by a suitable solid or liquid electrolyte from a charge balancing counter electrode, and the color changes occur by charging and discharging the electrochemical cell with applied potential of a few volts [44].

A dual-type ECD consists of two electrochromic materials (one revealing anodic coloration, the other revealing cathodic coloration) deposited on transparent ITO, placed in a position to face each other and a gel electrolyte in between. In order to maintain a balanced number of redox sites for switching, the redox charges of the two complementary polymer films were matched by chronocoulometry. Before constructing the ECD, the anodically coloring polymer film was fully reduced and the cathodically coloring polymer film was fully oxidized. Upon application of voltage, the doped polymer will be neutralized, whereas the other will be reduced, thus will result in the color change. Schematic representation of devices is given in Figure 2.12.

**Figure 2.12** Schematic representation of ECDs

The construction of an ECD consists of two thin polymer films deposited on transparent indium tin oxide coated glass (ITO), and separated by a viscous gel electrolyte. Polymer films used to assemble a device were obtained by constant potential oxidative polymerization at potentials slightly higher than the monomer oxidation onset to ensure a slow rate and uniform film deposition. Film thicknesses were controlled by monitoring the total charge density passed during electrosynthesis. Polymer-coated electrodes were removed from the polymerization medium and placed in monomer-free electrolyte. Cathodically coloring films were fully oxidized and anodically coloring polymers were fully neutralized before rinsing with ACN, to ensure charge balance prior to device assembly. The films were then coated with gel electrolyte casting solution until the entire polymer surface was uniformly covered. The gel electrolyte formed a seal around the edges, the devices becoming self-encapsulated.

2.7 Colorimetry

In-situ colorimetric analysis is rapidly becoming a popular technique in the study of electrochromic polymers. This method allows for accurately reporting a quantitative measure of the color and graphically representing the track of doping-induced color changes of an electrochromic material or device. There are three attributes that are used to describe the color: hue (a), saturation (b) and brightness (L). Hue represents the wavelength of maximum contrast (dominant wavelength) and is commonly referred to color. Saturation takes into consideration the purity (intensity) of a certain color, whereas the third attribute, brightness, deals with the luminance of the material, which is the transmittance of light through a sample as seen by the human eye. A commonly used scale that numerically defines colors has been established in 1931 by The Commission Internationale de l'Eclairge (CIE system). This method takes into consideration the response of a standard observer to various color stimuli, the nature of the light source, and the light reflected by the object under study. These functions are used to calculate values (L a b) that define the CIE color spaces. To simplify the representation of a color, the value L represents the brightness of a material, whereas a and b are used to define its

chromaticity, and they can be easily represented on a two-dimensional graph (Fig.2.13).

The experimental setup for colorimetry analysis is similar to the one used for spectroelectrochemistry. The applied potential is controlled by a Voltalab PST50 potentiostat. The polymer coated ITO/cuvette assembly is placed in a grey painted light booth (chromaticity box) that has a light source D50 (5000 K) located in the back. L, a and b data at different polymer doping levels are recorded with a Minolta CS-100 Chroma Meter colorimeter. In order to obtain accurate values, a background measurement on a bare ITO/cuvette assembly was taken either at the beginning or at the end of the polymer colorimetric analysis.
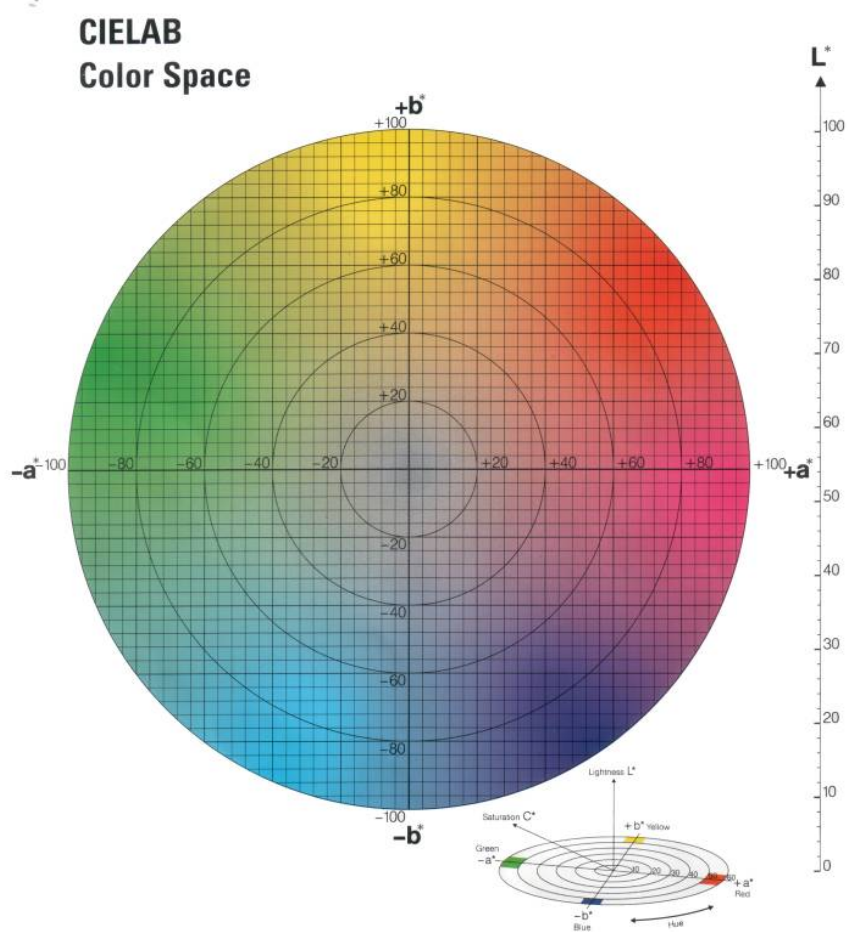
Figure 2.13 CIELAB color space

CHAPTER III

RESULTS AND DISCUSSION

3.1 Characterization of Monomers

3.1.1 Characterization of monomers by NMR Spectroscopy

NMR spectra of the monomers were taken by using $CDCl_3$ as the solvent and chemical shifts (δ) were given relative to tetramethylsilane as the internal standard.

3.1.1.1 ^{1}H-NMR spectrum of HMTA

^{1}H-NMR spectrum of HMTA (Fig. 3.1) evidences resonance signals of thiophene (Th), Th-CH$_2$, NH and CH$_2$ protons of relative intensities corresponding to the number and type of protons. ^{1}H-NMR (δ, ppm) data for HMTA: 7.4-6.9 ppm (m 6H), 5.6 (br, 2H), 3.7 ppm (s 4H), 3.22 ppm (m 4H), 1.54 (m 4H), 1.25 ppm (m 4H).

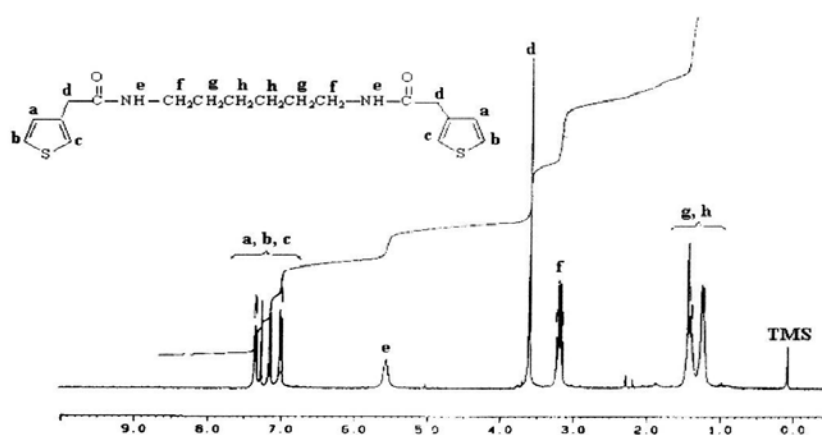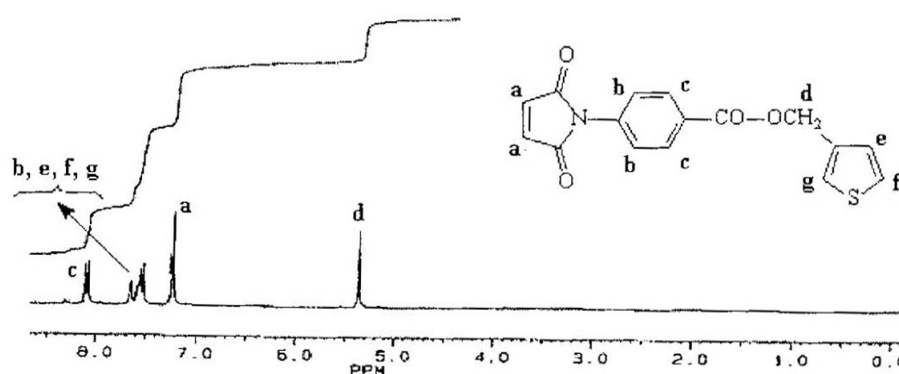**Figure 3.1** ^{1}H NMR spectra of HMTA

61

3.1.1.2 ^{1}H-NMR spectrum of MBThi

^{1}H-NMR (δ, ppm from TMS in DMSO): 8.26-8.23 (d, 2H, Ar-H, ortho to ester group); 7.64-7.59 (d, 2H, Ar-H, ortho to imide group); 7.56-7.53 (m, 1H, 2-position in thiophene ring); 7.26 (s, 1H, 4-position in thiophene ring); 7.23 (s, 2H, CH=CH)); 7.17-7.15 (d, 1H, 5-position in thiophene ring); 4.01 (s, 2H, CH$_2$) (Fig.3.2)
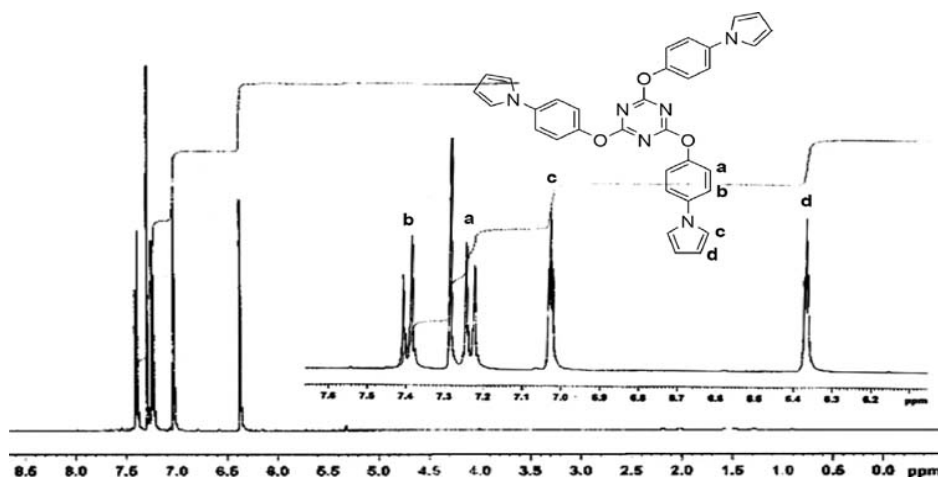

Figure 3.2 ^{1}H NMR spectrum of MBThi

3.1.1.3 ^{1}H-NMR and ^{13}C-NMR Spectra of TriaPy

The structure of TriaPy was confirmed by ^{1}H-NMR and ^{13}C-NMR spectral analysis. ^{1}H-NMR spectrum of the monomer has the characteristic peaks of the structure, as shown in Figure 3.3. ^{1}H-NMR (400MHz, 25 °C, in CDCl$_3$) δ/ppm: 7.36-7.42 (m, J=8.8 Hz, 6H), 7.2-7.26 (m, J=8.8 Hz, 6H), 7.25 (t, J=2.1 Hz, 6H), 6.38 (t, J=2.1 Hz, 6H)

^{13}C-NMR spectrum of TriaPy is shown in Figure 3.4. ^{13}C-NMR (400MHz, 25 °C, in CDCl$_3$) δ/ppm: 173.8, 149.0, 138.9, 122.5, 121.5, 119.4, 110.7.

Figure 3.3 ^{1}H-NMR spectrum of TriaPy
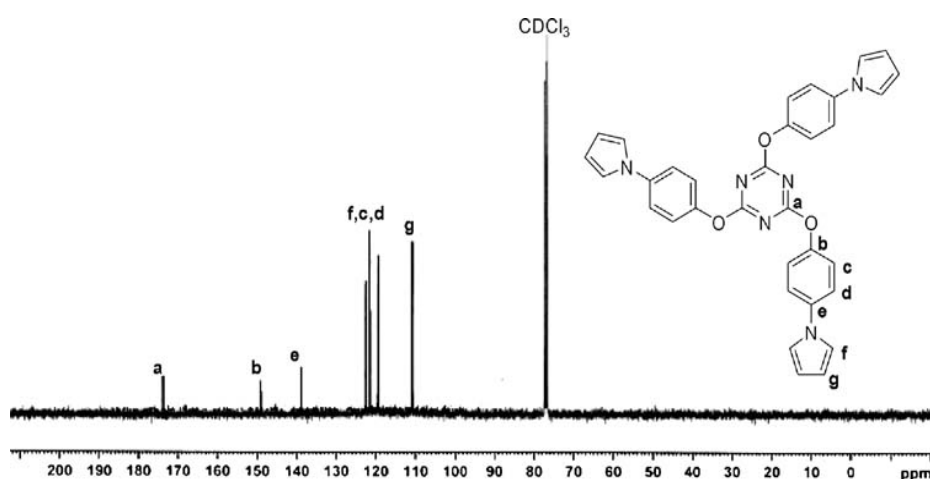
Figure 3.4 ^{13}C-NMR spectrum of the TriaPy

3.1.1.4 ^{1}H-NMR and ^{13}C-NMR Spectra of TriaTh

The structure of TriaTh was confirmed by ^{1}H-NMR and ^{13}C-NMR spectral analysis. ^{1}H-NMR spectrum of the TriaTh has the characteristic peaks of the structure, as shown in Figure 3.5.

^{1}H-NMR (400MHz, 25 °C, in CDCl$_3$) δ/ppm: 7.41 (m, 3H), 7.34 (m, 3H), 7.18 (m, 3H), 5.48 (s, 6H)

63
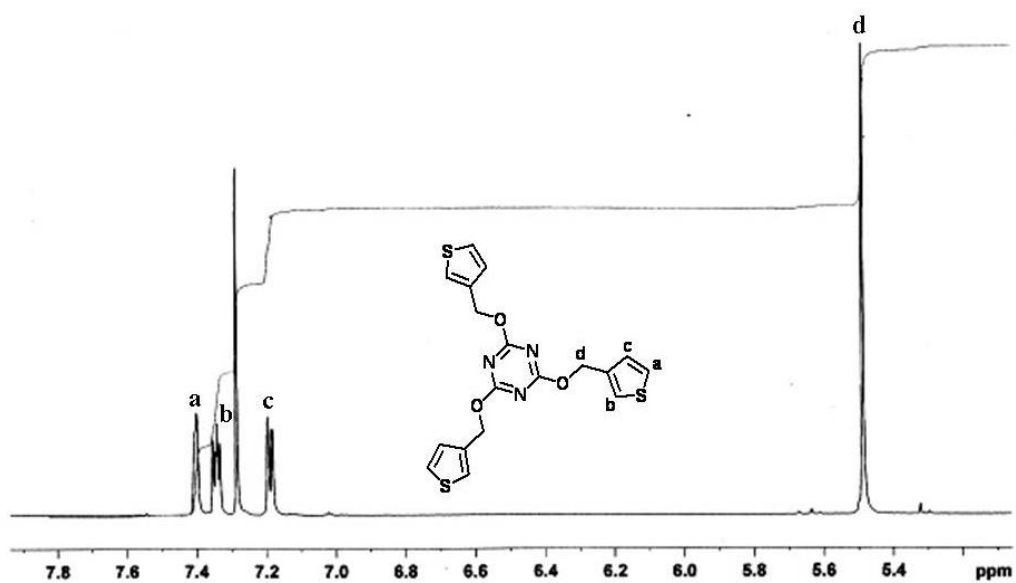
Figure 3.5 ^{1}H-NMR spectrum of TriaTh

^{13}C-NMR spectrum of TriaTh is shown in Figure 3.6. ^{13}C-NMR (400MHz, 25 $^{\circ}$C, in CDCl$_3$) δ/ppm: 173.8, 136.0, 127.6, 126.3, 124.8, 65.0
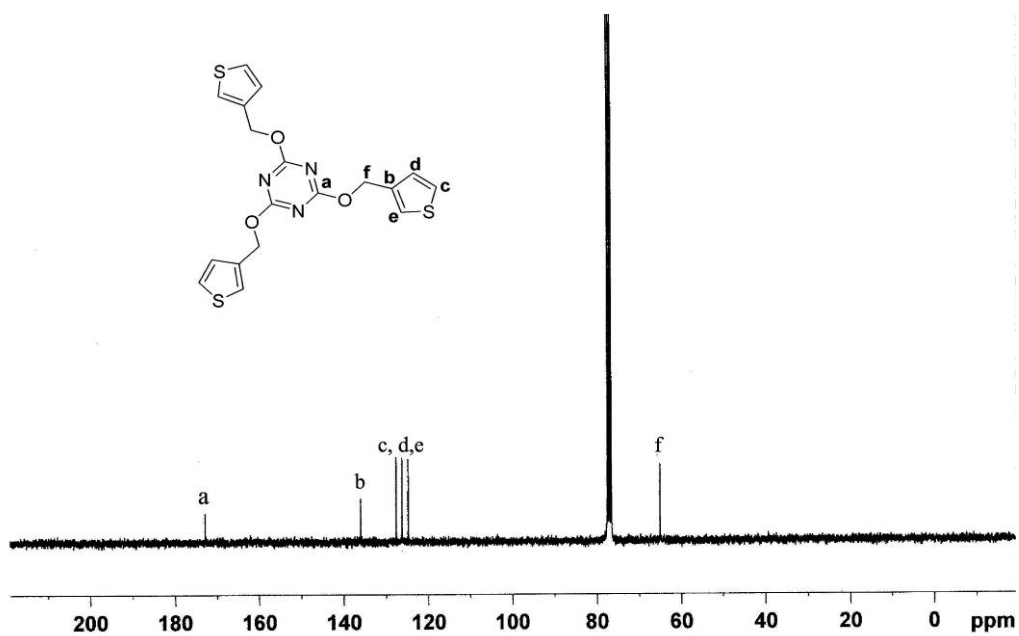
Figure 3.6 ^{13}C-NMR spectrum of TriaTh

64

3.1.1.5 ^{1}H-NMR Spectra of NMT

NMR spectrum of NMT (Fig. 3.7) evidences resonance signals of thiophene, CH_2 and maleimide protons of relative intensities corresponding to the number and type of protons.

^{1}H-NMR ($CDCl_3$) δ ppm: 7.17-7.21 (m, 1H, H_a), 7.06 (s, 1H, H_b), 6.95 (d, 1H, H_c), 6.44 (s, 2H, H_g), 4.19 (t, 2H, $j= 20$ Hz, H_e), 3.70 (t, 2H, $j= 20$ Hz, H_f), 3.54 (s, 2H, H_d),
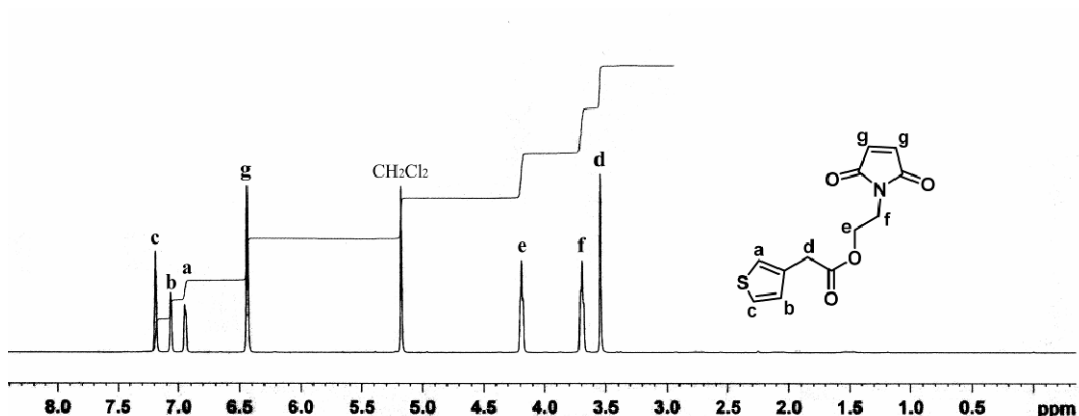
Figure 3.7 ^{1}H-NMR spectrum of NMT

3.1.2 Characterization of Monomers by FTIR

The IR spectral characteristics of the monomers were discussed together with that of the polymers in section 3.2.1.

3.1.3 Characterization of Monomers by Cyclic Voltammetry

3.1.3.1 Cyclic Voltammogram of HMTA

CV's of HMTA in AN-TBAFB system implied that the precursor monomer is not electroactive since it lacks any redox peaks. Upon addition of Th into the medium, an increasing redox peak with increasing scan number was observed

(Fig.3.8b). The number of cycles observed up to a certain current value was different from that of pure polythiophene (PTh) (Fig.3.8a).
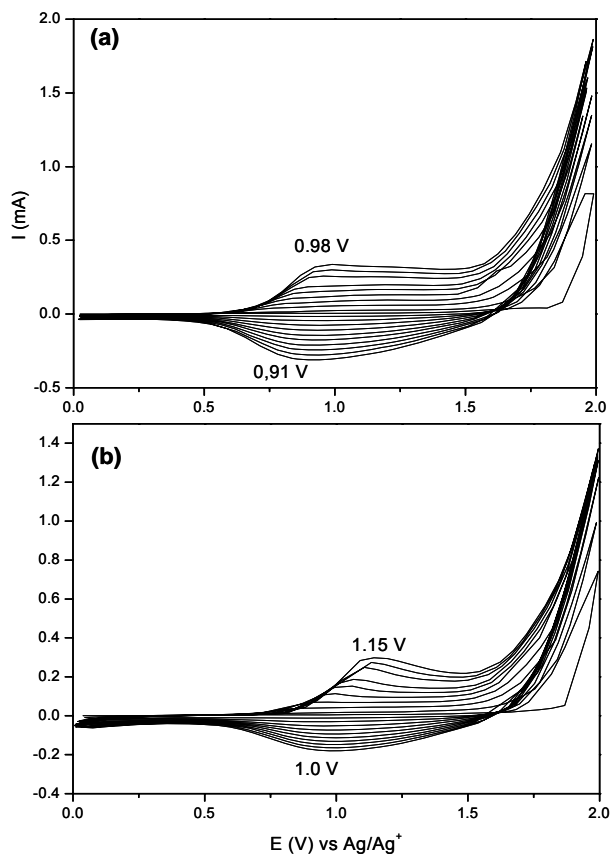
Figure 3.8 Cyclic voltammogram of (a) pure polythiophene (b) HMTA in the presence of thiophene in 0.1 M TBAFB/AN at 250 mV/s scan rate

3.1.3.2 Cyclic Voltammogram of MBThi

CV's of MBThi in AN-TBAFB system implied that the precursor monomer is not electroactive since it lacks any redox peaks. In order to investigate the CV behavior of the copolymer, we performed CV studies in the presence of thiophene. There was a drastic change in the voltammogram, both the increase in the increments between consecutive cycles and the oxidation potential of the

material was different from those of pure thiophene, which in fact could be interpreted as the formation of copolymer. (Fig.3.9).
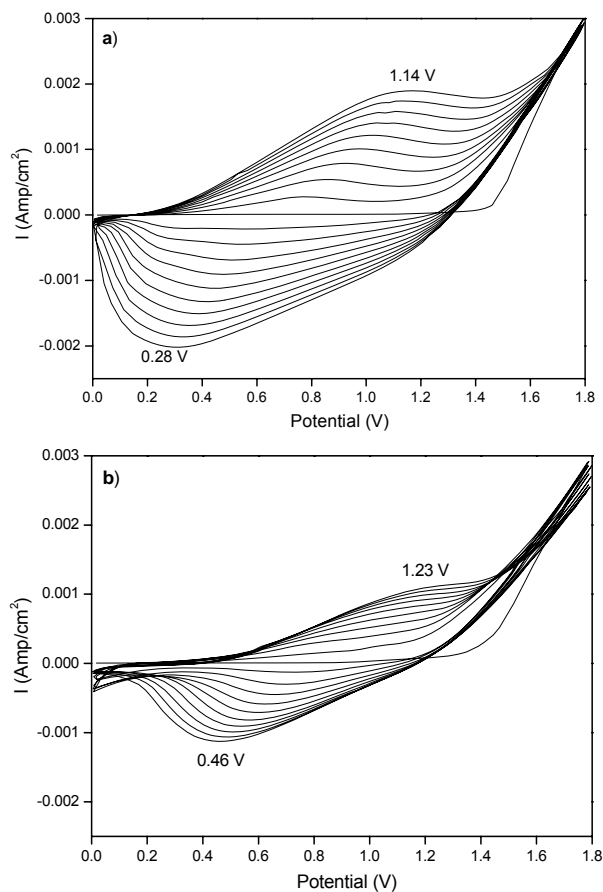

Figure 3.9 Cyclic voltammogram of (a) pure polythiophene (b) MBThi in the presence of thiophene in 0.1 M TBAFB/AN at 250 mV/s scan rate

3.1.3.3 Cyclic Voltammogram of TriaPy

Cyclic voltammogram of TriaPy (Fig.3.10) at 250 mV/s. indicated an oxidation peak at 0.82 V and a reduction peak at -0.2 V. When the range between –1.0 V and +1.8 V was studied, it was seen that the electroactivity increased with increasing scan number. This process promotes a color change of the film from turquoise to red.

Figure 3.10 Cyclic voltammogram of TriaPy between -1.0 and +1.8 V at 250 mV/s scan rate

In order to investigate the CV behavior of the P(TriaPy-co-Py), we performed CV studies in the presence of pyrrole. There was a drastic change in the voltammogram, both the increase in the increments b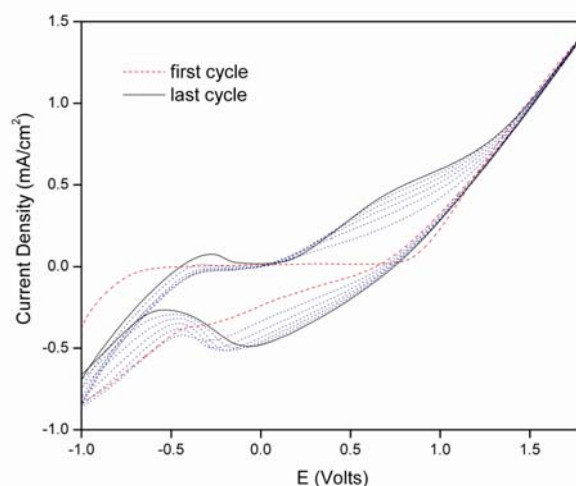etween consecutive cycles and the oxidation potential of the material were different than those of pure pyrrole and TriaPy, which in fact could be interpreted as the formation of copolymer. (Fig.3.11).

Figure 3.11 Cyclic voltammogram of (a) pure polypyrrole (b) TriaPy in the presence of pyrrole in 0.1 M TBAFB/AN at 250 mV/s scan rate

3.1.3.4 Cyclic Voltammogram of TriaTh

CV's of TriaTh in AN-TBAFB system implied that the precursor monomer is not electroactive. Upon addition of Th into the reaction medium, an increasing redox peak with increasing scan number was observed (Fig.3.12b). The number of cycles observed up to a certain current value didn't similar that of pure polythiophene (PTh) (Fig.3.12a).
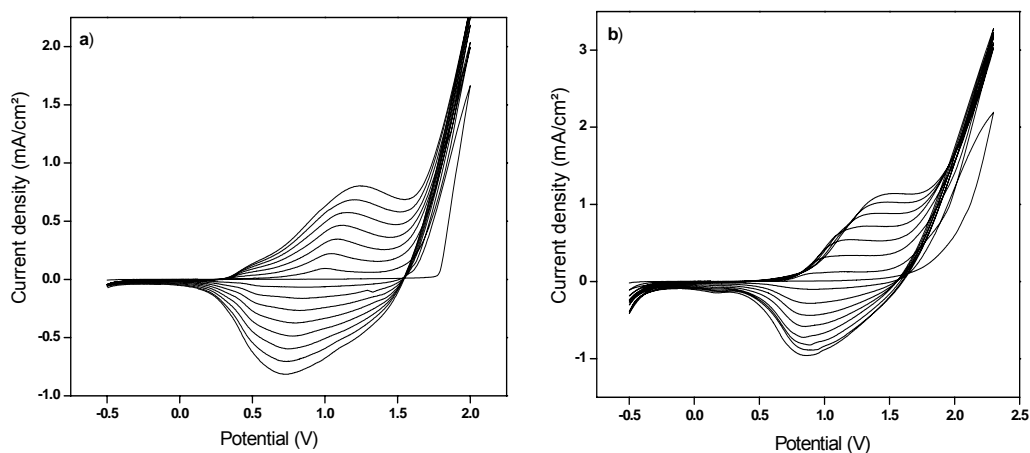
Figure 3.12 Cyclic voltammogram of (a) pure thiophene (b) TriaTh in the presence of thiophene in 0.1 M TBAFB/AN at 250 mV/s scan rate
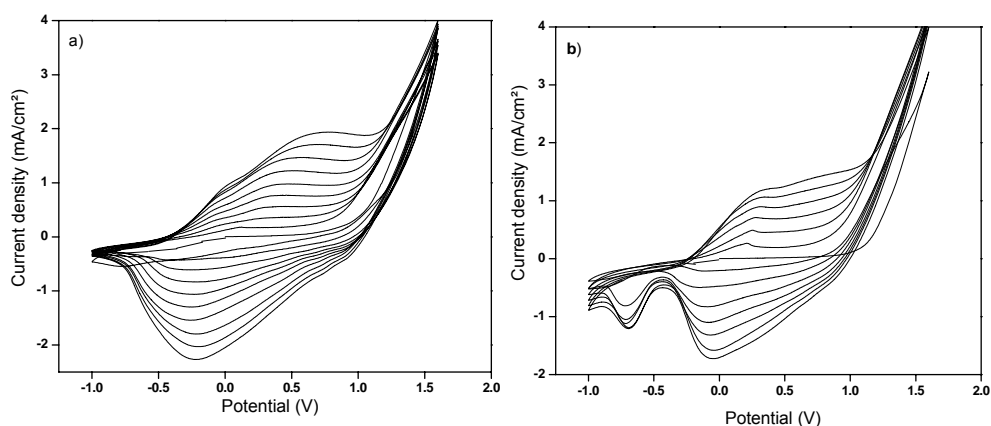
3.1.3.5 Cyclic Voltammogram of NMT

In the cyclic voltammogram of NMT (Fig. 3.13), at 1.34 V (a) the monomer is oxidized to its radical cation. Monomer oxidation is immediately followed by chemical coupling that affords oligomers in the vicinity of the electrode. Once these oligomers reach a certain length, they precipitate onto the electrode surface where the chains can continue to grow in length. The electroactivity of the polymer deposited onto the WE can be monitored by the appearance of a peak (-0.35 V) corresponding to the reduction of the oxidized polymer while scanning in the cathodic direction (b). A second positive scan reveals another oxidation peak (0.68 V) at a lower potential than the monomer

69

oxidation peak (c). This is due to the oxidized polymer. Another noticeable fact is the increase in monomer oxidation peak current in the subsequent scans. As the peak current is directly proportional with the electrode area, this increase in the peak current could be attributed to an increase of the WE area due to the electrodeposited polymer.
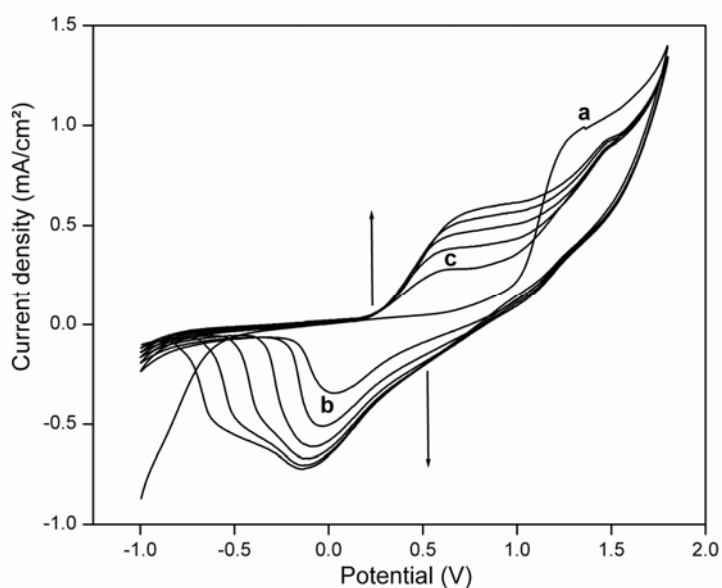
Figure 3.13 Cyclic voltammograms of the NMT in BFEE/AN at 250 mV/sec

In order to investigate the CV behavior of the copolymer, we performed CV studies in the presence of thiophene under same experimental conditions. There was a drastic change in the voltammogram, both the increase in the increments between consecutive cycles and the oxidation potential of the material were different than those of from NMT and thiophene, which, in fact, could be interpreted as the formation of copolymer (Fig. 3.14).
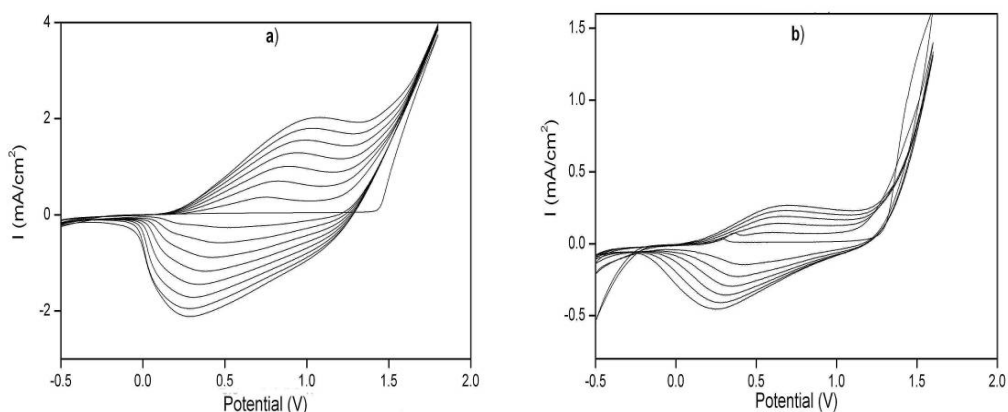
Figure 3.14 Cyclic Voltammogram of a) Th b) NMT in the presence of thiophene in AN:BFEE (1:1, v:v)

3.2 Characterization of Polymers

3.2.1 FTIR Spectroscopy

The IR spectral characteristics of the monomers were discussed together with that of the polymers.

3.2.1.1 FTIR Spectra of HMTA and P(HMTA-co-Th)

HMTA showed a characteristic, intense peak at 1640 cm^{-1}, which belongs to C=O (amide carbonyl) stretching vibrations. Two peaks at 2948 cm^{-1} and 2867 cm^{-1} correspond to aliphatic methylene stretchings. The peak at 1251 cm^{-1} indicates C–O–C ester group vibrations while the peak at 3265 cm^{-1} is attributed to N-H streching vibration. Also, the peak at 739 cm^{-1} is the result of aromatic C–H$_\alpha$ stretching of thiophene units.

FTIR spectrum of P(HMTA-co-Th) showed intense peak at 1082 cm^{-1} which belongs to dopant ions. A characteristic peak 1640 cm^{-1} belonging to carbonyl group of HMTA was also observed. These results prove copolymerization. Figure 3.15 shows FTIR spectra of HMTA and its copolymer with thiophene.

71
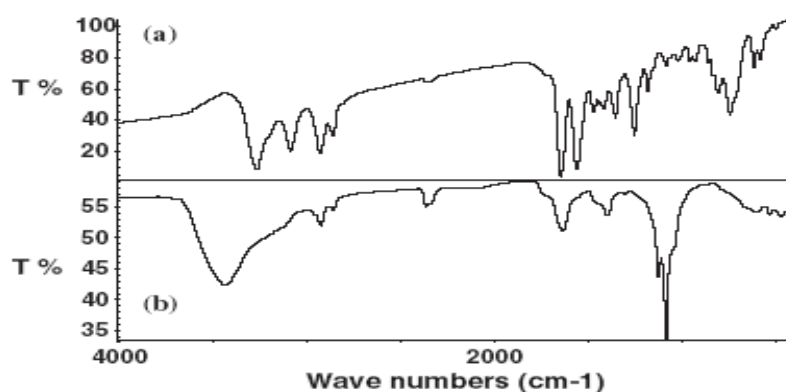
Figure 3.15. IR spectrum of (a) HMTA and (b) P(HMTA-co-Th)

3.2.1.2 FTIR Spectra of MBThi and P(MBThi-co-Th)

The FTIR spectrum of the MBThi showed the usual features of substituted thiophenes (Fig.3.16b). The absorption bands at 3170 and 3105 cm^{-1} correspond to the aromatic C-H stretching originating from the benzene ring and thiophene moiety, the bands at 2955 cm^{-1} corresponds to the aliphatic substituents (methyl group) of the monomer. The presence of the intense peak at 1718 cm^{-1} was attributed to C=O stretching vibrations and the bands in the region of 1100-1213 cm^{-1} were attributed to C-O-C (ester group) stretching vibrations. The bands at 1605 and 1513 cm^{-1} were attributed to the C=C units of benzene ring and thiophene, the bands at 1389 and 1280 cm^{-1} to the C-N vibrations of the maleimide group respectively. Thiophene moiety of the monomer was further characterized by the presence of the bands at 769 and 832 cm^{-1} (C-H$_\alpha$ and C-H$_\beta$ stretching respectively).

The FTIR spectrum of electrochemically synthesized copolymer (Fig.3.16a) revealed the presence of C=O, C-O-C and C=C stretching vibrations at 1711 cm^{-1}, 1115 cm^{-1} and 1510 cm^{-1} due to ester and phenyl groups of the monomer respectively. Besides, 2945 cm^{-1} is due to C-H stretching vibrations of methyl group, the peak at 1395 cm^{-1} are due to C-C and C-N stretching vibrations. The bands at 769 cm^{-1} and 832 cm^{-1} indicating C-Hα and C-Hβ stretching of the thiophene group of the monomer disappeared

completely, whereas evolution of a new absorption peak at 840 cm^{-1} (2,3,5-trisubstituted thiophene) was observed. The peaks around 1078 and 1611 cm^{-1} indicated the presence of dopant anion and polyconjugation.
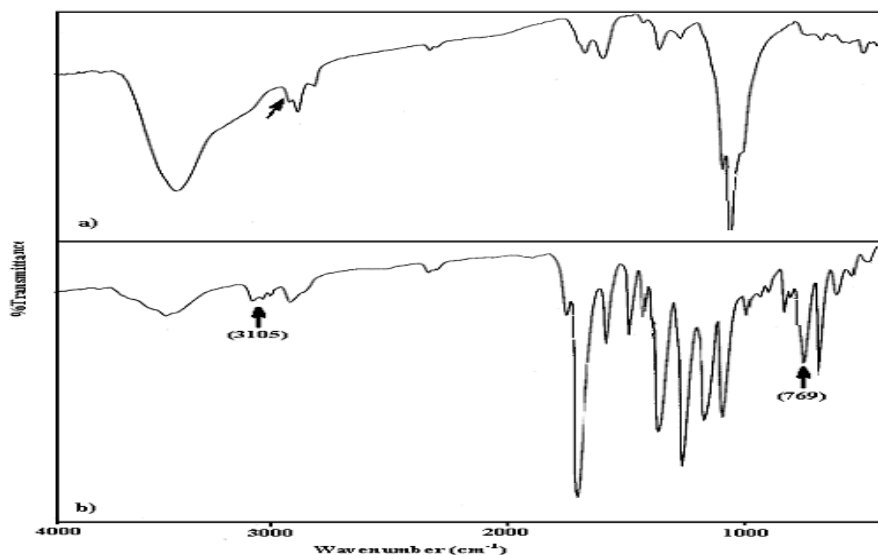
Figure 3.16 IR spectrum of (a) P(MBThi-co-Th) and (b) MBThi

3.2.1.3 FTIR Spectra of TriaPy, P(TriaPy) and P(TriaPy-co-Py)

The FTIR spectrum of TriaPy (Fig. 3.17a) exhibits characteristic features of N-substituted pyrroles and triazines. The absorption bands at 733, 1018 and 1080 cm^{-1} correspond to C-H stretching of N-substituted pyrroles. C-O-C stretching vibrations are observed in the region of 1200–1220 cm^{-1}. The absorption band at 1511 cm^{-1} indicates the presence of benzene ring. The strong absorption bands at 1573, 1373 and 1327 cm^{-1} were assigned to the C=N of the *s*-triazine ring.

FTIR spectrum of electrochemically prepared P(TriaPy) (Fig. 3.17b) showed an intense peak at 1082 cm^{-1} which belongs to dopant ions. A new band appears at 1640 cm^{-1} indicating the conjugation in addition to characteristic bands of TriaPy.

FTIR spectrum of electrochemically prepared P(TriaPy-co-Py) (Fig. 3.17c) showed characteristic bands of TriaPy.
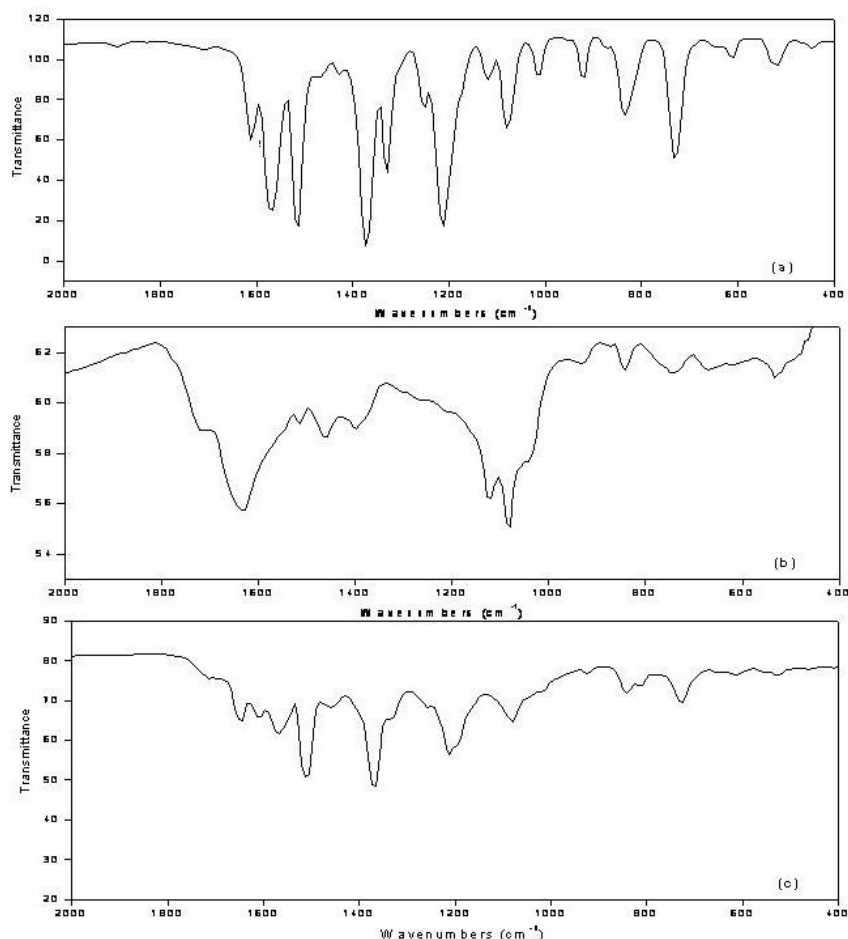
Figure 3.17 FTIR spectra of (a)TriaPy (b) P(TriaPy) and c) P(TriaPy-co-Py)

3.2.1.4 FTIR Spectra of TriaTh and P(TriaTh-co-Th)

FTIR spectrum for the TriaTh (Fig. 3.18a) shows peaks at 3078 cm^{-1} (aromatic C-H), 2937-2900 cm^{-1} (aliphatic C-H) and strong absorption bands at 1566, 1382 and 1328 cm^{-1} (C=N of the *s*-triazine ring). 1260-1000 cm^{-1} (C-O-C symmetric and asymmetric stretching), 780 cm^{-1} (thienylene out of plane C-H$_\alpha$

74

stretching), 820 cm^{-1} (thienylene out of plane C-H$_\beta$ stretching), 1423, 1347 cm^{-1} (aromatic C=C, C-C ring stretching), 612 cm^{-1} (C-S-C stretching)

FTIR spectrum of electrochemically prepared P(TriaTh) (Fig. 3.18b). showed an intense peak at 1082 cm^{-1} which belongs to dopant ions. A new band appears at 1640 cm^{-1} indicating the conjugation in addition to characteristic bands of TriaTh.
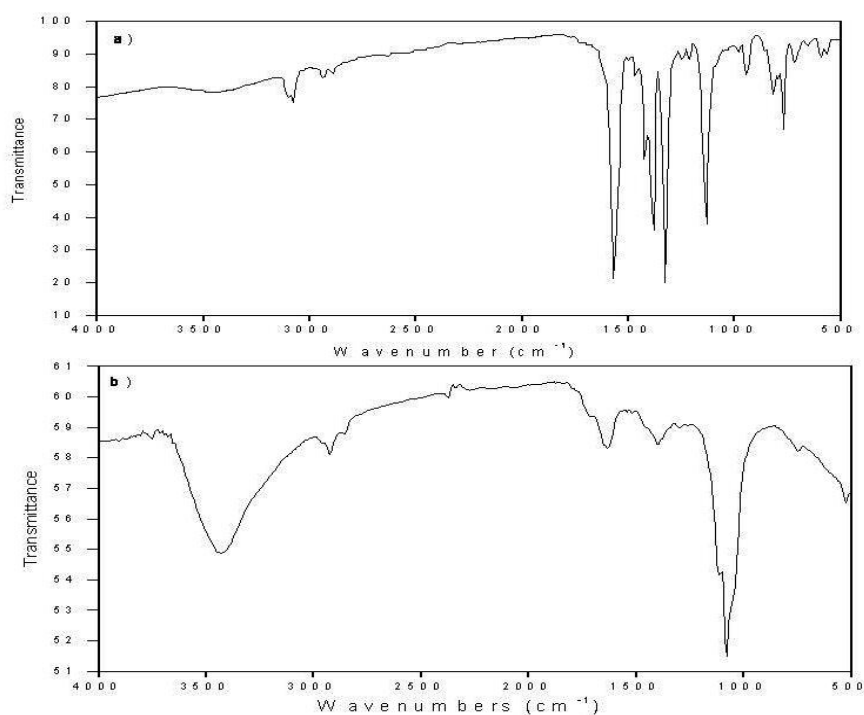
Figure 3.18 FTIR spectra of (a)TriaTh (b) P(TriaTh-co-Th)

3.2.1.5 FTIR Spectra of NMT, P(NMT) and P(NMT-co-Th)

Figure 3.19 (a) shows the FT-IR spectrum of the NMT product in the range 4000-500 cm^{-1}. The absorption bands at 1543, 1410, 855, 788 and 665 cm-1 are due to the vibrations of C-H and C=C bonds of thiophene rings. 3100 attributed to CH stretching of maleimide and two peaks at 1735 and 1697 cm^{-1}

75

are related to CO stretching vibrations of ester and maleimide ring respectively. Peaks at 2948 and 2867 cm^{-1} correspond to aliphatic methylene stretchings and the bands in the region of 1100-1250 cm^{-1} is due to C-O-C symmetric and asymmetric stretching vibrations of spacing methyl chain.

As seen in Figure 3.19(b), besides the characteristic monomer peaks, FTIR spectra of P(NMT) also contains a new shoulder appeared at 1637 cm^{-1} indicating the polyconjugation upon polymerization and the peak appeared at 1083 cm^{-1} revealed the presence of the dopant ion (BF_4^-).
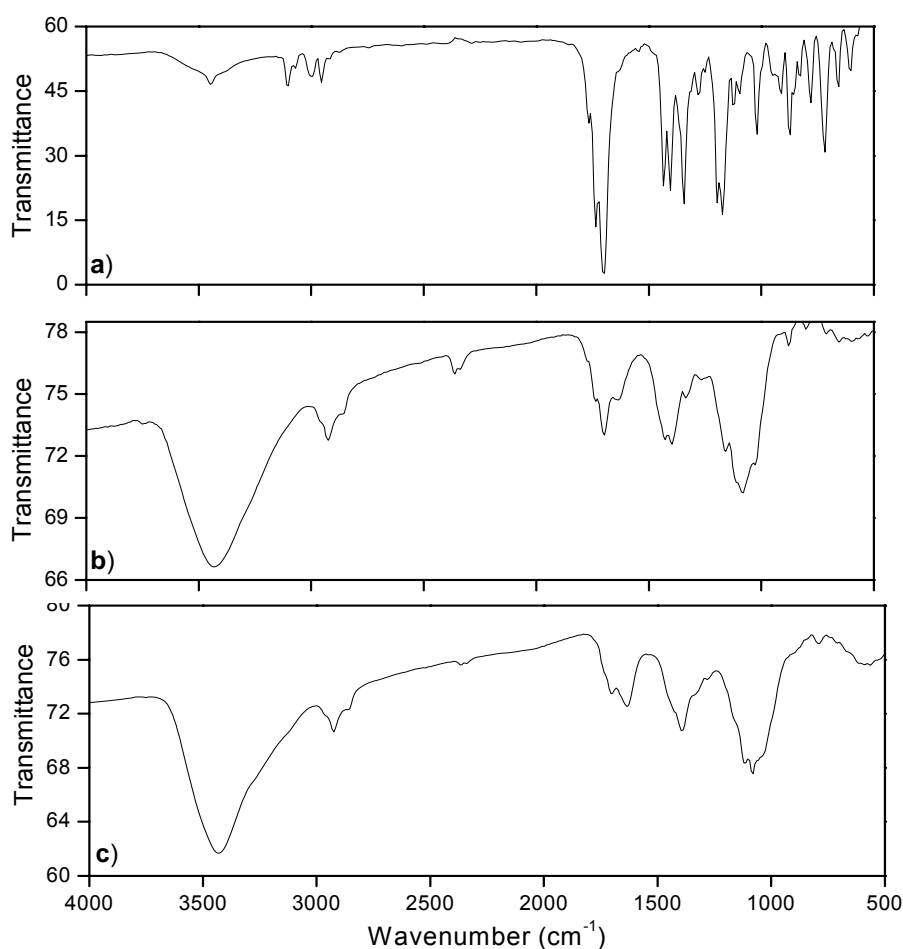
Figure 3.19 FTIR spectra of (a) NMT (b) P(NMT) (c) P(NMT-co-Th)

3.2.2 Conductivity Measurements

Electrical conductivity measurements were carried out by using four-point probe technique. The conductivities of the polymer films are shown in Table 3.1.

Table 3.1 Conductivities of the polymer films

Polymer	Conductivity
P(HMTA-co-Th)	$2.4.10^{-3}$
P(MBThi-co-Th)	$4.4.10^{-4}$
P(TriaPy)*	$3.7.10^{-6}$
P(TriaPy-co-Py)	$8.3.10^{-3}$
P(TriaTh-co-Th)	$6.2.10^{-4}$
P(NMT)*	$6.8.10^{-5}$
P(NMT-co-Th)	$4.1.10^{-4}$

*Conductivity measurements of polymers were done on pellets

3.2.3 Scanning Electron Micrographs

As seen in Figure 3.20, P(HMTA-co-Th) and P(MBThi-co-Th) reveal droplets on the surface which is quite different from pure polythiophene morphology.

The surface morphology of electrochemically synthesized P(TriaPy) film (solution side) has a spongy structure (Fig. 3.21a), which is quite different than P(TriaPy-co-Py) (Fig. 3.21b) and a regular cauliflower structure for polypyrrole.
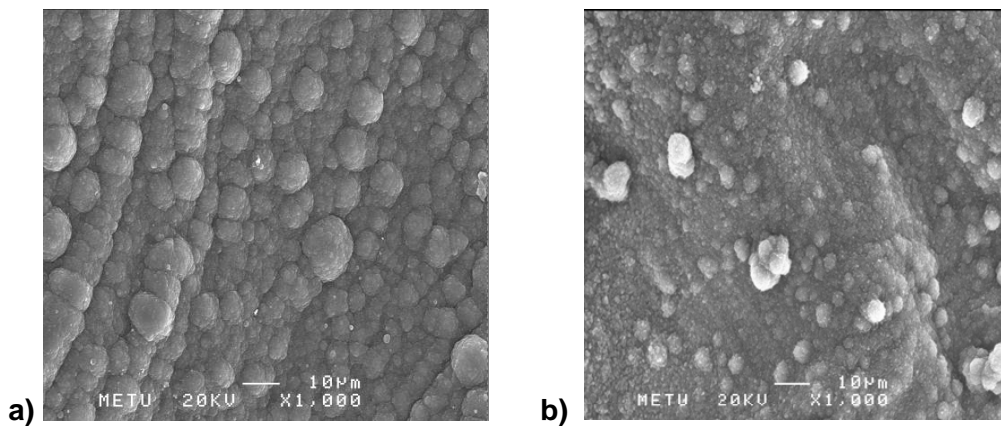
Figure 3.20 Surface morphology of a) P(HMTA-co-Th) and b) P(MBThi-coTh)
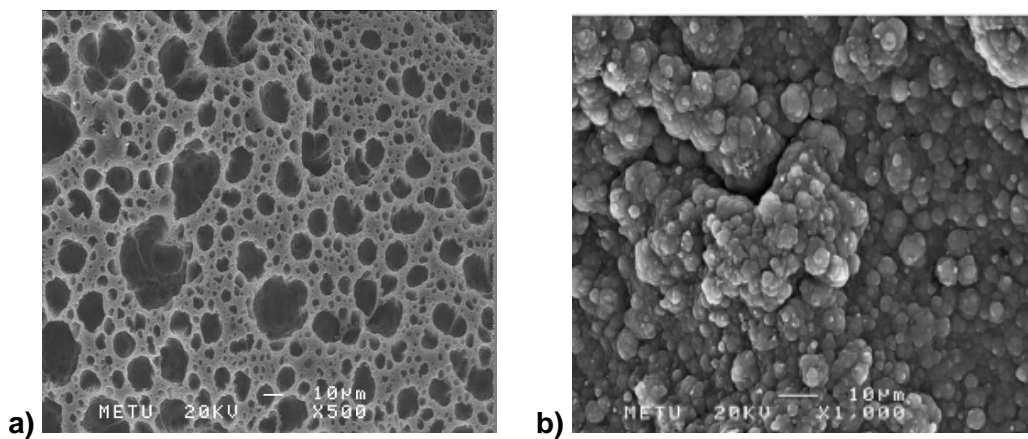
Figure 3.21 Surface morphology of a) P(TriaPy) and b) P(TriaPy-co-Py)

The surface morphology of electrochemically synthesized P(TriaTh-co-Th) film (solution side) is shown in Figure 3.22.
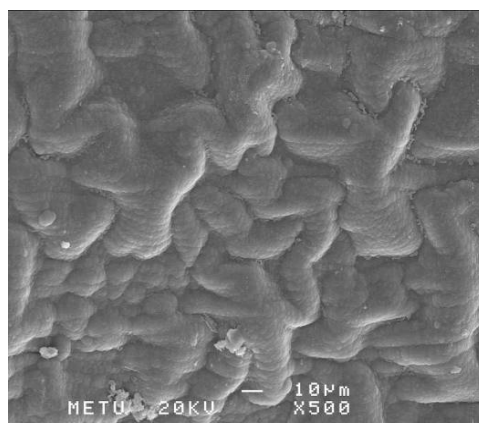
Figure 3.22 Surface morphology of P(TriaTh-co-Th)

Solution side of P(NMT) film showed uniform and very smooth structure (Fig.3.23a). SEM micrograph of P(NMT-co-Th) (Fig. 3.23b) was significantly different than pure PTh and P(NMT). These completely different morphologies indicate the formation of a new material other than the monomers and thiophene.
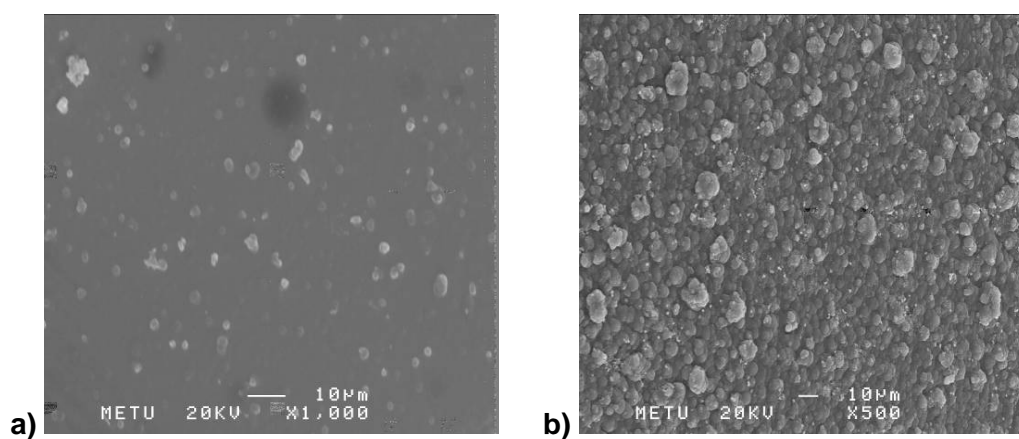
Figure 3.23 Surface morphology of a) P(NMT) and b) P(NMT-co-Th)

3.3. Electrochromic Properties of Conducting Polymers

3.3.1 Spectroelectrochemistry of the Conducting Polymers

3.3.1.1 Spectroelectrochemistry of P(HMTA-co-Th)

The film was deposited on ITO via potentiostatic electrochemical copolymerization of HMTA (0.01 M) in the presence of TBAFB and Th in AN at 1.9V. Copolymer coated ITO was investigated by UV-Vis spectroscopy in the monomer free electrolytic system by switching between +0.2V and +1.6V (Fig. 3.24). The onset energy for the π-π* transition (electronic band gap) was found to be 1.95 eV and λ_{max} was 505 nm. Appearance of the peak around 741 nm could be attributed to the evolution of polaron band. Upon further oxidation, appearance of another absorption was observed at longer wavelengths (>1000 nm) due to bipolaron change carriers.

3.3.1.2 Spectroelectrochemistry of P(MBThi-co-Th)

P(MBThi-co-Th) films were potentiodynamically deposited onto ITO-coated glass slides in TBAFB/AN/BFEE between 0.0V and 1.8V. Spectroelectrochemical properties were studied in the same but monomer free solution. The λ_{max} value for the π-π* transitions in the neutral state of copolymer was found to be 440 nm, revealing light orange color which are all significantly different than pure polythiophene (λ_{max}=495 nm). The electronic band gap defined as the onset energy for the π-π* transition was found to be 1.74 eV. Upon increase in the applied voltage, the evolution of a new absorption band at 730 nm was observed due to evolution of charge carriers (Fig. 3.25), which was accompanied by gradual decrease in the intensity of the bands at λ_{max}. At 1.1 V the extreme oxidation was achieved, where color of the copolymer was blue.
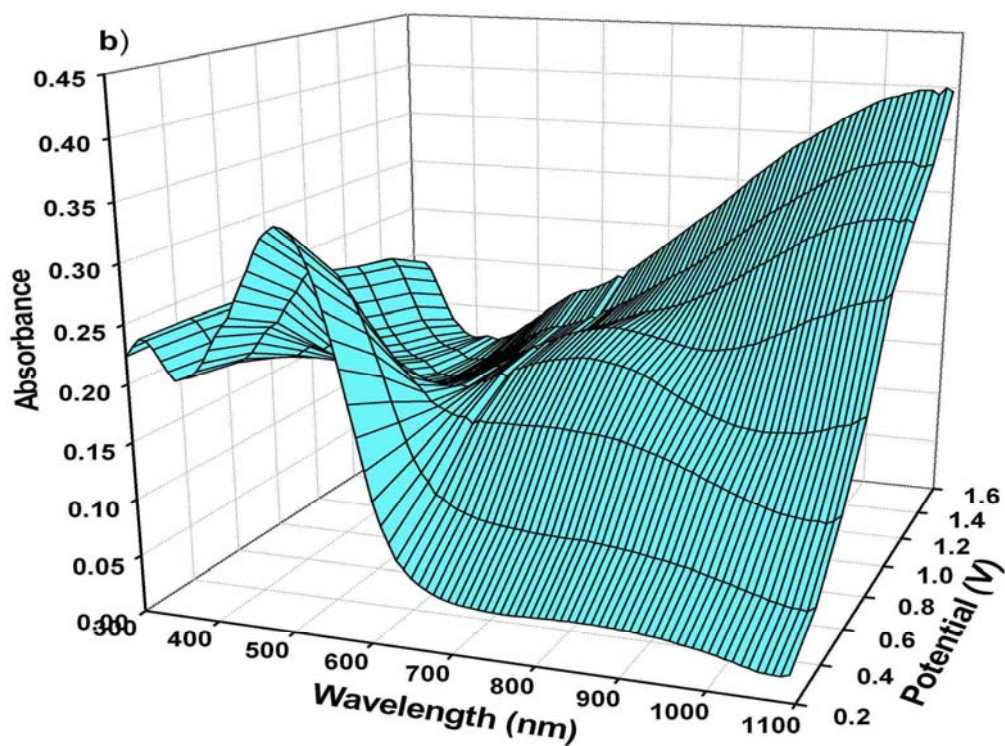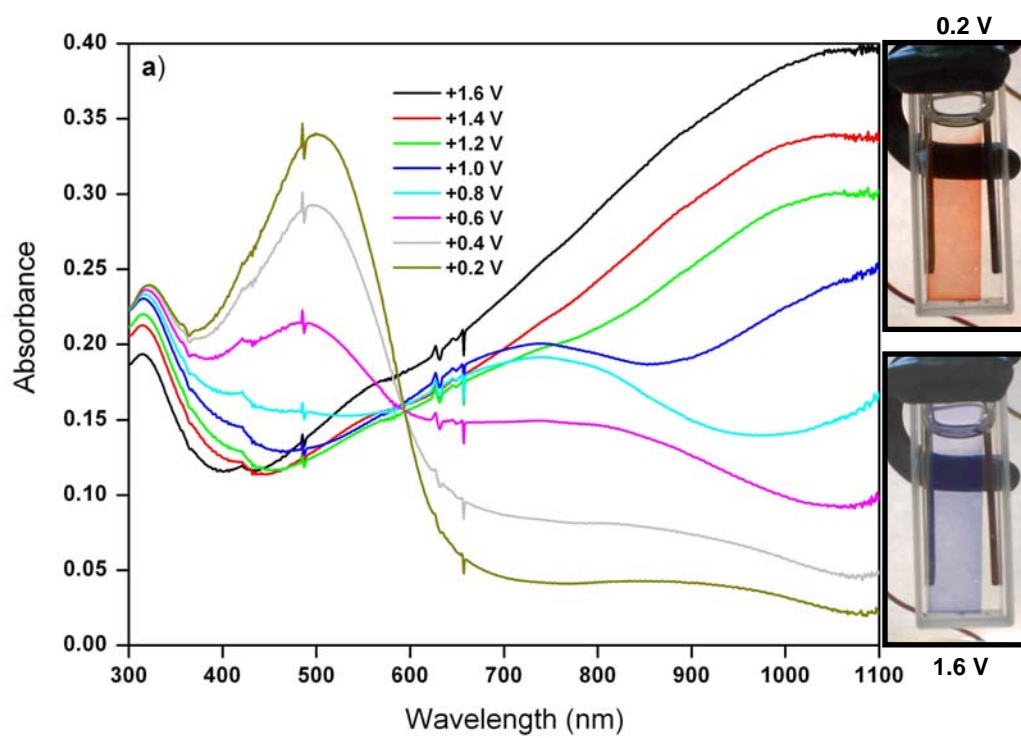
Figure 3.24 Optoelectrochemical spectrum of P(HMTA-co-Th) at applied potentials between 0.2 and +1.6 V in 0.1 M TBAFB/AN a) 2D b)3D
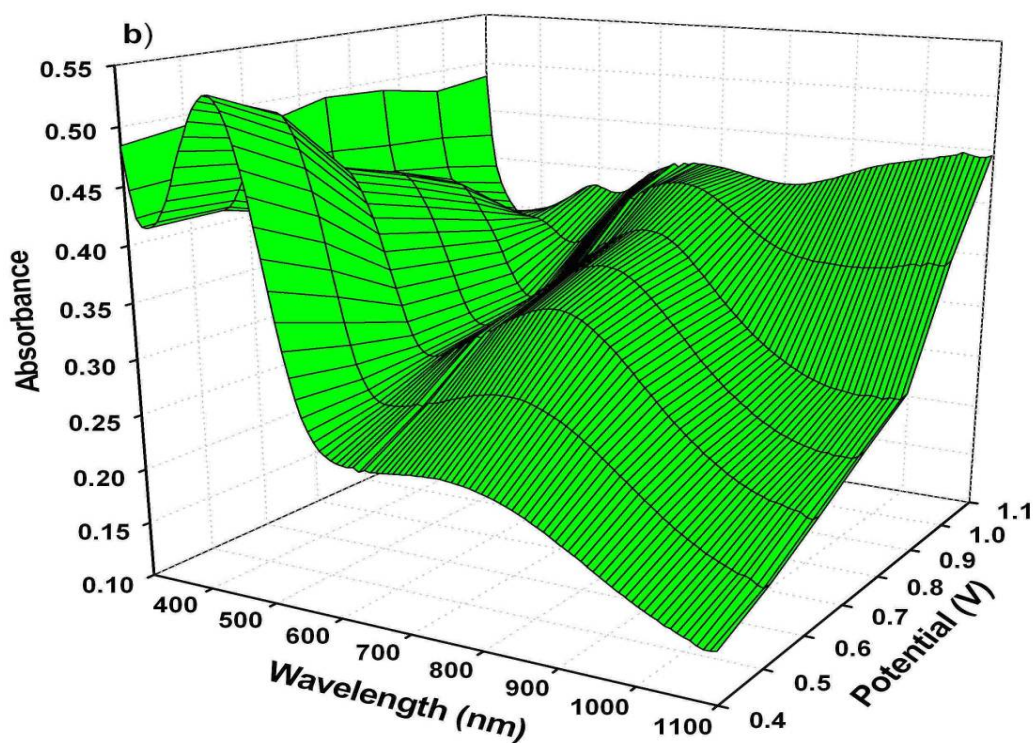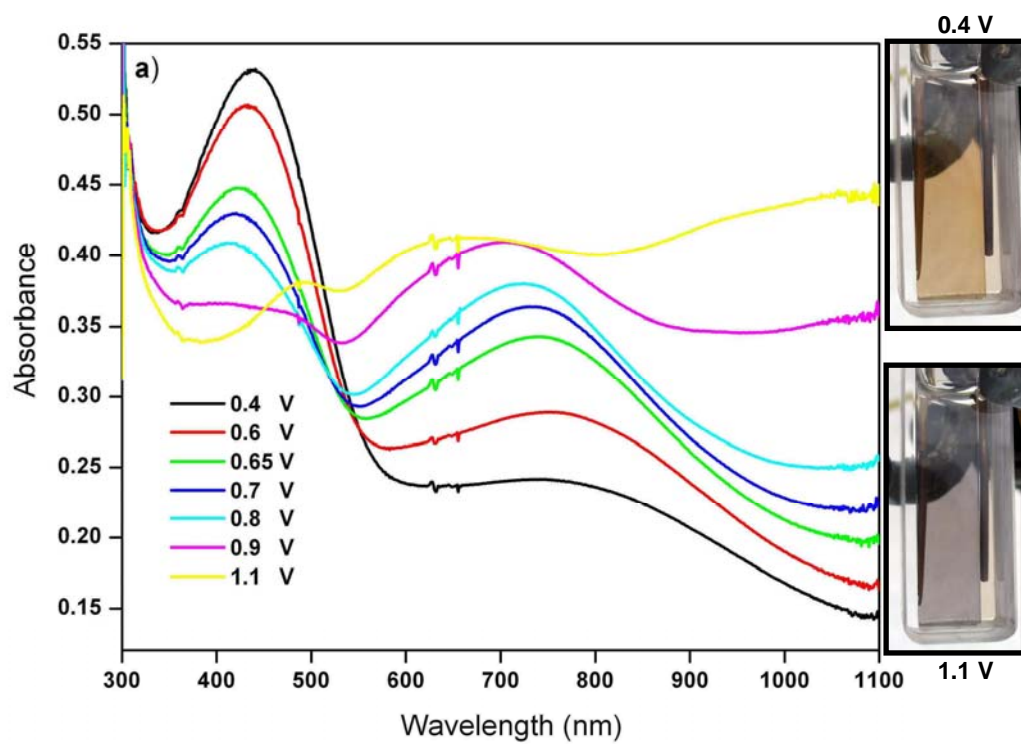
Figure 3.25 Optoelectrochemical spectrum of P(MBThi-co-Th) at applied potentials between 0.4 and +1.1 V in 0.2 M TBAFB/AN a) 2D b)3D

3.3.1.3 Spectroelectrochemistry of P(TriaPy)

Spectroelectrochemical analysis of the P(TriaPy) film was studied in order to elucidate electronic transitions upon doping of the polymer (Fig. 3.26).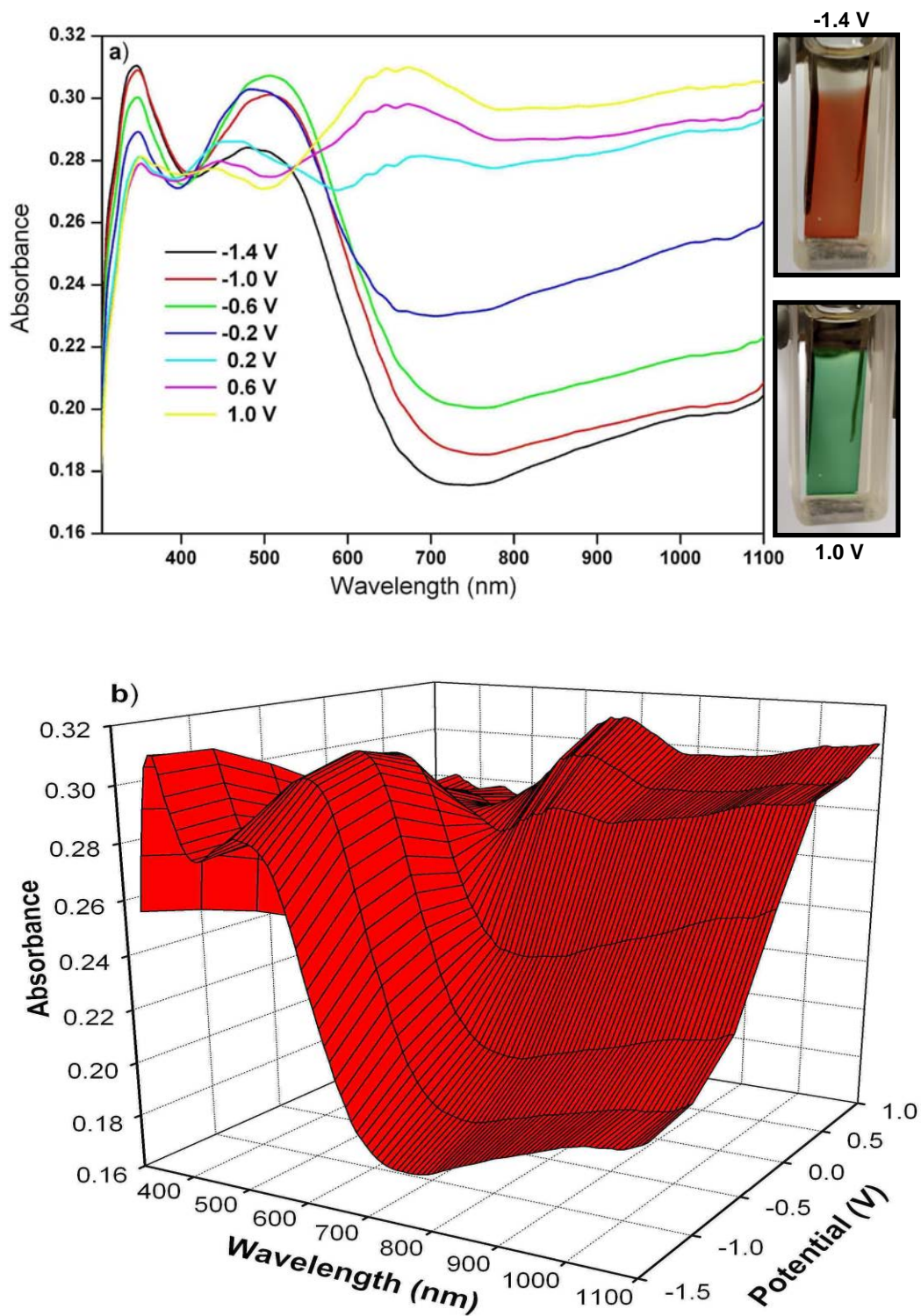 The film was deposited on ITO via potentiostatic electrochemical polymerization of TriaPy (0.1 M) in the TBAFB/DM:AN (1:3) at +1.2 V. P(TriaPy) coated ITO glass electrodes was investigated by UV–vis spectroscopy in the same but monomer free electrolytic system via switching between -1.4 and +1.0 V with incremental increases in applied potential. Upon applied voltage, decrease in the intensity of the π-π^* transition and formation of charge carrier bands were observed. There was a gradual decrease in the peak intensity at around 346 nm upon increase in the applied potential, which was accompanied by the increase in the intensity of peaks at around 508 nm due to the formation of polaron bands at interval potentials. Upon further oxidation, appearance of another absorption was observed at 665 nm due to bipolaron change carriers. The onset energy for the π-π^* transition (electronic band gap) was found to be 2.97 eV.

3.3.1.4 Spectroelectrochemistry of P(TriaPy-co-Py)

P(TriaPy-co-Py) films were potentiodynamically deposited onto ITO-coated glass slides in TBAFB/AN between -0.4 V and 1.2 V. The λ_{max} value for the π-π^* transitions in the neutral state of copolymer was found to be 371 nm, revealing light orange color. The electronic band gap defined as the onset energy for the π-π^* transition was found to be 2.37 eV. Upon increase in the applied voltage, the evolution of a new absorption band at ~500 nm was observed due to evolution of charge carriers (Fig. 3.27), which was accompanied by gradual decrease in the intensity of the bands at λ_{max}. At 1.2 V the extreme oxidation was achieved, where color of the copolymer was blue.

Figure 3.26 Optoelectrochemical spectrum of P(TriaPy) film a) 2D b)3D
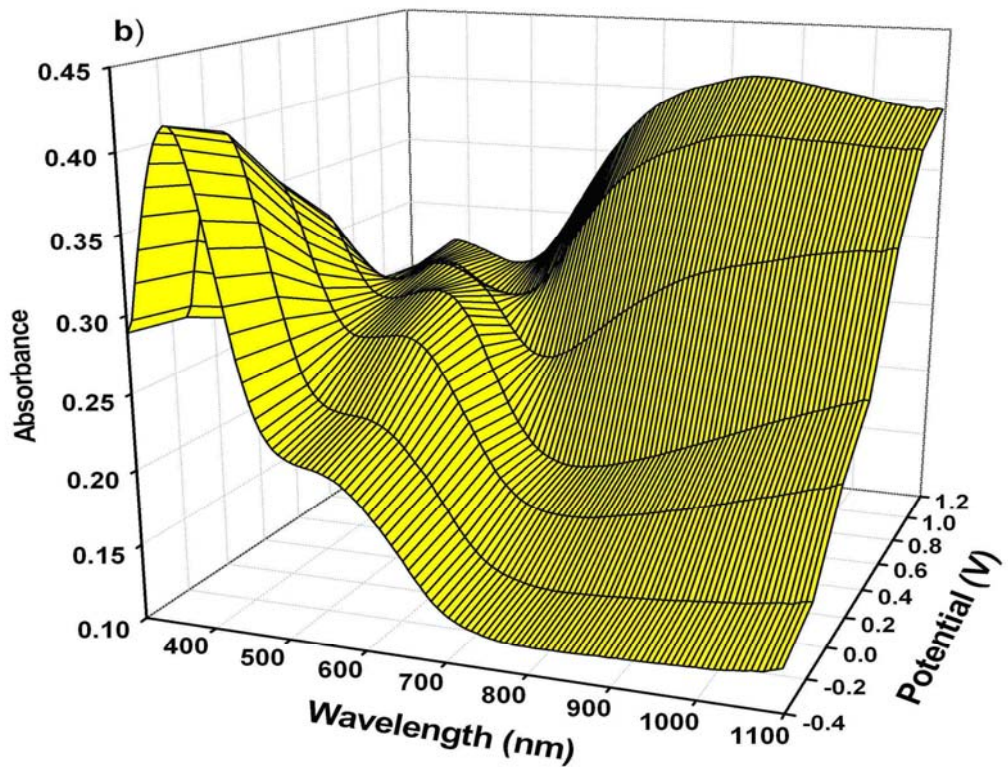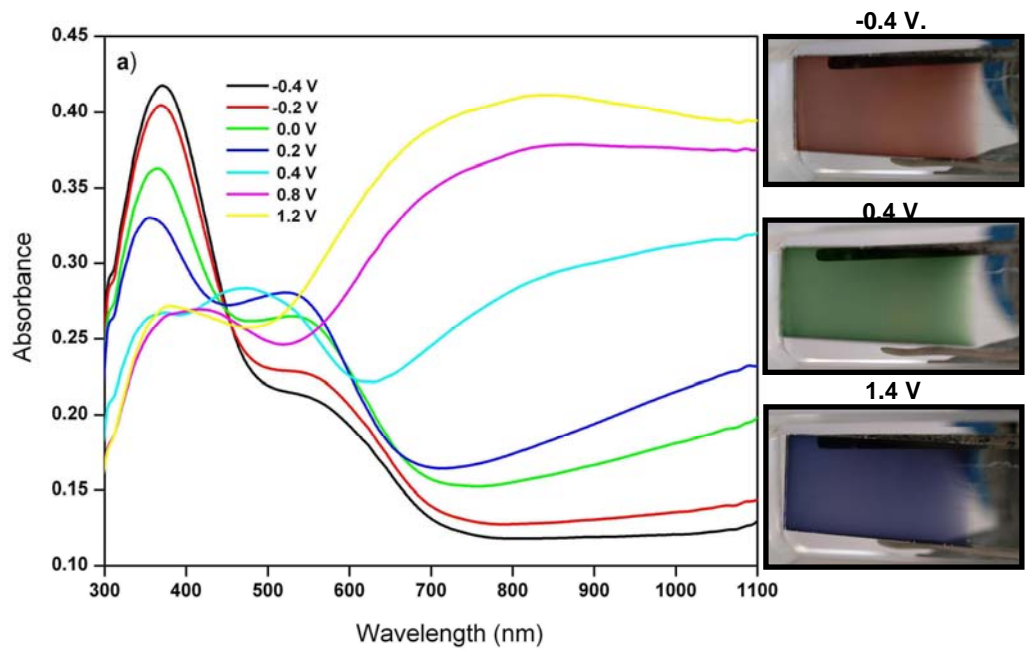
Figure 3.27 Optoelectrochemical spectrum of P(TriaPy-co-Py) film a) 2D b)3D

3.3.1.5 Spectroelectrochemistry of P(TriaTh-co-Th)

The copolymer film was deposited on ITO via potentiostatic electrochemical polymerization in the TBAFB/DM:AN (1:3) at +1.9 V. P(TriaTh-co-Th) coated ITO glass electrodes was investigated by UV–vis spectroscopy in the same but monomer free electrolytic system via switching between -0.2 and +1.8 V . There was a gradual decrease in the peak intensity at around 390 nm upon increase in the applied potential. The onset energy for the π-π^* transition (electronic band gap) was found to be 1.97 eV (Fig. 3.28).

3.3.1.6 Spectroelectrochemistry of P(NMT)

P(NMT) coated ITO was investigated by switching between +0.2V and +1.2V (Fig. 3.29). The onset energy for the π-π^* transition (electronic band gap) was 2.34 eV and λ_{max} was 417 nm. There was a gradual decrease in the peak intensity at 417 nm upon increase in the applied potential, which was accompanied by the increase in the intensity of peaks at 733 nm due to the formation of charge carrier bands (Fig. 3.29). Appearance of the peak 733 nm could be attributed to the evolution of a polaron band. Upon further oxidation, due to formation of bipolaron change carriers there was a decrease in the intensity of the polaron band.

3.3.1.7 Spectroelectrochemistry of P(NMT-co-Th)

P(NMT-co-Th) film was potentiostatically synthesized at 1.7 V on ITO electrode. Electrolyte solution composed of 0.01 M NMT, 0.005 M Th, AN:BFEE (1:1, v:v) and TBATFB (0.1 M). The spectroelectrochemical and electrochromic properties of the resultant copolymer were studied by applying potentials ranging between -0.8 V and +1.2 V in monomer free (1:1, v:v) AN:BFEE/TBATFB (0.1 M) medium. At the neutral state λ_{max} due to the π-π^* transition of the copolymer was found to be 488 nm and Eg was calculated as 1.99 eV. There was a gradual decrease in the peak intensity at 488 nm upon increase in the applied potential, which was accompanied by the increase in the intensity of peaks at 716 nm due to the formation of charge carrier

(polaron) bands (Fig. 3.30). Upon further oxidation, due to formation of bipolaron change carriers there was a decrease in the intensity of the polaron band.
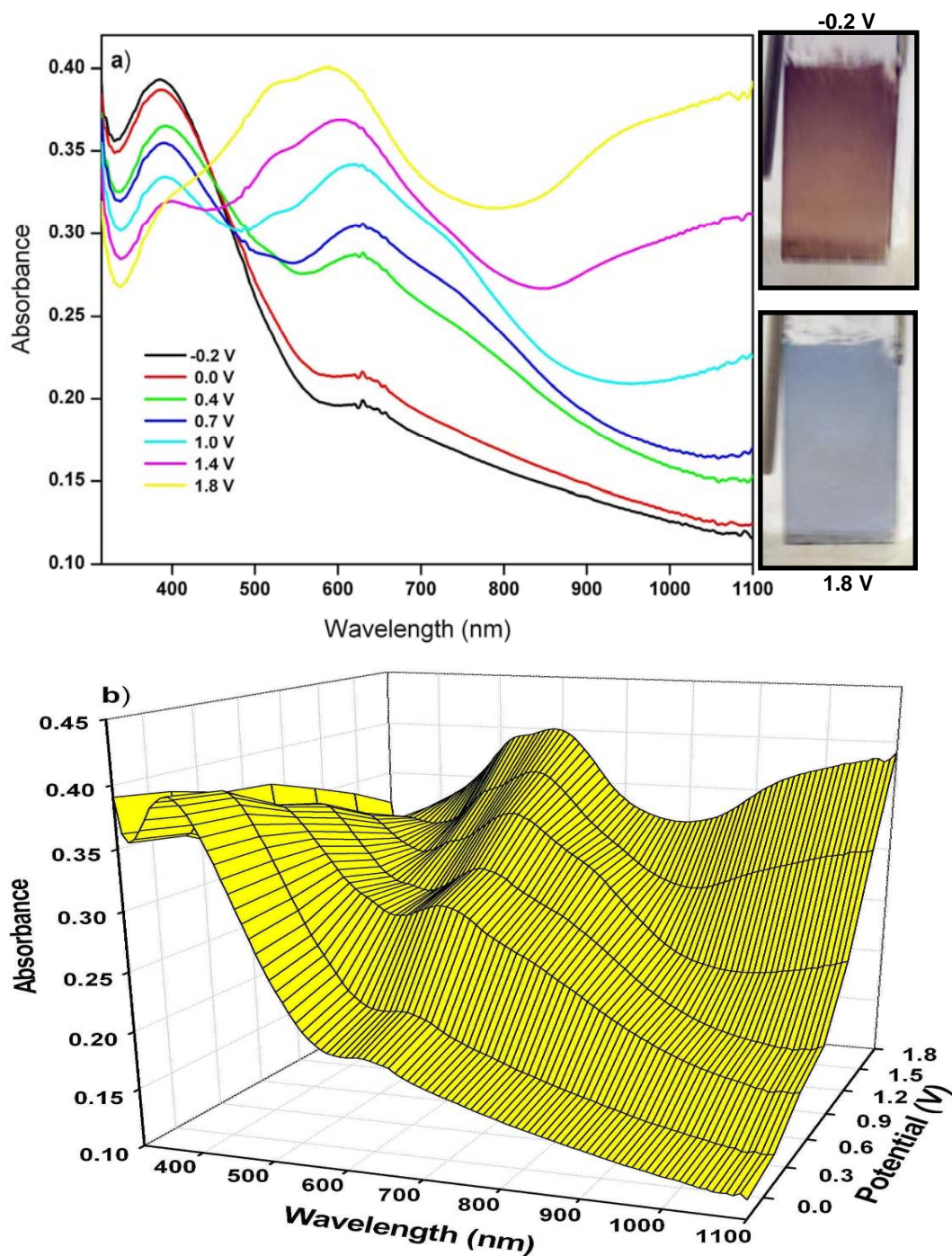
Figure 3.28 Optoelectrochemical spectrum of P(TriaTh-co-Th) film a) 2D b)3D
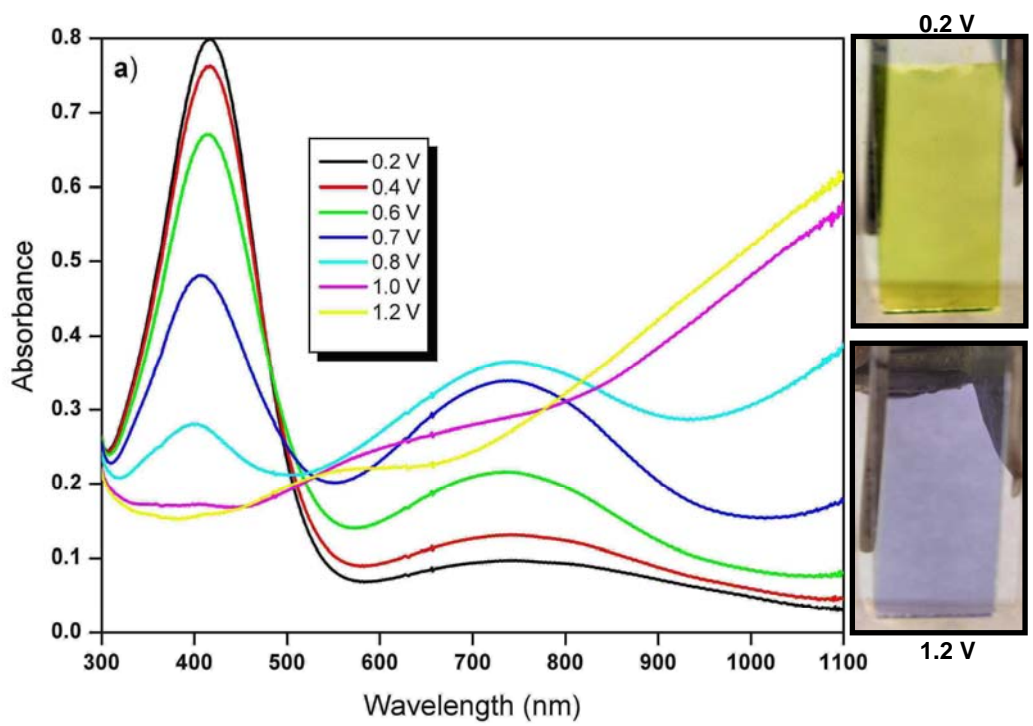
Figure 3.29 Optoelectrochemical spectrum of P(NMT) film a) 2D b)3D
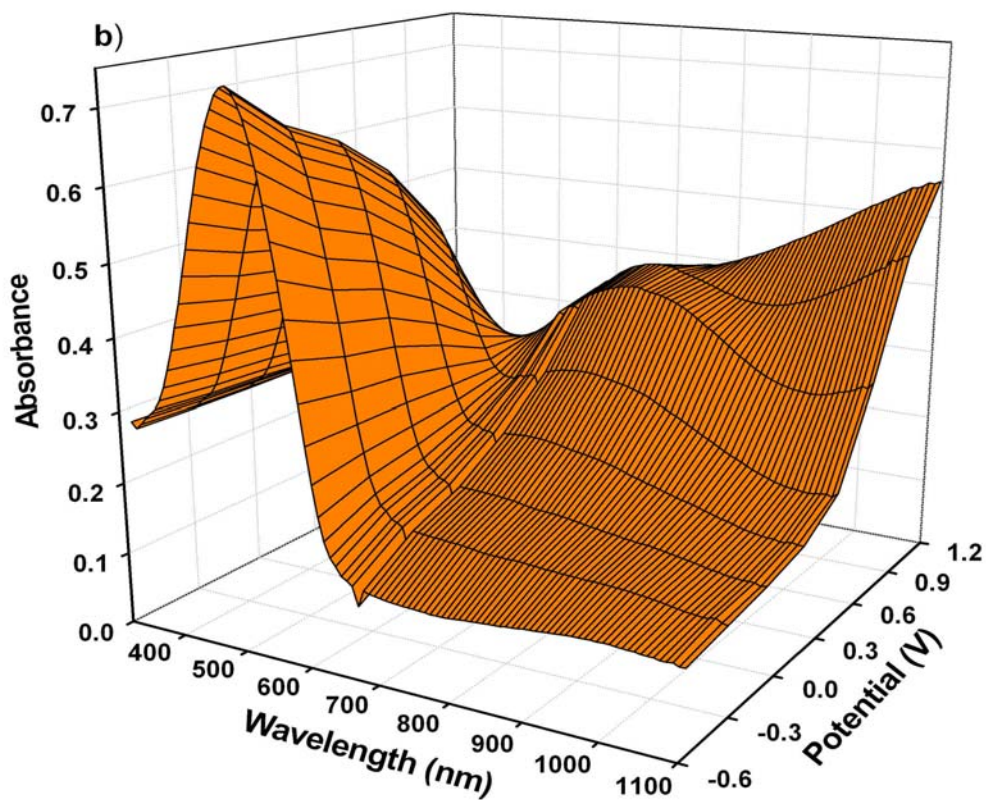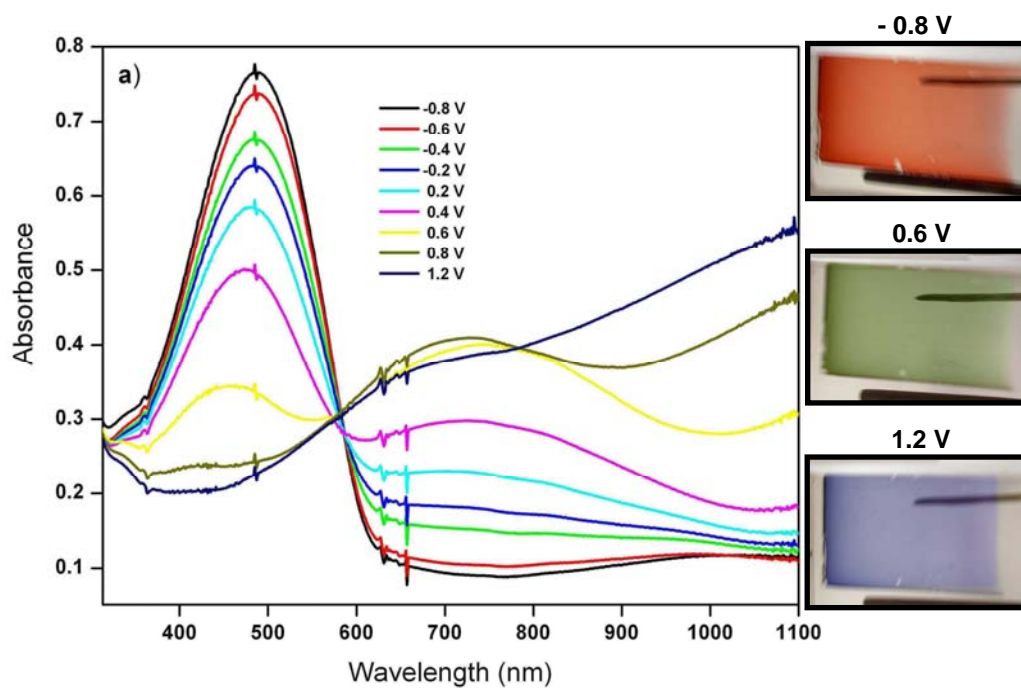
Figure 3.30 Optoelectrochemical spectrum of P(NMT-co-Th) film a) 2D b)3D

3.3.2 Electrochromic Switching

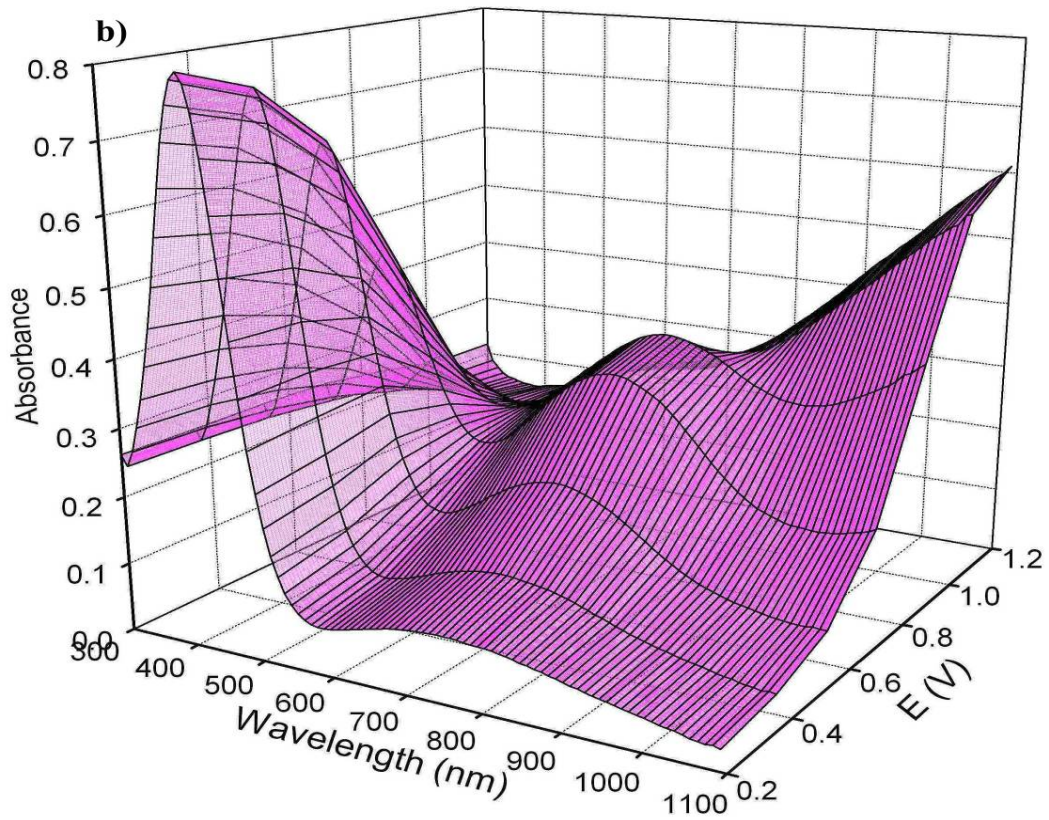Spectroelectrochemistry studies revealed the ability of the polymers to switch between their redox states with a change in transmittance at a fixed wavelength.

3.3.2.1 Switching of P(HMTA-coTh) and P(MBThi-co-Th)

For P(HMTA-co-Th) maximum contrast (%ΔT) was measured as 20.02 and switching time was 1.1 seconds by stepping the potential between 0.0 V and + 1.6 V with a residence time of 5 s (Fig. 3.31a). For P(MBThi-co-Th) switching time of the copolymer was determined by monitoring the % T change at 440 nm through switching the applied potential in a square wave form between 0.4 V and 1.1 V (Fig. 3.31b).
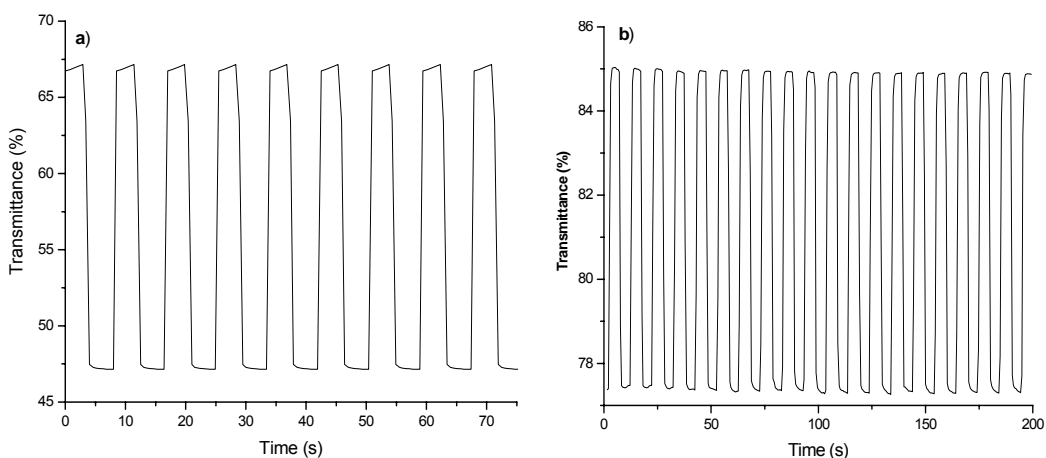
Figure 3.31 Electrochromic switching, optical absorbance change monitored for a) P(HMTA-co-Th) and b) P(MBThi-co-Th)

3.3.2.2 Switching of P(TriaPy)

The transmittance, %T, was monitored at λ_{max} of the polymer while the polymer was switched from -1.4 to +1.0 V. For P(TriaPy) maximum contrast was obtained for bipolaronic state absorption (~700 nm). Hence, optical contrast of the P(TriaPy) between its neutral and doped states were measured at 700 nm, and found as 20 % with a switching time of 1.1 s (Fig.3.32).
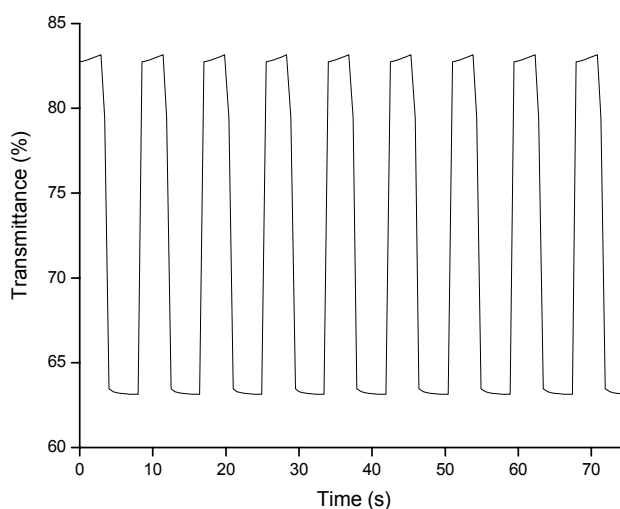
Figure 3.32 Electrochromic switching, optical absorbance change monitored for P(TriaPy)

3.3.2.3 Switching of P(TriaPy-co-Py) and P(TriaTh-co-Th)

For P(TriaPy-co-Py) maximum contrast (%ΔT) was measured as 31.8 (at 800 nm) and switching time was 1.7 seconds by stepping the potential between -0.4 V and +1.2 V with a residence time of 5 s.(Fig. 3.33a). For P(TriaTh-co-Th) switching time of the copolymer was determined by monitoring the % T change at 600 nm through switching the applied potential in a square wave form between -0.2 V and 1.8 V (Fig. 3.33b).
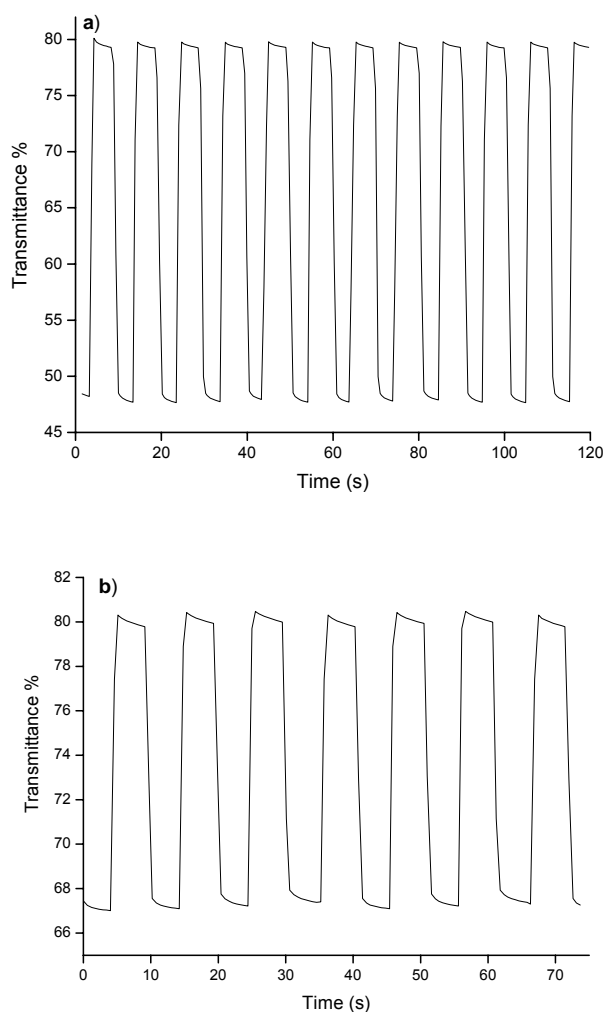
Figure 3.33 Electrochromic switching, optical absorbance change monitored for a) P(TriaPy-co-Py) and b) P(TriaTh-coTh)

3.3.2.4 Switching of P(HMD) and P(HMD-co-Th)

%T is monitored at 417 nm while the P(HMD) is switched from +0.2 V to +1.2V. The contrast is measured as the difference between %T in the reduced and oxidized forms and noted as 41. As seen in Figure 3.34a, P(NMT) has reasonable stability and less than 1.7 s switching time.

For P(HMD-co-Th), the optical contrast was monitored by switching the copolymer between -0.8 V and 1.2 V at 546. As seen in Figure 3.34b, copolymer has good stability, fast switching time (1.2 sec.) and high optical contrast (%37).
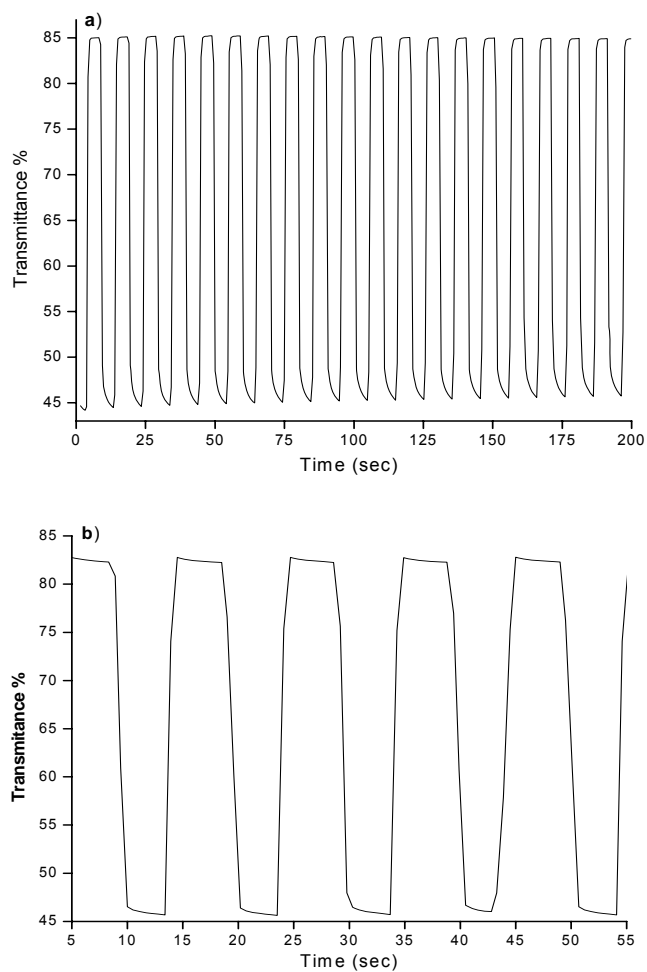
Figure 3.34 Electrochromic switching, optical absorbance change monitored for a) P(HMD) and b) P(HMD-coTh)

3.3.3 Colorimetry

L a b values of the polymer films were measured at the fully oxidized and the fully reduced states and the results were recorded in Table 3.2.

3.4 Electrochromic Devices Application

A dual-type ECD consists of two electrochromic materials (one revealing anodic coloration, the other revealing cathodic coloration) deposited on transparent ITO, placed in a position to face each other and a gel electrolyte in between. Before constructing the ECD, the anodically coloring polymer films were fully reduced and the cathodically coloring polymer (PEDOT) was fully oxidized. Upon application of the potential, the doped polymer will be neutralized with concurrent oxidation of the complementary polymer, including color formation.

3.4.1 Spectroelectrochemistry of ECDs

3.4.1.1 Spectroelectrochemistry of P(HMTA-co-Th)/PEDOT device

Spectroelectrochemical study of P(HMTA-co-Th)/PEDOT device at voltages varying between 0.0 V and +1.6 V is shown in Figure 3.35. Due to π-π^* transition there is a maximum absorption at 496 nm revealing the red color. In that state PEDOT layer was in transparent blue color and device revealed red color. When the applied potential was increased due to reduction of PEDOT layer, blue color became dominant and maximum absorption was observed at 608 nm.
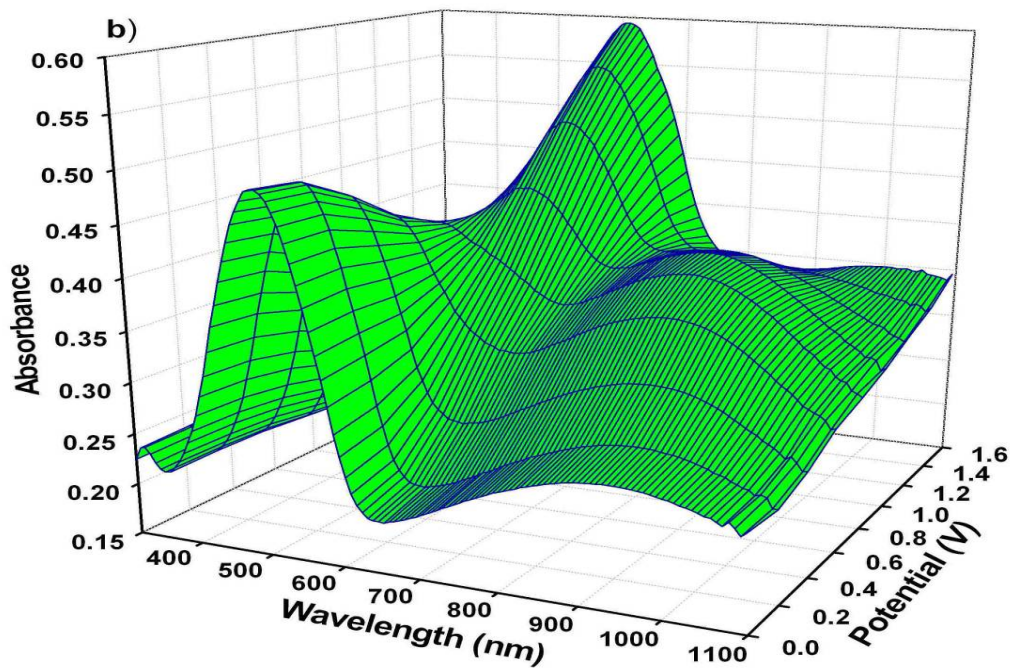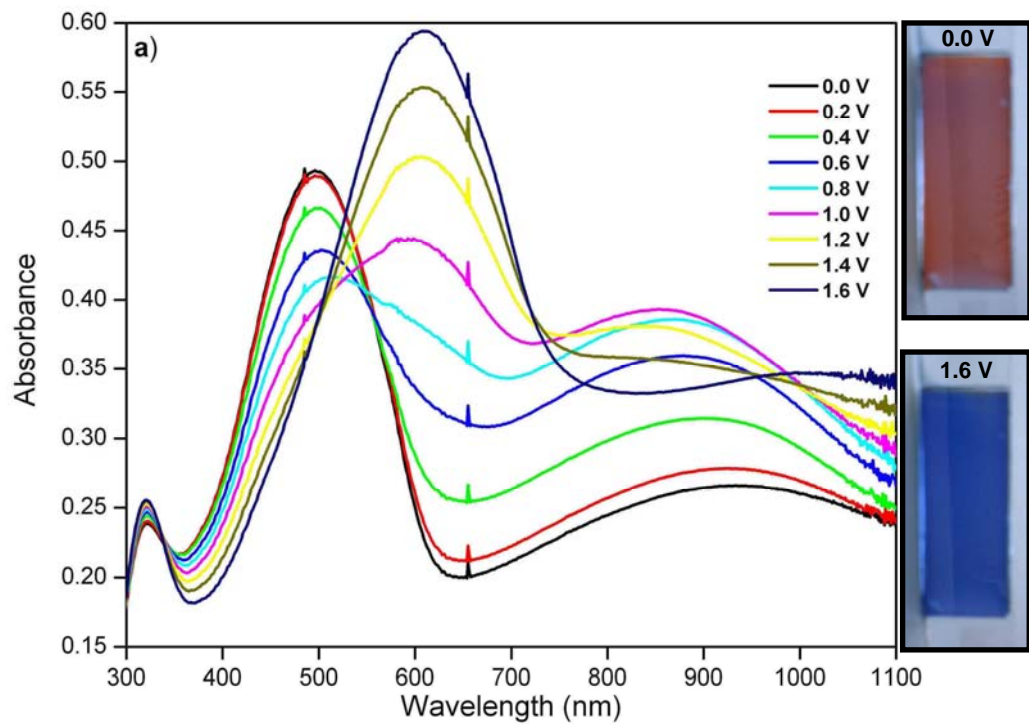
Figure 3.35 Optoelectrochemical spectrum of P(HMTA-co-Th)/PEDOT device
a) 2D b)3D

3.4.1.2 Spectroelectrochemistry of P(MBThi-co-Th)/PEDOT device

Optoelectrochemical spectra of the dual-type P(MBThi-co-Th)/PEDOT ECD as a function of applied voltage are shown in Figure 3.36. At 0.0 V the device revealed a maximum absorption at 450 nm. At this stage the copolymer was in its neutral state revealing light orange color and PEDOT was in its oxidized form (highly transparent) revealing on significant absorption at the visible region. Upon incremental increase in the applied potential, oxidation of the copolymer layer, which was signified with the decrease in the intensity of the peak due to π-π^* transition was observed. Beyond 2 V evolution of the new peak around 650 nm (π-π^* transition of PEDOT itself) was observed, due to reduction of this layer. At 2 V the spectra of the device is very similar to pure PEDOT, indicating that the PEDOT and copolymer were in their fully neutral and oxidized states, respectively.

3.4.1.3 Spectroelectrochemistry of P(TriaPy)/PEDOT device

Figure 3.37 shows the spectroelectrochemical data of the P(TriaPy)/PEDOT device at voltages varying between -1.2 and +1.5 V. When a negative voltage applied to the PEDOT layer, the polymer was in its neutral state with a π-π^* transition λ_{max} at around 595 nm which was responsible for the blue color. At this voltage, P(TriaPy) was in oxidized state and device reveals the dark blue color. When a positive voltage was applied to the PEDOT layer, the polymer film was oxidized and it exhibited transmissive sky blue color. At this stage, P(TriaPy) layer had an absorptive red color with the a π-π^* transition at 357 nm. The relative luminance L and the a, b values of the devices (Table 3.2) were measured at -1.2 and +1.5 V.
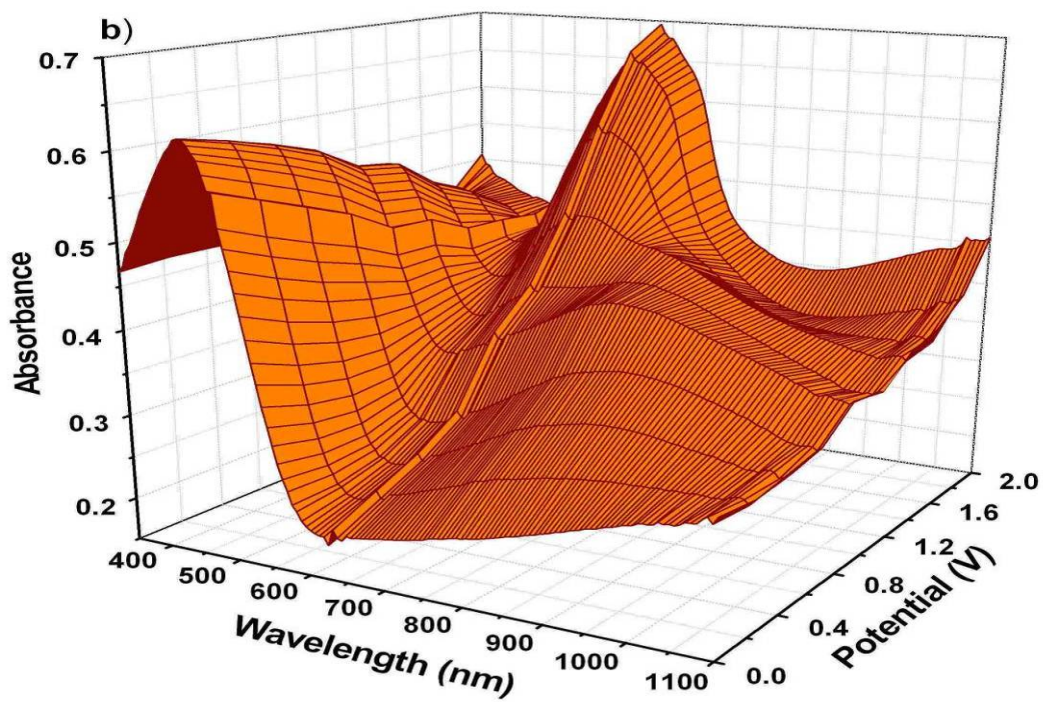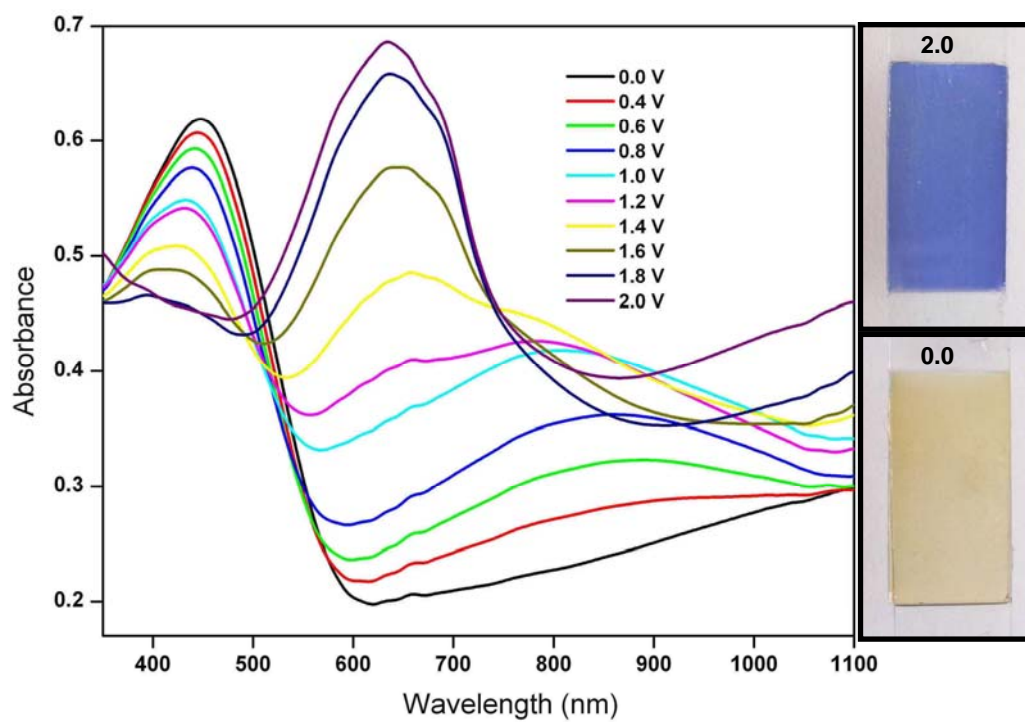
Figure 3.36 Optoelectrochemical spectrum of P(MBThi-co-Th)/PEDOT device
a) 2D b)3D
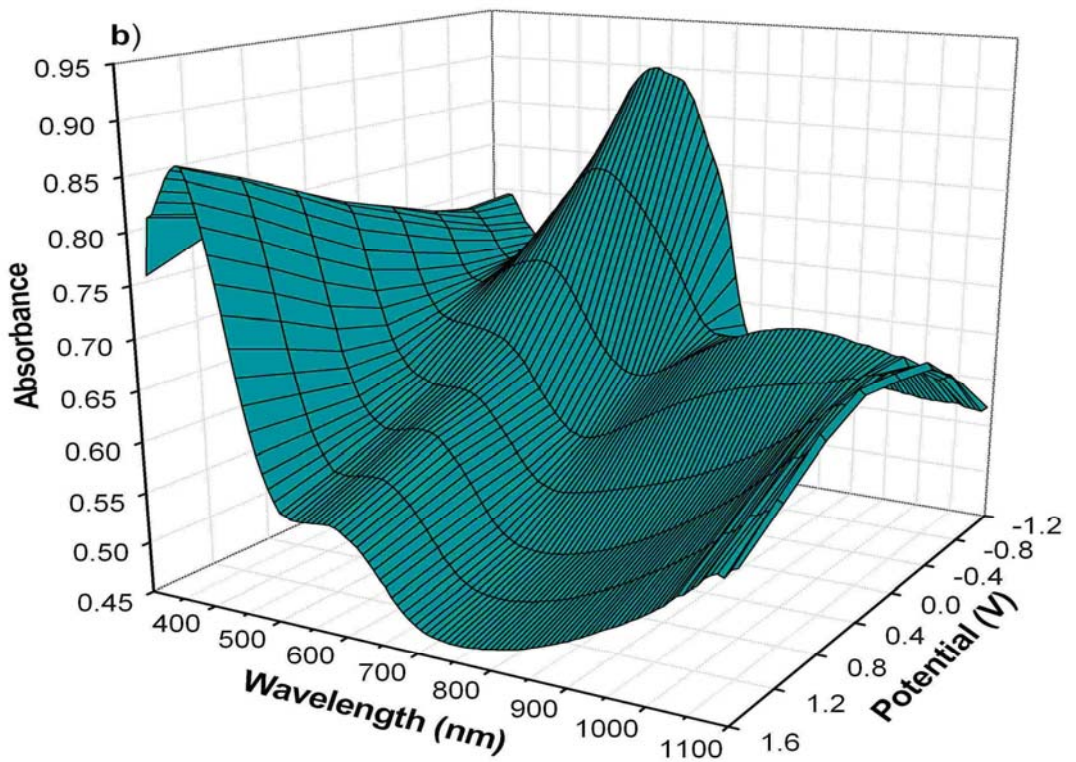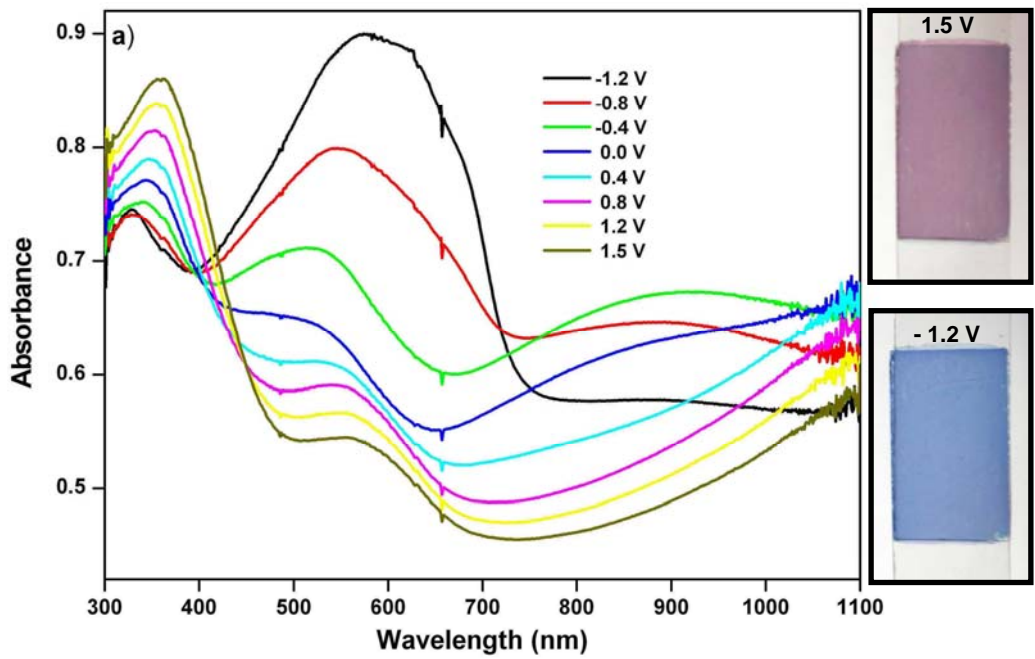
Figure 3.37 Optoelectrochemical spectrum of P(TriaPy)/PEDOT device a) 2D b)3D

3.4.1.4 Spectroelectrochemistry of P(NMT)/PEDOT and P(NMT-coTh)/PEDOTdevice

For P(NMT)/PEDOT device, maximum absorption at 417 nm revealing yellow color was observed due to π-π* transition upon application of positive voltages. At that state, PEDOT did not reveal an obvious absorption at the UV-Vis region of the spectrum and device revealed yellow color. When the applied potential decreased, due to reduction of PEDOT layer, blue color became dominant and a new absorption observed at 622 nm (Fig. 3.38a).

Copolymer device has maximum absorptions at 488 nm and 640 due to π-π* transition of P(NMT-co-Th) and PEDOT layers (Fig. 3.38b).
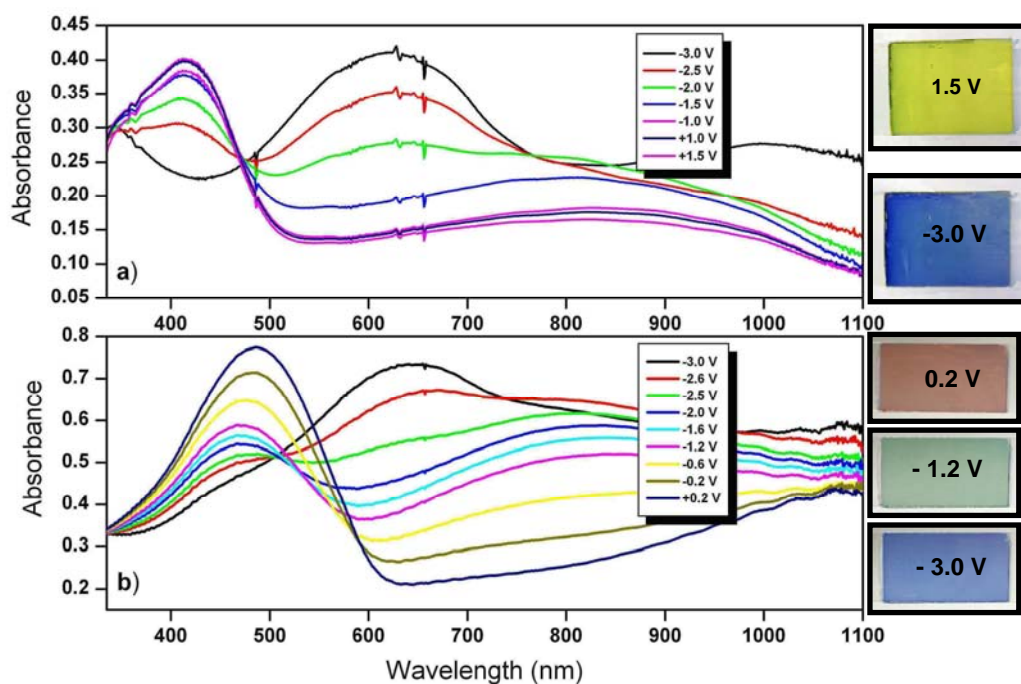
Figure 3.38 Optoelectrochemical spectrum of a) P(NMT)/PEDOT b) P(NMT-co-Th)/PEDOT devices

3.4.2 Switching of the Electrochromic Devices

One of the most important characteristics of ECD's is the response time needed to perform switching between two colored states. A square wave potential step method coupled with optical spectroscopy known as chronoabsorptometry is used to probe switching times and contrast in these polymers. During the experiment, the % transmittance (%T) at the wavelength of maximum contrast was measured by using a UV-Vis spectrophotometer.

Switching time and %ΔT values for P(HMTA-co-Th)/PEDOT device measured as 1.7 s and 23.95 respectively while stepping the potential between -0.5 V and +1.5 V. Figure 3.39a shows transmittance-time profile of the P(HMTA-co-Th)/PEDOT device recorded during double step spectrochronoamperometry.

Figure 3.39b demonstrates the transmittance change of at 650 nm, where the maximum contrast was observed, for P(MBThi-co-Th)/PEDOT. During the experiment, potentials were stepped between 0.0 and 2.0 V with a residence time of 5 s. Results showed that time required to reach ultimate % T was 1.6 s.
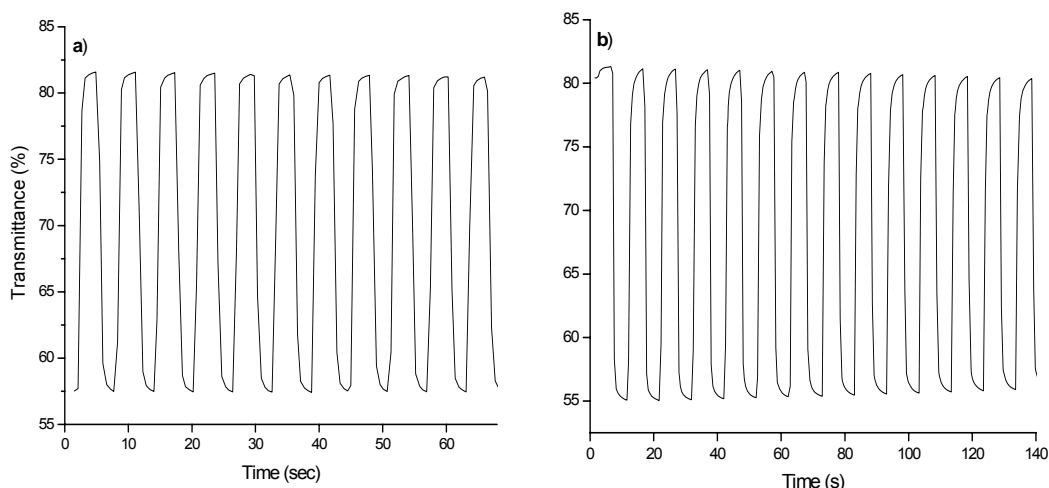
Figure 3.39 Electrochromic switching, optical absorbance change monitored for a) P(HMTA-co-Th)/PEDOT and b) P(MBThi-co-Th)/PEDOT devices

During the chronoabsorptometry experiment for P(Tria-Py)/PEDOT by stepping the potential between -1.2 and 1.5 V with a residence time of 5 s, the contrast was measured as the difference between %T in the reduced and oxidized forms and switching time were found to be 25% and 2.2 s (Fig. 3.40).
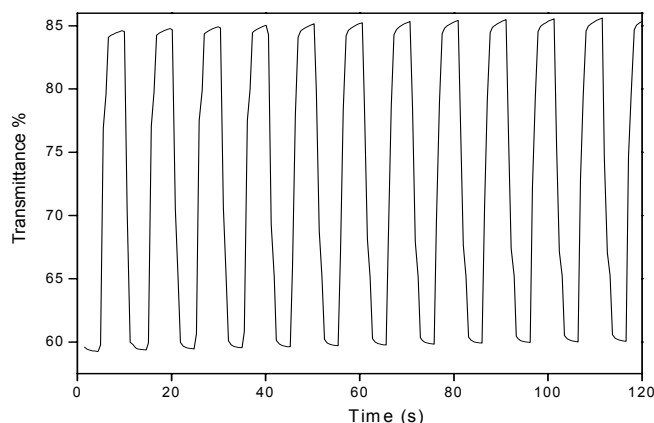
Figure 3.40 Electrochromic switching, optical absorbance change monitored for P(Tria-Py)/PEDOT device

For the P(NMThi)/PEDOT device, maximum contrast (T %) and switching time was measured as 20 % and 1.7 sec at 622 nm. (Fig.3.41a). Maximum contrast (T %) and switching time of the P(NMThi-coTh)/PEDOT device at 640 nm were measured %37 and 1.7 sec (Fig 3.41b).

3.4.3 Stability of Electrochromic Devices

3.4.3.1 Stability of P(HMTA-co-Th)/PEDOT and P(MBThi-co-Th)/PEDOT Devices

Redox stability is an important requirement for production of reliable electrochromic devices with long lifetimes. For this purpose we accomplished non-stop cycling of the applied potential between 0.0-1.6 V with 500 mV/s scan rate for P(HMTA-co-Th)/PEDOT device. As seen in Figure 3.42a even after

1000 th run, device showed only a slight decrease in electroactivity accompanied by unperturbed color change.
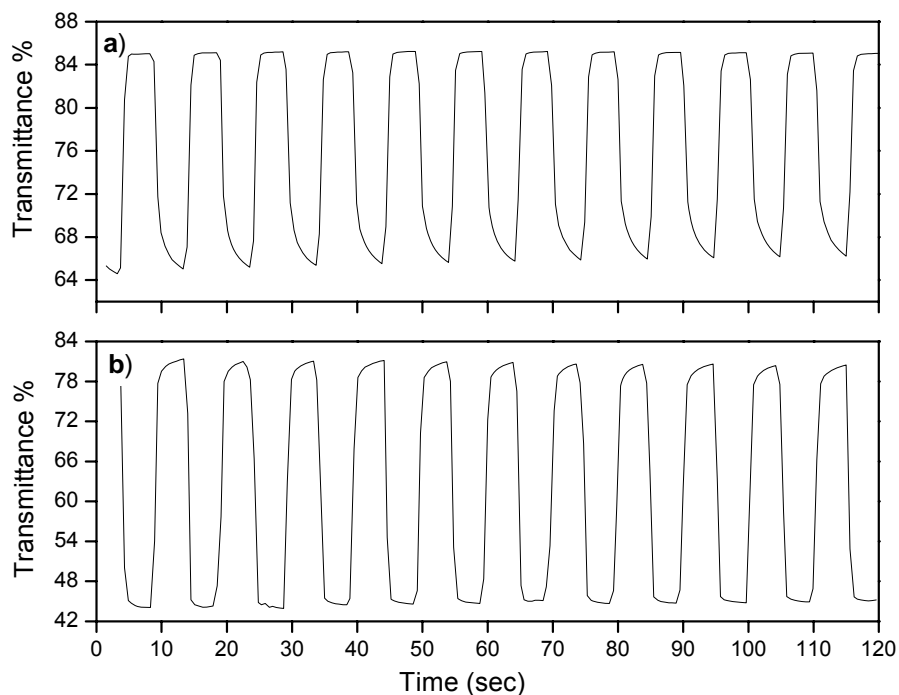
Figure 3.41 Electrochromic switching, optical absorbance change monitored for a) P(NMThi)/PEDOT and b) P(NMThi-coTh)/PEDOT devices

Redox stability of the P(MBThi-co-Th)/PEDOT device was investigated by applying continuous potentiodynamic scans between 0.0 V and 2.0 V at a scan rate of 500 mV/s. Results indicated the reasonable stability of the device under atmospheric conditions, where there is only limited decrease in current after 1000 cycles (Fig. 3.42b).
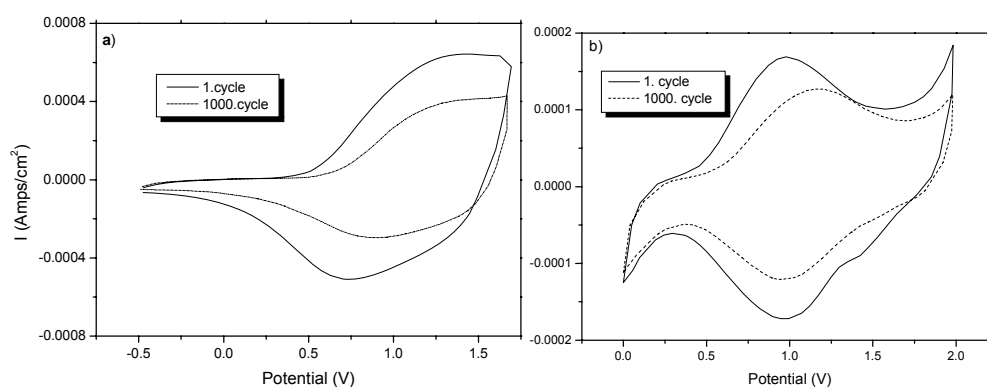
Figure 3.42 Switching stability of a) P(HMTA-co-Th)/PEDOT b) P(MBThi-co-Th)/PEDOT devices

3.4.3.2 Stability of P(TriaPy)/PEDOT, P(HMD)/PEDOT and P(HMD-co-Th)/PEDOT Devices

Redox stability of the P(TriaPy)/PEDOT, P(HMD)/PEDOT and P(HMD-co-Th)/PEDOT devices were investigated by applying continuous potentiodynamic scans between -1.6/1.4 V, -3.0/2.6 V and -2.5/0.0 V respectively at a scan rate of 500 mV/s. After 1000 cycles, results indicated the reasonable stability of the devices under atmospheric conditions, where there is only limited decrease in current response (Fig. 3.43 and Fig. 3.44).
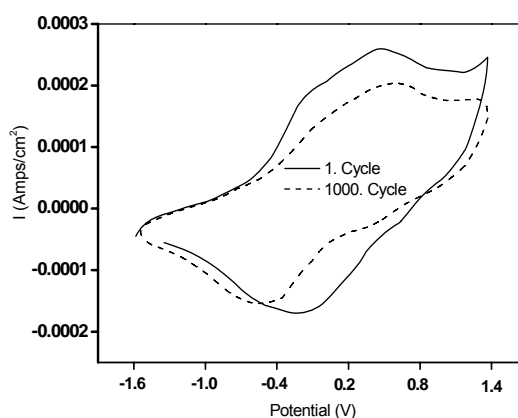
Figure 3.43 Switching stability of P(TriaPy)/PEDOT device
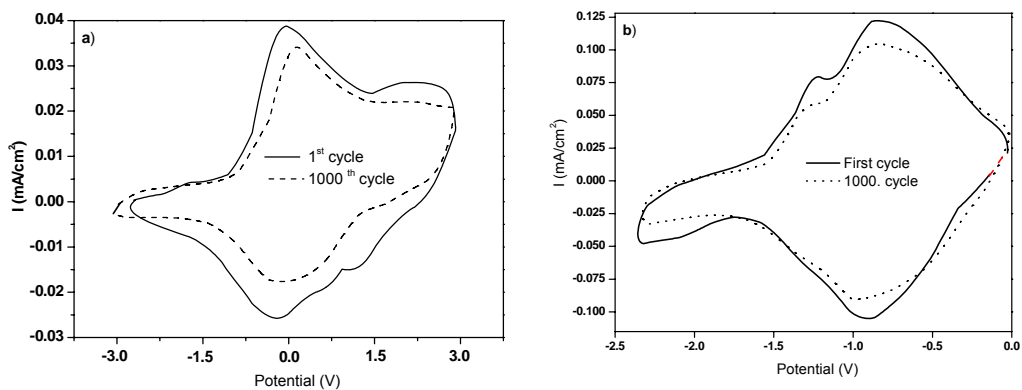
Figure 3.44 Switching stability of a) P(HMD)/PEDOT b) P(HMD-co-Th)/PEDOT devices

3.4.4. Colorimetry Studies of Electrochromic Devices

L*a*b values of the devices colors were measured at the fully oxidized and fully reduced states and the results are given in Table 3.2.

Table 3.2 Electrochromic and optical properties of polymers and devices

Polymer	λ_{max} (nm) (π-π*)	λ_{max} (nm) (polaron)	Switch. time (s)	Optical contrast	ox-red pot. (V)	Eg (eV) (Band gap)	Colors and L a b Values		
							Ox. (L a b)	Half ox. (L a b)	Red. (L a b)
P(HMTA-co-Th)	505	741	1.1	20	0.2/1.6	1.95	Blue (57,-7,-1)	-	Red (51,52,46)
P(MBThi-co-Th)	440	730	1.1	8	0.0/1.8	1.74	Blue (53,-7,-20)	-	Orange (70,9,42)
P(TriaPy)	346	508	1.1	20	-1.4/1.0	2.97	Turquise (64,-37,11)	-	Red (66,23,31)
P(TriaPy-co-Py)	371	500	1.1	32	-1.0/1.6	2.37	(Turquise (68,-30,8)	-	Red (55,45,40)
P(TriaTh-co-Th)	386	588	1.1	13	-0.2/1.8	1.97	Blue (58,-10,-5)	-	Red (53,58,45)
P(NMT)	417	733	1.5	41	0.2/1.2	2.34	Blue (65,3,0)	-	Yellow (90,-8,46)
P(NMT-co-Th)	488	718	1.2	37	-0.8/1.2	1.99	Blue (61,-3,3)	Green (57,-13,30)	Red (51,21,26)

Devices	λ_{max} (nm) (π-π*)	λ_{max} (nm) (polaron)	Switch. time (s)	Optical contrast	ox-red pot. (V)	Colors and L a b Values		
						Ox. (L a b)	Half ox. (L a b)	Red. (L a b)
P(HMTA-co-Th)/PEDOT	496	608	1.7	24	-0.5/1.5	Blue (50,-6,-19)	-	Red (61,18,7)
P(MBThi-co-Th)/PEDOT	450	650	1.6	23	0.0/2.0	Blue (50,-5,-23)	-	Orange (77,8,40)
P(TriaPy/PEDOT)	357	595	2.2	25	-1.2/1.5	Blue (56,1,-33)	-	Red (53,33,44)
P(NMT)/PEDOT	417	622	1.7	20	-3.0/1.5	Yellow (81,-12,41)	-	Blue (66,-10,-19)
P(NMT-co-Th)/PEDOT	488	640	1.7	37	-3.0/0.2	Red (47,33,34)	Green (53,-22,31)	Blue (35,0,-26)

CHAPTER IV

CONCLUSIONS

There are numerous processes possible for the modulation of visible light. Among them are electrochromic techniques that use the reversible change of color and/or optical density obtained by an electrochemical redox process in which the oxidized and the reduced forms have different colors, indices of refraction, or optical densities.

For electrochromic windows an ideal cathodically coloring material has a low band gap around 1.8-2.0 eV in order for the π-π^* transition to occur in the visible region where the human eye is highly sensitive. An anodically coloring polymer is chosen to have a high band gap (E_g) > 2.0 eV with all of the absorption lying in the ultraviolet region of the spectrum. Generally cathodically coloring materials for use in ECDs are based on PEDOT and its derivatives, as they exhibit high electrochromic contrasts, low oxidation potentials and high conductivity, as well as good electrochemical and thermal stability. In this thesis, new thiophene and pyrrole based monomers used for anodically coloring materials for electrochromic windows were synthesized.

In first part of the this thesis, different substituted thiophene and pyrrole monomers, namely hexamethylene (bis-3-thiopheneacetamide) (HMTA), N-(4-(3-thienyl methylene)-oxycarbonylphenyl)maleimide (MBThi), 2,4,6-Tris-(4-pyrrol-1-yl-phenoxy)-[1,3,5]triazine (TriaPy), 2,4,6-Tris-(thiophen-3-ylmethoxy)-[1,3,5]triazine (TriaTh), and N-(2-(thiophen-3-yl)methylcarbonyloxyethyl) maleimide (NMT) were synthesized. Main application of these monomers is use in electrochromic windows as the anodically coloring polymers. The chemical structures of the monomers were characterized by Nuclear Magnetic

106

Resonance (^{1}H-NMR and ^{13}C-NMR) and Fourier Transform Infrared (FTIR). Electrochemical behavior of the monomers in the presence and absence of comonomers were studied by cyclic voltammetry. Subsequently, monomers were homopolymerized and copolymerized via electrochemical methods and the resultant polymers were characterized by FTIR, Scanning Electron Microscopy (SEM) and conductivity measurements.

Second part of this thesis was devoted mainly to the investigation of spectroelectrochromic properties and electrochromic window applications of these polymers. For this purpose we used some important set of electrochemical experiments such as spectroelectrochemistry, chronoabsorptometry, colorimetry and redox stability experiments.

Spectroelectrohemical experiments reveal key properties of conjugated polymers such as the electronic band gap (Eg) and the intergap states that appear upon doping as well as provide insights into fine structure. Spectroelectrochemistry of the homopolymers, copolymers and corresponding devices were investigated by UV-Vis spectroscopy. Results (λ_{max}, band gap energy, wavelength of the π-π^* transition and polaron bands) were shown in Table 4.1

Contrast ratios were then calculated by the transmittance change between the neutral state and the oxidized state of polymer for corresponding devices with chronoabsorptometry experiments. An extension of this technique is electrochromic switching studies where the step time is shortened to measure the response time of conjugated polymers which are measured as the time required to reach full optical contrast. Measured switching times and optical contrast values of all polymers and corresponding devices are given in Table 4.1.

Colorimetry is a quantitative analytical tool that has proven an effective objective method to compare and evaluate the optical responses of electrochromic polymers and devices. Color can be described in terms of three attributes; hue, saturation, and luminance, since the subjective nature of the art, color matching can be difficult. Using CIE system of colorimetry, neutral and oxidized colors of the all polymers and devices were determined. The results were shown in Table 4.1.

Cyclic voltammetry technique was used for the stability experiments of the devices. Results indicated reasonable stability of the devices under atmospheric conditions, where there exists only limited decrease in the current response.

REFERENCES

[1]   H.Letheby, *J. Chem. Soc.* 1862 15 161

[2]   E. Noelting, *Scientific and Industrial History of Aniline Black*; J. Matheson: New York, 1989

[3]   G. Natta, G. Mazzanti, P. Corradini, *Atti Accad. Lincei Cl. Sci. Fis. Mat. Nat. Rend.* 1958 25 3

[4]   F. B. Burt, *J. Chem. Soc.* 1910 68 105

[5]   A. G. MacDiarmid, *J. Am. Chem. Soc.*, 1976 98 3884

[6]   J. Gerratt, S.J. McNicholas, M. Sironi, D.L. Cooper, P.B. Karadakov, *J. Am. Chem. Soc.* 1996118 6472

[7]   H. Shirakawa, F. J. Louis, A. G. MacDiarmid, C. K. Chiang, A.J. Heeger, *J. Chem. Soc., Chem. Commun.* 1977, 578

[8]   (a) H. Shirakawa, *Angew. Chem. Int. Ed.* 2001, 40, 2574. (b) A. G. MacDiarmid, *Angew. Chem. Int. Ed.* 2001, 40, 2581. (c) A.J. Heeger, Angew. Chem. Int. Ed. 2001,40, 2591. (d) H. Shirakawa, *Synth. Met.* 2002, 125, 3. (e) A. G. MacDiarmid, *Synth.Met.* 2002, 125, 11. (f) A. J. Heeger, *Synth. Met.* 2002, 125, 23

[9]   H. Shirakawa, E.J. Louis, A.G. MacDiarmid, C.K. Chiang, A.J. Heeger, *J. Chem. Soc. Chem. Commun.* 1977 578

[10] C.K. Chiang, C.R. Fischer, Y.W. Park, A.J. Heeger, H. Shirakawa, E.J. Louis, S.C. Gau, A.G. MacDiarmid, *Phys. Rev. Letters,* 1977 39 1098

[11] A. Gandini, M. N. Belgancem, *Prog. Polym. Sci.* 1997 *22* 1203

[12] (a) A. F. Diaz, K. K. Kanazawa, G. P. Gardini, *J. Chem. Soc., Chem. Commun.* 1979 635 (b) A. F. Diaz, J. I. Castillo, J. A. Logan, W. Lee, *J. Electroanal. Chem.* 1981 129 115 (c) K. Lee, A. J. Heeger, *Synth. Met.* 1997 *84* 715

[13] (a) A.G. Bayer Eur. Patent 339,340, 1988 (b) F. Jonas, L. Schrader, Synth.Met. 1991 41 831 (c) G. Heywang, F. Jonas, *Adv. Mater.* 1992 4 116

[14] G. Grem, G. Leditzky, B. Ullrich, G. Leising, *Adv. Mater.* 1992 4 36

[15] J.H. Burroughes, D.D.C. Bradley, A.R. Brown, R.N. Marks, K. MacKay, R.H. Friend, P.L. Burn, A.B. Holmes, *Nature* 1990 347 539

[16] J. Rault-Berthelot, J. Simonet, *J. Electrochem. Soc.* 1985 182 187

[17] A. G. MacDiarmid, A.J. Epstein, *Farad. Discuss. Chem. Soc.* 1989 88 317

[18] A. Desbene-Monvernay, P.-C.Lacaze,J.-E. Dubois, *J. Electroanal. Chem.* 1981 129 229

[19] P. Bäuerle, U. Segelbacher, A. Maier, M. Mehring, *J. Am. Chem. Soc.* 1993 115 10217

[20] D.C. Trivedi, *In Organic Conductive Molecules and Polymers*, H.S. Nalwa, Ed.; John Wiley & Sons: Chichester, 1997, Vol. 2

[21] U. Salzner, J.B. Lagowski, P.G. Pickup, P.A. Poirier, *Synth. Met.* 1998 96 177

[22] I. F. Perepichka, D. F. Perepichka, H. Meng, F. Wudl, *Adv. Mater.* 2005 17 1

[23] M. Leclerc, K. Faid *Handbook of Conducting Polymers*. eds T.A. Skotheim, R.A .Elsenbaumer, J.R. Reynolds, New York: Marcel Dekker, 1998 Ch 24

[24] A.J. Heeger, S. Kivelson, J.R. Schrieffer, W.P. Su, *Reviews of Modern Physics*, 1988 60 781

[25] A. Johansson, S. Stafstrom, *Physical Review B*, 2002 6504 no: 045207

[26] J.L. Bredas, D. Beljonne, J. Cornil, J.P. Calbert, Z. Shuai, R. Silbey, *Synth. Met.* 2001 125 107

[27] J.-L. Brédas, G.B. Street, *Acc. Chem. Res.* 1985 18 309

[28] S.N. Hoier, S.-M. Park, *J. Phys. Chem.* 1992 96 5188

[29] J.F. Oudard, R.D. Allendoerfer, R.A. Osteryoung, *J. Electroanal. Chem.* 1988 241 231

[30] K. Fesser, A.R. Bishop, D.K. Campbell, *Phys. Rev.* B 1983 27 4804

[31] M.G. Hill, J.F. Penneau, B. Zinger, K.R. Mann, L.L. Miller, *Chem. Mater.* 1992 4 1106

[32] P. Bäuerle, W. Segelbacher, A. Maier, M. Mehring, *J. Am. Chem. Soc.* 1993 115 10217

[33] Y. Furukawa, *J. Phys. Chem.* 100 (1996) 15644

[34] J.J. Apperloo, R.A.J. Janssen, *Synth. Met.* 1999 101 373

[35] J.J. Apperloo, L. Groenendaal, H. Verheyen, M. Jayakannan, R.A.J. Janssen, A. Dkhissi, D. Beljonne, R. Lassaroni, J.L. Brédas, *Chem. Eur. J.* 2002 8 2384

[36] E.Kalacioglu, L. Toppare, Y.Yagci Synt. Met., 2000, 108, 1

[37] E.M. Genies, G. Bidan, A.F. Diaz, *J. Electroanal. Chem.* 1983 149 101

[38] R.J. Waltman, J. Bargon, *Tetrahedron* 1984 40 3963

[39] A. Yassar, J. Roncali, F. Garnier, *Macromolecules* 1989 22 804

[40] J. Roncali, A. Yassar, F. Garnier, *J. Chem. Soc., Chem. Commun.* 1988 581

[41] J. Roncali, A. Yassar, F. Garnier, *Journal De Chimie Physique Et De Physico-Chimie Biologique* 1989 86 85

[42] J. Roncali, A. Yassar, F. Garnier, *Synth. Met.* 1989 28, C275

[43] P. Marque, J. Roncali, F. Garnier, *J. Electroanal. Chem.* 1987 218 107

[44] B. Krische, M. Zagorska, *Synth. Met.* 1989 28 263

[45] M. Gratzl, D.F. Hsu, A.M. Riley, J .Janata, *J .Phys. Chem.* 1990 94 5973

[46] B. D. Malhotra, N. Kumar, S. Chandra, *Prog. Polym. Sci.,* 1986 12 179

[47] A. F. Diaz, K. K. Kanazawa, in: J. S. Miller (Ed.), *Extended Linear Chain Compounds*, V3, Plenum Press, 1982

[48] K. Gurunathan, A. Vadivel Murugan, R. Marimuthu, U.P. Mulik, D.P. Amalnerkar, *Mater. Chem. Phys.,* 1999 61 173

[49]   S. Hotta, S.D.D.V. Rughooputh, A. J. Heeger*, Synth. Met.*, 1987 22 79

[50]   J. Rodriguez, H.J. Grande, T. F. Otero, *Handbook of Organic Conductive Molecules and Polymers*, (Ed. H. S. Nalwa), John Wiley &Sons, 1997

[51]   S. Sadki, P. Schottland, N. Brodie, G. Sabouraud, *Chem. Soc. Rev.*, 2000 29 283

[52]   J. Margolis, *Conductive Polymers and Plastics*, Chapman and Hall, 1989, P.121

[53]   J. Margolis, *Conductive Polymers and Plastics,* Chapman and Hall, 1989, P.120

[54]   A. Barlow, Entone-OMI representative, 1997

[55]   L. Alcacer, *Conducting Polymers Special Applications*, D. Reidel Publishing Company, 1987, p5

[56]   W. R. Salaneck, D. T. Clark, E. J. Samuelsen, *Science and Application of Conducting Polymers*, IOP Publishing, 1991, p135

[57]   W. R. Salaneck D. T. Clark E. J. Samuelsen, *Science and Application of Conducting Polymers*, IOP Publishing, 1991, p 55

[58]   L. Alcacer, *Conducting Polymers Special Applications* , D. Reidel Publishing Company, 1987, p192

[59]   J. Margolis, *Conductive Polymers and Plastics*, Chapman and Hall*,* 1989, P. 121

[60]   J. Margolis, *Conductive Polymers and Plastics*, Chapman and Hall, 1989, P. 33

[61]   W. R. Salaneck, D.T. Clark, E.J. Samuelsen, *Science and Application of Conducting Polymers*, IOP Publishing, 1991, p52

[62]   R.A. Huggins, *Phill. Trans. R. Soc. London A.*, 1996 354 1555

[63]   S.A. Hashimi, R.J. Latham, R.G. Lindford, W.S. Schlidwein, *Ionics*, 1997 3 177

[64]   G.G. Wallace, C.O. Too, D.O. Officer, P. Dastoor, *Chemical Innovations*, 2000 3 15

[65]   S. Varis, M. Ak, C. Tanyeli, I. M Akhmedov, L. Toppare, Eur. Polym. J. 2006, 42, 2352

[66]   D. R. Rosseinsky, R .J. Mortimer, *Adv. Mater.* 2001 13 783

[67]   R.J. Mortimer, *Electrochim. Acta* 1999 44 2971

[68]   M A. De Paoli, W. A. Gazotti, *J. Braz. Chem. Soc.,* 2002 13 410

[69]   G. Sonmez, I. Schwendeman, P. Schottland, K. Zong, J. R. Reynolds *Macromolecules* 2003 36 639

[70]   K. Fesser, A.R. Bishop, D.K. Campbell, *Phys. Rev. B* 1983 27 4804

[71]   B.C. Thompson, P. Schottland, G. Sonmez, J.R. Reynolds, *Synth. Met.,* 2001 119 333

[72]   J. Roncali, *Chem. Rev.* 1997, 97, 173

[73]   J. L.Bredas, *J. Chem Phys.* 1985 82 (8) 3808

[74]   F. Wudl, M. Kobayashi, A. J. Heeger, *J. Org. Chem.* 1984 49 3382

[75]   R.D. McCullough, *Adv. Mater.* 1998 10 93

[76]   G. A. Sotzing, J. L. Reddinger, A. R. Katritzky, J. Soloducho, R. Musgrave, J. R. Reynolds, *Chem. Mater.* 1997 9 1578

[77]   G.A. Sotzing, J.L. Reddinger, A.R. Katritzy, J. Soloducho, R. Musgarave, J.R. Reynolds, Chem. Mater 1997 9 1578

[78]   G. A. Soltzing, J. R. Reynolds, *J Chem. Soc. Chem. Commun* 1995 703

[79]   L. B. Groenendaal, G. Zotti, P.H. Aubert, S.M. Waybright, J.R. Reynolds *Adv. Mater.* 2003 15 855

[80]   H. Rossotti, *Colour,* Princeton University Press, 1983

[81]   K. Nassau, *The Physics and Chemistry of Color John Wiley*, New York,   1983

VITA

Metin Ak was born in Elazığ on 20th February 1977. He graduated from Antalya Çağlayan Lisesi in 1994. He received his B.S. degree in Chemistry Department in Pamukkale University in 1998. He had worked for Boyasan A.Ş. (Uslu Holding) for 7 month in 1998 and joined the Pamukkale University Chemistry department as a research assistant in the same year. He completed his M.S. degree in 2001 under the supervision of Prof. Dr. Halil Çetişli in the field of "Dissolution kinetic of the calcium in hydrate cement paste". He began his PhD. study in 2002 under the supervision of Prof. Dr. Levent Toppare in the field of conducting polymers, and electrochromism in Middle East Technical University. He worked as a visiting scientist at Bulgarian Academy of Sciences (BAS) in Bulgaria in 2006. Up to date he has published five papers in international journals.